NASA/TM-2001-209984/VER.1/VOL.1

GEOSAT Follow-On (GFO) Altimeter Document Series

Volume 1

GFO Altimeter Engineering Assessment Report

From Launch to Acceptance

10 February 1998 to 29 November 2000

Version 1

D. W. Hancock, III
G. S. Hayne
R. L. Brooks
D. W. Lockwood

December 2000

Observational Science Branch
Laboratory for Hydrospheric Processes
NASA Goddard Space Flight Center
Wallops Flight Facility

Foreword

The Navy's Geosat Follow-On (GFO) Mission, launched on February 10, 1998, is the latest in a series of altimetric satellites which include Seasat, Geosat, ERS-1, and TOPEX/POSEIDON (T/P). Data and results from these missions lead to vast improvements in our knowledge of ocean circulation, ice sheet topography, and climate change. In order to capture the maximum amount of information from the altimetric data, accurate altimeter calibrations are required for the GFO civilian data set which NOAA will produce. NASA/Goddard Space Flight Center/Wallops Flight Facility (GSFC/WFF) has provided these products for the Geosat and T/P missions and is doing the same for GFO.

Wallops' multiple roles with regard to GFO are:

- NASA Representative for Radar Altimeter Performance
- Calibration Collaboration
- Member of GFO Cal-Val Team
- Data distribution to members of Cal-Val Team
- Validate sensor-related corrections
- Provide corrections for sensor changes

For the latest updates on the performance of the GFO Radar Altimeter, and for accessing many of our reports, readers are encouraged to contact our WFF/GFO Home Page at http://gfo.wff.nasa.gov/

This WFF GFO Altimeter Engineering Assessment Report has been prepared by Raytheon/ITSS under Contract NAS5-00181 with the NASA Goddard Space Flight Center, Greenbelt, Maryland. This work was performed under the direction of David W. Hancock, III, WFF GFO Altimeter Verification Manager, Observational Science Branch, Laboratory for Hydrospheric Processes, NASA Goddard Space Flight Center, Wallops Flight Facility, Wallops Island, Virginia, who may be contacted at (757) 824-1238, hancock@osb1.wff.nasa.gov (e-mail), or (757) 824-1036 (fax).

Acknowledgments

This document includes contributions by the following members of the Wallops Flight Facility GFO Team:

- David Hancock (NASA GSFC / WFF)
  WFF GFO Altimeter Verification Manager
- George Hayne (NASA GSFC / WFF)
- Anita Brenner (Raytheon ITSS / Greenbelt)
- Lisa Brittingham (Raytheon ITSS)
- Ronald Brooks (Raytheon ITSS)
- Jeffrey Lee (Raytheon ITSS)
- Dennis Lockwood (Raytheon ITSS)
- Carol Purdy (Raytheon ITSS)
- Ngan Tran (Raytheon ITSS)

Table of Contents

Foreword iii
Acknowledgments v
Table of Contents vii
List of Figures ix
List of Tables xi

Section 1 Introduction

1.1 Identification of Document 1-1
1.2 Definition of a GFO Cycle 1-1
1.3 Data Flow to/from Wallops 1-1

Section 2 On-Orbit Instrument Performance

2.1 Internal Calibrations 2-1
2.2 GFO Cycle (17.05 days) Summaries 2-10
2.3 GFO Key Events 2-12

Section 3 Assessment of Instrument Performance

3.1 Range Measurement Noise 3-1
3.2 GFO Sigma Naught Comparison with TOPEX 3-3
3.3 GFO SWH Comparison of GFO and TOPEX 3-5
3.4 Wind Speeds 3-6
3.5 GFO Sigma0 and SWH Calibration Correction 3-8
3.6 Waveform Fitting in GFO Data 3-9
3.7 GFO “Smile Patch” and its Consequences 3-21
3.8 GFO Range and SWH Consequences of Thermal Change 3-25
3.9 Sigma0 Blooms and Examples in GFO Data 3-28

Section 4 WFF’s Processing Recommendations to GFO Project

4.1 Temperature Correction for AGC 4-1
4.2 WFF Recommended Sigma0 and SWH Corrections 4-3

Section 5 Engineering Assessment Synopsis

5.1 Performance Overview 5-1
5.2 Open Issues 5-1

Section 6 References

6.1 Supporting Documentation 6-1

Appendix A GFO Altimeter Sigma0 and SWH Calibration Correction

Abbreviations & Acronyms AB-1

List of Figures

Figure 2-1 Launch-to-Date Cal 1 Range / Temperature 2-2
Figure 2-2 Period 1999-180 to 1999-229 Cal 1 Range / Temperature 2-3
Figure 2-3 Period 2000-122 to 2000-190 Cal 1 Range / Temperature 2-4
Figure 2-4 Period 2000-243 to 2000-277 Cal 1 Range / Temperature 2-4
Figure 2-5 Launch-to-Date Cal 1 AGC. 2-5
Figure 2-6 Launch-to-Date Cal 2 AGC. 2-6
Figure 2-7 Period 1999-180 to 1999-229 Cal 1 AGC 2-7
Figure 2-8 Period 1999-180 to 1999-229 Cal 2 AGC 2-7
Figure 2-9 Period 2000-122 to 2000-190 Cal 1 AGC 2-8
Figure 2-10 Period 2000-122 to 2000-190 Cal 2 AGC 2-8
Figure 2-11 Period 2000-243 to 2000-277 Cal 1 AGC 2-9
Figure 2-12 Period 2000-243 to 2000-277 Cal 2 AGC 2-9
Figure 3-1 Noise in Altimetry - Spectra Derived by Differencing Repeat Tracks 3-2
Figure 3-2 GFO Noise Level 3-2
Figure 3-3 Comparison of GFO and TOPEX Sigma0. 3-4
Figure 3-4 Comparison of GFO and TOPEX SWH 3-6
Figure 3-5 Distribution of Open Ocean Collected Data 3-7
Figure 3-6 Comparison Between GFO and QSCAT Wind Speeds 3-7
Figure 3-7 Standard Deviation Comparison Between GFO and QSCAT Wind Speeds 3-8
Figure 3-8 GFO Waveform Data from Calibration Mode 1 Fitted to Ideal Sinc^2 with 3.125 ns Width. 3-12
Figure 3-9 GFO Waveform Data from Calibration Mode 2 3-13
Figure 3-10 GFO Waveform Sample Data and Model Waveform Fits 3-14
Figure 3-11 GFO Waveform Fit Comparisons of Attitude / SWH Correction to Range for Gate Index 1 and 2. 3-15
Figure 3-12 GFO Waveform Fit Comparisons of Attitude / SWH Correction to Range for Gate Index 3 and 4. 3-16
Figure 3-13 GFO Attitude Diff. (Fit - SDR) for All Gate Index (1-4) 3-17
Figure 3-14 GFO Waveform Fit Comparisons of SWH Estimates for Gate Index 1 and 2 3-18

Figure 3-15 GFO Waveform Fit Comparisons of SWH Estimates for Gate Index 3 and 4 3-19
Figure 3-16 GFO Noise Baseline Examples 3-20
Figure 3-17 GFO Waveform “Smile Patch” Values 3-22
Figure 3-18 GFO Range Correction Error vs. SWH, With NO Patch 3-23
Figure 3-19 GFO SWH Error vs. SWH, With NO Patch 3-24
Figure 3-20 GFO Individual Waveform Sample Gains from Cal-2 with Patch, at Temperatures 30 and 45C 3-25
Figure 3-21 GFO Range Correction Difference vs. SWH Comparing 45C to 30C Cal-2 Data 3-26
Figure 3-22 GFO SWH Correction Difference vs. SWH Comparing 45C to 30C Cal-2 Data 3-27
Figure 3-23 NGDR Sigma0 vs. Time 3-28
Figure 3-24 NGDR Wind Speed vs. time 3-29
Figure 3-25 GFO 1-Sec Waveform Fit SWH vs. Time 3-29
Figure 3-26 NGDR Vatt vs. Time 3-30
Figure 3-27 GFO 1-Sec Waveform Fit Attitude vs. Time 3-31
Figure 3-28 SSHU STD vs. Time for GFO Data Segment B, in 2000 Day 252 3-31
Figure 3-29 NGDR SSHU STD Standard Deviation vs. Time 3-32
Figure 3-30 NGDR Vatt Standard Deviation vs. Time 3-33
Figure 4-1 Temperature Correction Analysis Plots 4-2

List of Tables

Table 2-1 Cycle Summaries 2-11

Table 2-2 GFO Key Events 2-12

Table 3-1 Comparison of GFO and TOPEX (Ku) Sigma0 Means for 10-Day TOPEX Cycles 3-3

Table 3-2 Comparison of GFO and TOPEX (Ku) SWH Means for 10-Day TOPEX Cycles 3-5

Table 3-3 GFO “Smile Patch” Values for Waveform Samples 1 - 128 3-21

Section 1

Introduction

1.1 Identification of Document

The purpose of this document is to present and document performance analyses and results for the Geosat Follow_on (GFO) altimeter. It is the first of an anticipated series of Wallops GFO performance documents, each of which will update WFF's assessment results. This report covers the altimeter performance from launch on February 10, 1998 to acceptance on November 29, 2000.

1.2 Definition of a GFO Cycle

Like its predecessor, GEOSAT, the GFO groundtrack has a repeat (+/-1 km) period of 17.05 days. For our analyses, the repeat periods are referred to as cycles, and are used as data dividers to assess sensor internal consistency, taking into account seasonal differences. Cycle numbers have not been assigned at this time.

1.3 Data Flow to/from Wallops

1.3.1 To Wallops

The daily near-real time GFO data flow from the Naval Oceanographic Office (NAVO), Altimetry Data Fusion Center (ADFC), Stennis Space Center, Bay St. Louis, MS to Wallops Flight Facility (WFF) consists of:

- Science data without waveforms (ra_data)
- Science data with waveforms (ra_cal_data)
- Engineering data (eng_data)
- Water Vapor Radiometer data (wvr_data)
- Sensor data (sdr)

Additional data are forwarded by the Navy to Wallops as soon as the data are available, consisting of:

- Navy Geophysical Data (ngdr)
- Operational Orbital Determination data (oodd)

1.3.2 From Wallops to Cal/Val Team Members

Wallops forwards the following GFO data types to the other members of the Cal/Val Team:

- Sensor data (sdr)
- Science data with waveforms (ra_cal_data)
- Operational Orbital Determination data (oodd)

Section 2

On-Orbit Instrument Performance

As of November 29, 2000, the GFO altimeter had acquired a cumulative total of approximately 700 days of data out of a possible 935 days. During the initial year-and-a-half of the GFO on-orbit mission, altimeter data collection was sporadic due to various spacecraft systems and software problems, the descriptions of which are outside the scope of this report. The following subsections will illustrate that the altimeter tracking data have been internally consistent. The subsections discuss:

- internal calibrations
- cycle summaries
- key events

2.1 Internal Calibrations

The GFO's internal calibration mode has two submodes, designated CAL-1 and CAL-2. CAL-1 is designed to detect changes in the internal path delays, to measure range drift. CAL-1 also monitors changes in the receiver automatic change control (AGC); the altimeter's estimates of the ocean surface radar backscattering cross-section are obtained from the AGC values. The purpose of the second mode, CAL-2, is to characterize the response of the receiver and digital filter bank.

During CAL-1, a portion of the transmitter output is fed back to the receiver through a digitally controlled calibration attenuator and a delay line, whereupon the altimeter acquires and tracks the signal. Then, during CAL-2, the altimeter processes receiver thermal noise with no transmitted signal present, to characterize the waveform sampler response.

Generally, the GFO Project provides at least two and sometimes three internal calibrations per day.

Prior to Wallops' receiving the calibration data, the GFO ground data processing system routinely does the following: (1) adds a large constant bias to the CAL-1 range, such that the magnitude of the resultant range sum is comparable to a nominal nadir altimeter range to the surface of the earth, and then (2) applies an oscillator drift correction to the total range.

To reconstruct a meaningful CAL-1 range, Wallops performs the following: (1) using the GFO-Project-provided VTCW (Vehicle Time Code Word), removes the oscillator drift correction, and then (2) removes a large constant bias.

The first series of plots which follow contains all the launch-to-date calibrations. These are followed, in turn, by the calibration plots for specific, smaller, cal / val periods of time. The cal / val periods (YYYY-DDD) are: 1999-180 to 1999-229; 2000-122 to 2000-190; and 2000-243 to 2000-277.

2.1.1 Range

2.1.1.1 Launch-to-Date 1998-133 to 2000-334

The launch-to-date CAL-1 range calibrations are shown in the middle of Figure 2-1, denoted by (+) and are referenced to the left vertical scale in millimeters. The data plotted nearer the bottom of the figure, denoted by (◆), are the Composite Temperatures corresponding to the times of the calibrations; the temperatures are referenced to the right vertical scale in degrees Centigrade.

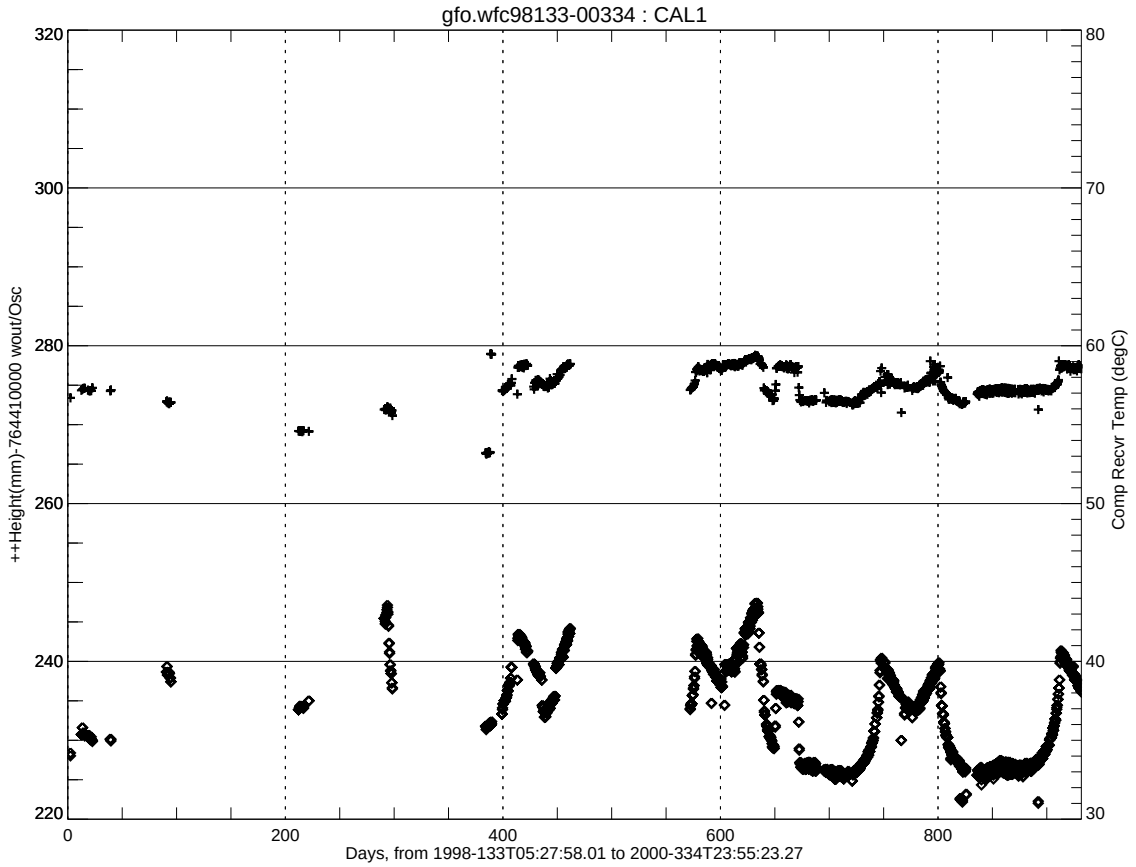

Figure 2-1 Launch-to-Date Cal 1 Range/Temperature

An apparent range calibration drift is observed during the first ~400 days (bottom scale). This is not a real drift, however; it only reflects the fact that we do not have the VTCWs for this early time period.

Subsequent to the time that we began receiving the VTCWs (via the SDRs), the range calibrations have stayed within a narrow window of five mm (273-278 mm). When correlating the range calibration measurements with the composite temperatures, it is apparent that the range measurements have a minor temperature dependency of ~0.55 mm / deg, and the narrow window could be reduced even further by applying a temperature correction, if desired. The internal consistency is already within such a

small window, however, that a temperature correction is not warranted. There is no evidence of any significant long-term range drift.

2.1.1.2 Cal Val Periods

The CAL-1 range for several of the cal / val periods are shown in Figure 2-2, Figure 2-3, and Figure 2-4 respectively. The Composite Temperatures are shown at the bottom of each figure, denoted by (◆) and referenced to the right vertical scale in degrees Centigrade. The CAL-1 range is denoted by (+) and referenced to the left vertical scale in millimeters. Each range is in a very narrow band and displays some temperature dependency.

2.1.1.2.1 Period 1999-180 to 1999-229

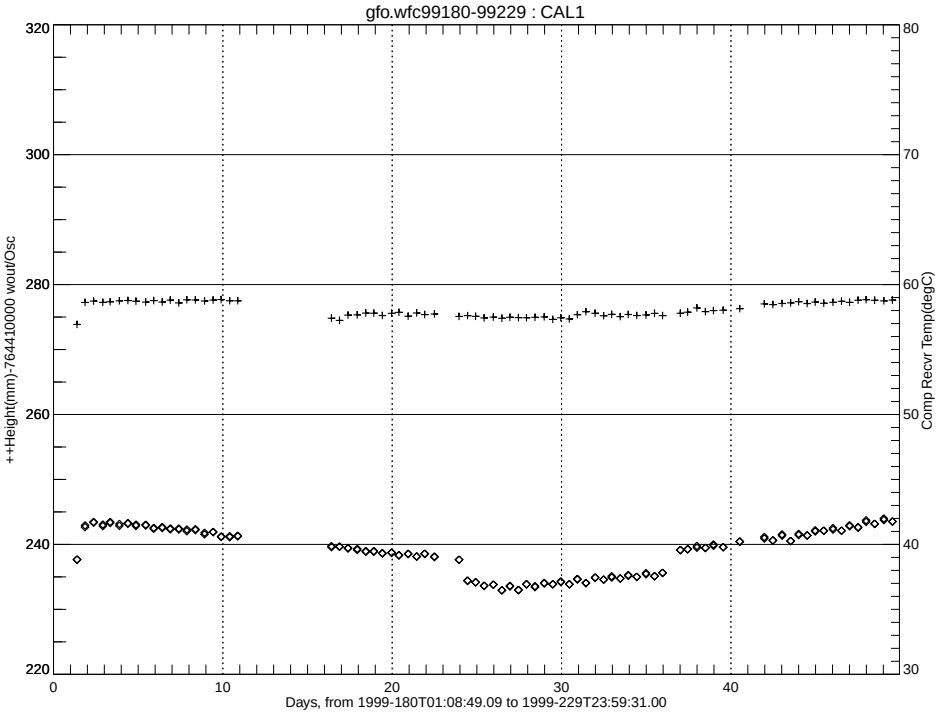

Figure 2-2 Period 1999-180 to 1999-229 Cal 1 Range/Temperature

2.1.1.2.2 Period 2000-122 to 2000-190

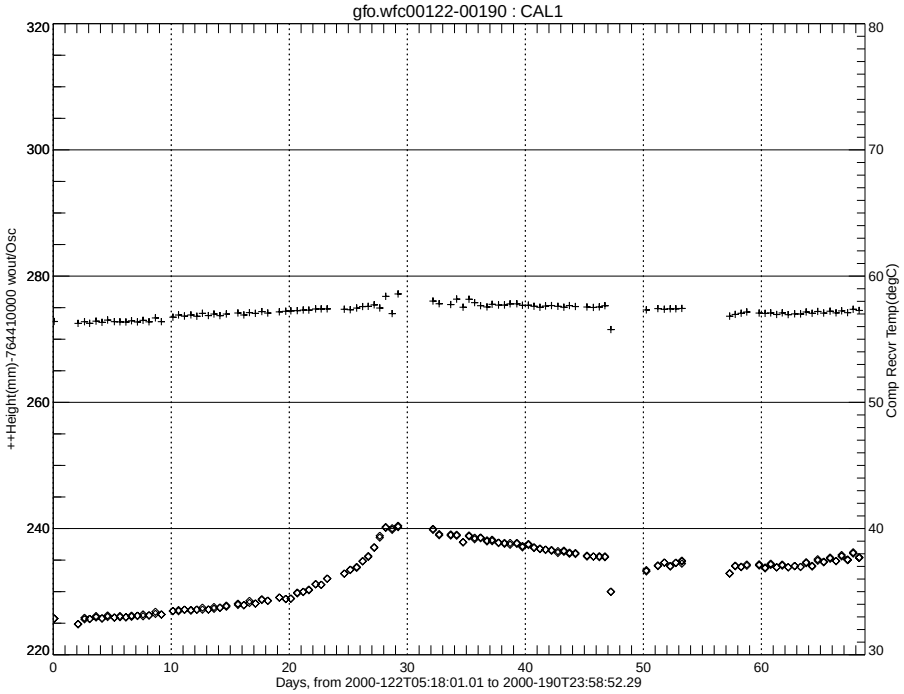

Figure 2-3 Period 2000-122 to 2000-190 Cal 1 Range/Temperature

2.1.1.2.3 Period 2000-243 to 2000-277

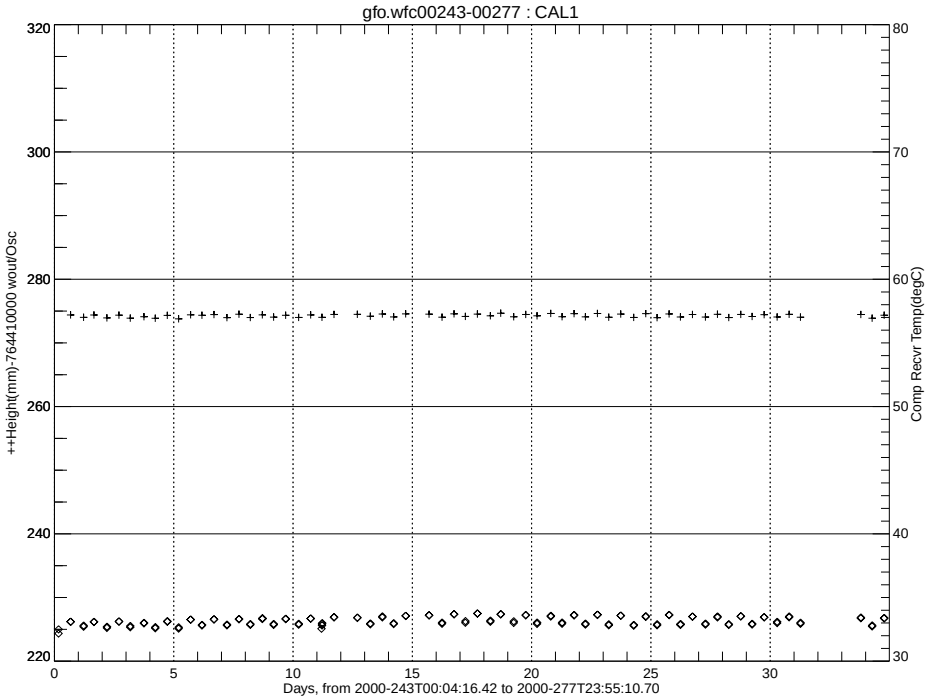

Figure 2-4 Period 2000-243 to 2000-277 Cal 1 Range/Temperature

2.1.2 AGC

2.1.2.1 Launch to Date 1998-133 to 2000-334

The launch-to-date CAL-1 AGCs are shown in Figure 2-5.The AGCs have been routinely temperature-corrected at the GFO processing center using an algorithm (see Section 4.1) derived by Wallops, and have remained in a fairly narrow band of 42.64 + 0.12 dB. Some minor AGC drift is noted, but no further temperature dependency is indicated.

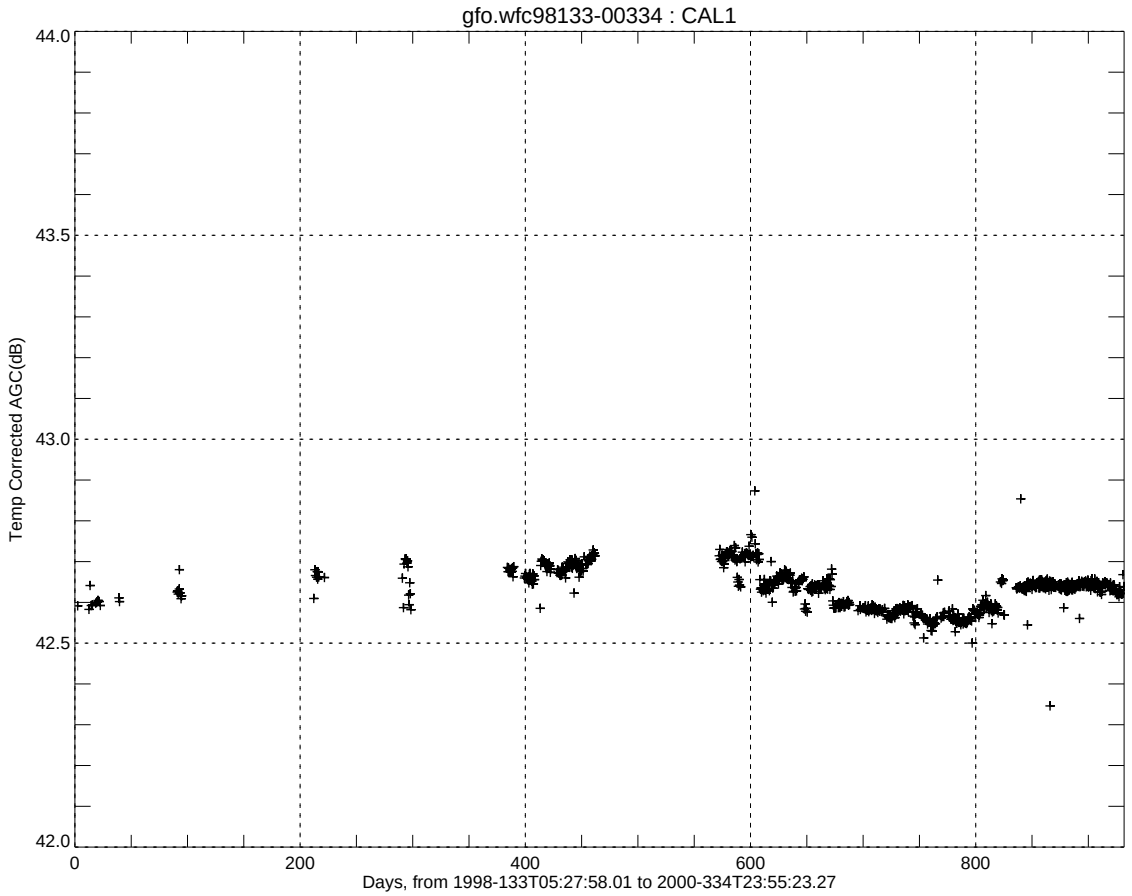

Figure 2-5 Launch-to-Date Cal 1 AGC

The launch-to-date CAL-2 AGCs are shown in Figure 2-6. A CAL-2 residual temperature dependency of ~0.06 dB / deg is evident, although the same processing correction applied in CAL-1 has been applied to the CAL-2 data. The CAL-1 mode is more like the actual tracking mode AGC. The WFF team opinion is that the applied correction is more like a normal system correction that includes the CAL-2 noise. Transmitters and other corrections when combined are different than just CAL-2.

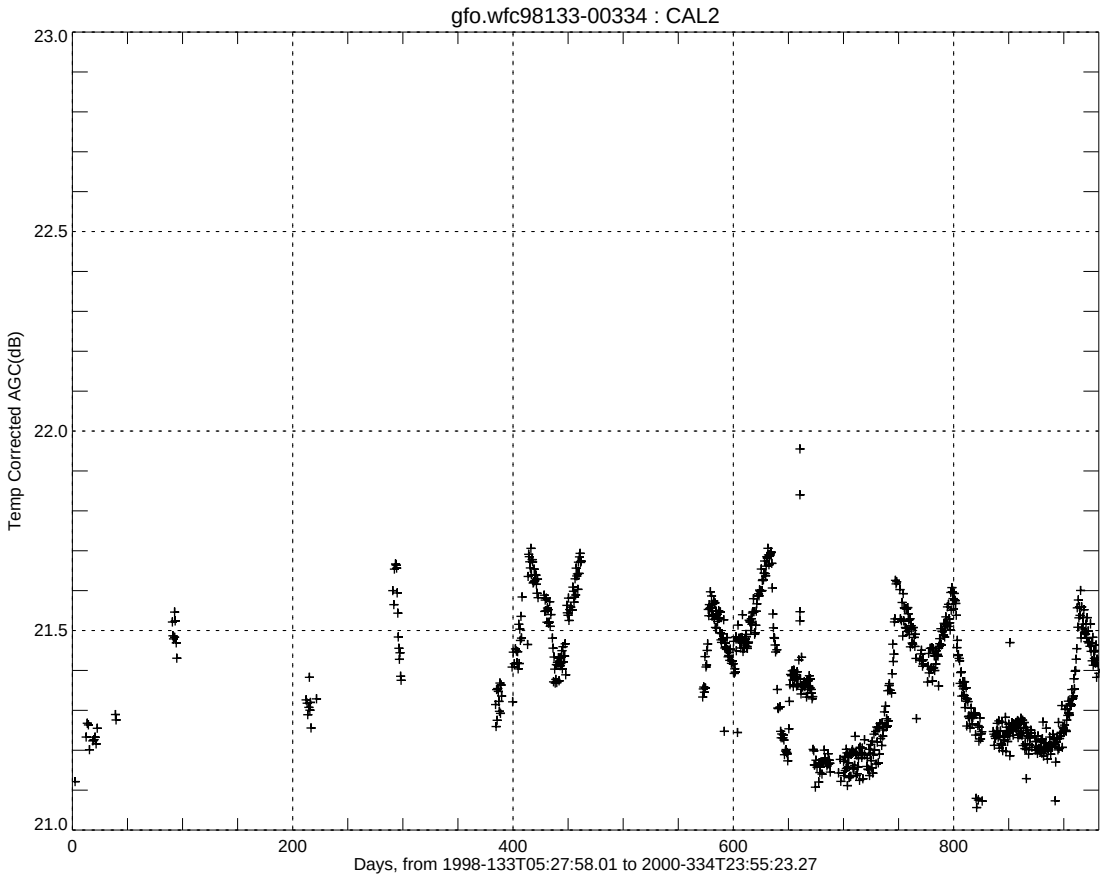

Figure 2-6 Launch-to-Date Cal 2 AGC

2.1.2.2 Cal-Val Periods

The CAL-1 AGC and the CAL-2 AGC for each cal/val periods are shown in Figures 2-7, Figure 2-8, Figure 2-9, Figure 2-10, Figure 2-11 and Figure 2-12, respectively. Similar to the launch-to-date calibration data, the CAL-1 AGC are each in very narrow bands; and the CAL-2 AGC each display some temperature dependency.

2.1.2.2.1 Period 1999-180 to 1999-229

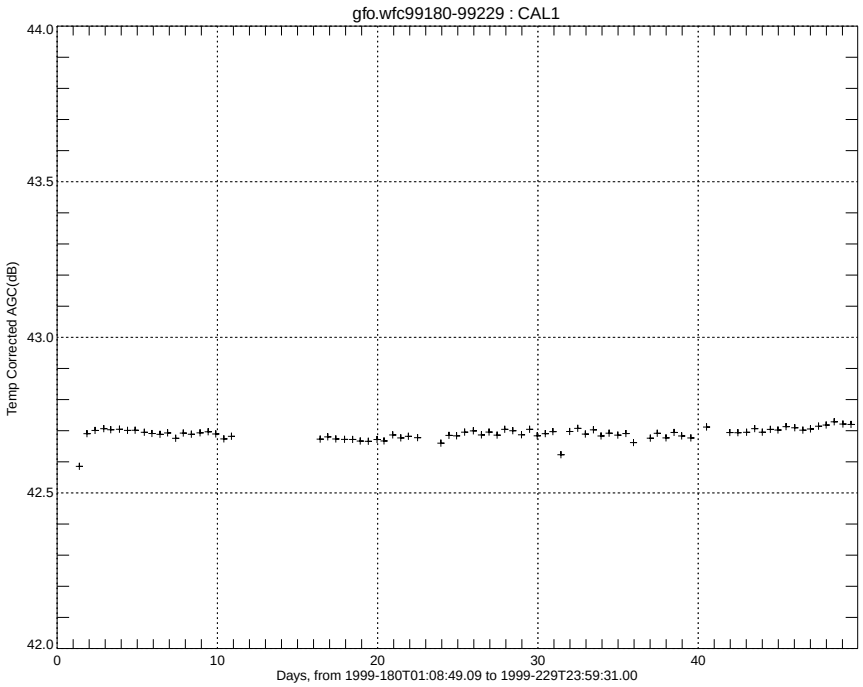

Figure 2-7 Period 1999-180 to 1999-229 Cal 1 AGC

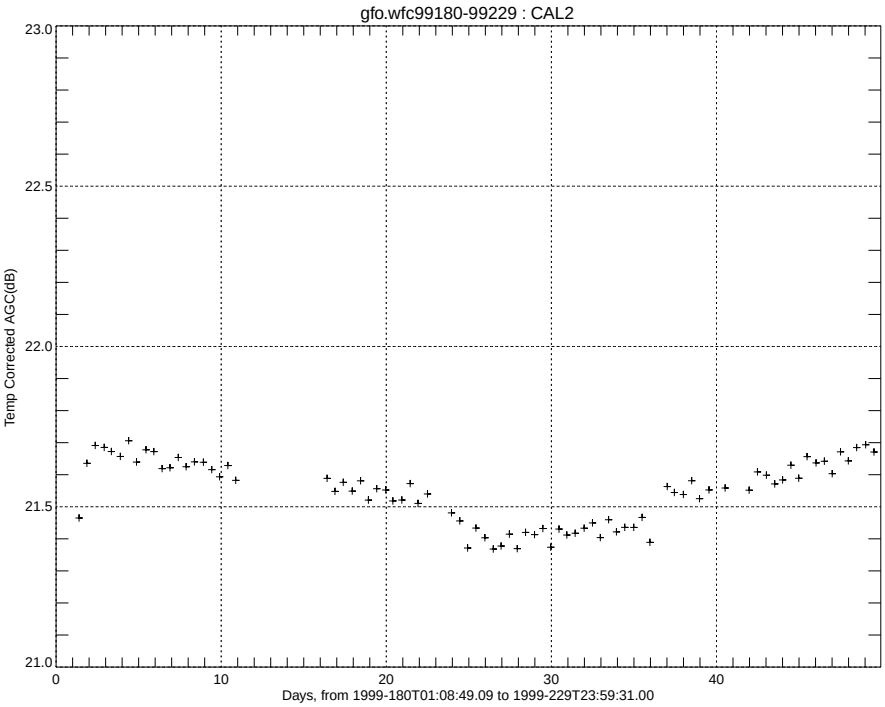

Figure 2-8 Period 1999-180 to 1999-229 Cal 2 AGC

2.1.2.2.2 Period 2000-122 to 2000-190.

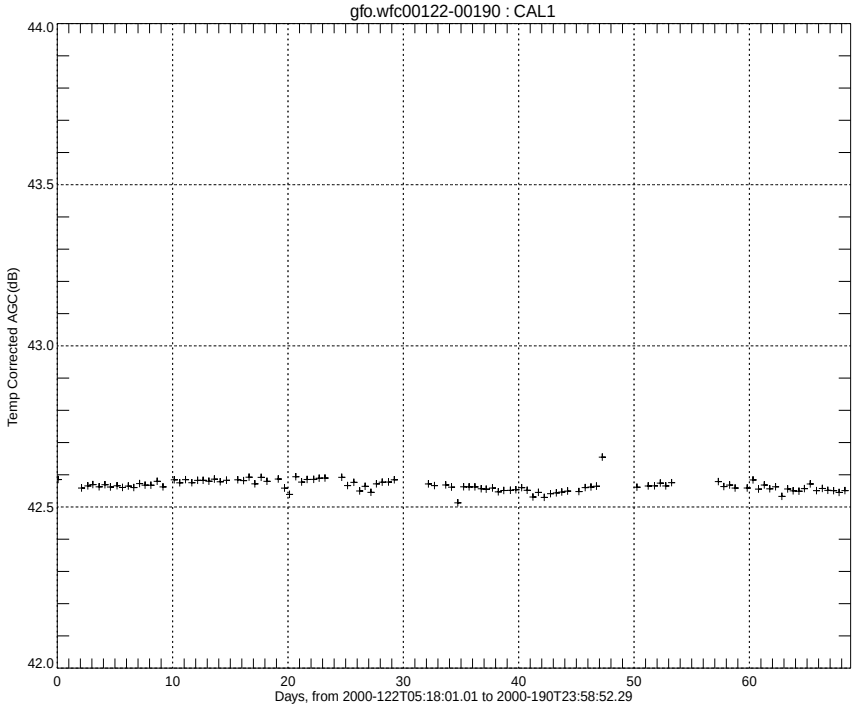

Figure 2-9 Period 2000-122 to 2000-190 Cal 1 AGC

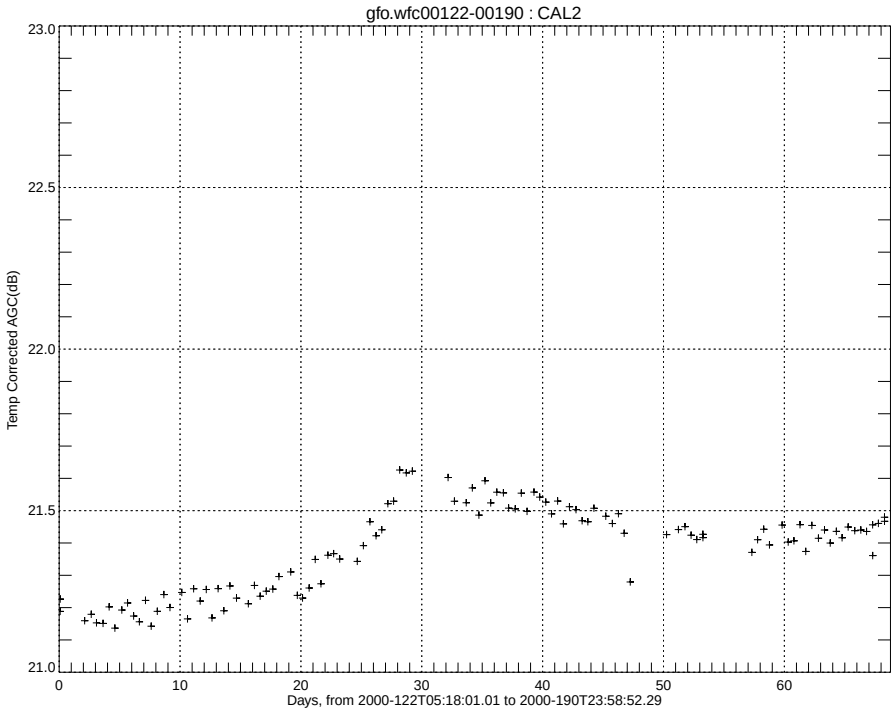

Figure 2-10 Period 2000-122 to 2000-190 Cal 2 AGC

2.1.2.2.3 Period 2000-243 to 2000-277

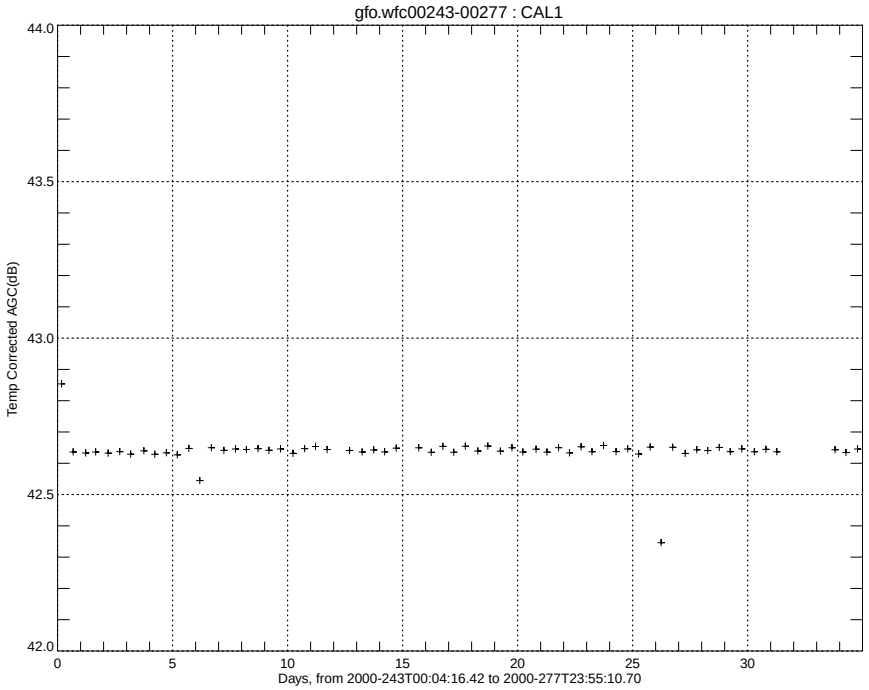

Figure 2-11 Period 2000-243 to 2000-277 Cal 1 AGC

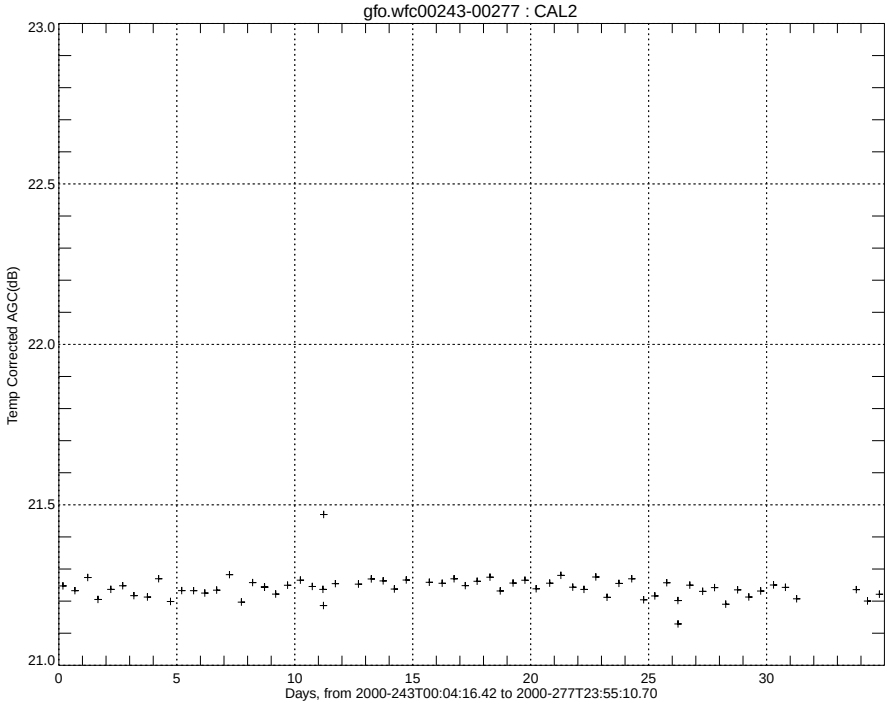

Figure 2-12 Period 2000-243 to 2000-277 Cal 2 AGC

2.2 GFO Cycle (17.05 days) Summaries

Another indication of the GFO altimeter's internal consistency is the agreement of cycle-to-cycle means for: global significant waveheights, sigma-naughts, and wind-speed. For this analysis, the measurements for complete cycles (17.05 days) were meaned, standard deviations were computed, and measurement histograms were produced.

Prior to the computations, the data sets were edited to eliminate suspect measurements. Our edit criteria, using Quality Word #1, are as follows:

- Bit 2: Record is zero-filled
- Bit 3: Altimeter not in Fine Track
- Bit 7: No smoothed VATT
- Bit 10: SWH bounds error
- Bit 18: Off-Nadir error
- Bit 19: SWH standard error
- Bits 22-31: More than 5 frames missing
- Default fill values indicative of bad data

We suggest the use of above criteria by data users for editing the GFO data.

The process by which the cycle summaries were produced involved the following criteria:

- 60 second averaging interval
- $0.2 < SWH < 12.0$
- $-66.0 < Latitude < 66.0$
- $6.0 < Sigma0 < 16.0$
- $45 <$ Numpoints in intervals < 62

All the cycle summaries produced at Wallops so far indicate excellent cycle-to-cycle consistency. Selected cycle summaries are shown in Table 2-1.

Column Definitions for Table 2-1 Cycle Summaries	
Day-of-Year	YYYY-DDDTHH:MM:SSZ YYYY = Year DDD = Jullian day HH = Hour of the day MM = Minute of the day SS = Second of the day Z = Greenwich Mean Time
Number of Data Points Processed	Total number of points processed in the Cycle period used in the Cycle average
Mean SWH	Cycle Average Significant Wave Height
Mean AGC	Cycle Average Automatic Gain Control
Mean Att	Cycle Average Attitude which is calculated from the Off-Nadir Angle
Mean Recvr. Temp.	Cycle Average Receiver Temperature

Table 2-1 Cycle Summaries

Start Day-of-Year	End Day-of-Year	Number of Data Points Processed	Mean SWH (m)	Mean Sigma0 (db)	Mean Att. (deg)	Mean Recvr. Temp. (c)
1999-196T00:11:41Z	1999-212T23:59:27Z	715861	2.608	10.773	0.224	38.035
1999-213T00:03:28Z	1999-229T23:34:50Z	583360	2.501	10.416	0.235	40.290
2000-131T00:01:28Z	2000-147T23:54:52Z	611929	2.676	10.948	0.210	34.753
2000-148T00:32:10Z	2000-164T23:24:42Z	569313	2.494	11.045	0.224	38.570
2000-196T00:03:40Z	2000-212T23:41:53Z	656248	2.519	11.061	0.222	37.971
2000-213T00:03:29Z	2000-229T06:20:20Z	367635	2.644	11.144	0.271	33.709
2000-243T00:01:29Z	2000-259T14:23:31Z	599581	2.485	10.987	0.210	32.913
2000-260T00:01:28Z	2000-277T23:33:42Z	766650	2.594	10.966	0.217	33.070

2.3 GFO Key Events

The key events for the GFO altimeter since its on-orbit turn-on are summarized in Table 2-2. These sensor-related key events are extracted from:

http://gfo.bmpcoe.org/Gfo/Event_Log/gfo_event_log.htm.

Additional key events from a Wallops perspective have been included in the Table.

Table 2-2 GFO Key Events

Event	Date & Time of Event	Comments
Launch	10 Feb 1998 1998041T14:30:00Z	Launched from Vandenberg AFB
Auto Reset	18 Feb 1998 1998049T02:23:00Z	Self-initiated Reset (#1A).
Auto Reset	18 Feb 1998 1998049T02:23:00Z	Self-initiated Reset (#1B). Again.
Auto Reset	23 Feb 1998 1998054T11:24:00Z	Self-initiated Reset (#2).
Auto Reset	28 Feb 1998 1998059T18:24:00Z	Self-initiated Reset (#3.
Auto Reset	05 Mar 1998 1998064T19:08:00Z	Self-initiated Reset (#4).
Auto Reset	11 Mar 1998 1998070T00:50:00Z	Self-initiated Reset (#5). Real time.
Auto Reset	15 Mar 1998 1998074T09:20:00Z	Self-initiated Reset (#6).
Manual Reset	18 Mar 1998 1998077T22:25:00Z	Manual Reset (#7).
Auto Reset	22 Mar 1998 1998081T19:08:00Z	Self-initiated Reset (#8).
Auto Reset	04 Apr 1998 1998094T08:26:00Z	Self-initiated Reset (#9).
Manual Reset	12 Apr 1998 1998102T16:57:00Z	Manual Reset (#10).
Manual Reset	15 Apr 1998 1998105T23:21:00Z	Manual Reset (#11).
Manual Reset	19 Apr 1998 1998109T18:21:00Z	Manual Reset (#12).
Auto Reset	29 Apr 1998 1998119T01:22:00Z	Self-initiated Reset (#13).
Auto Reset	04 May 1998 1998124T03:48:00Z	Self-initiated Reset (#14).
Auto Reset	10 May 1998 1998130T15:45:00Z	Self-initiated Reset (#15).
S/W Change	11 May 1998 1998131T00:00:00Z	Algorithm change - Changed delta_h_init from 796.44002 km to 000.0000 km.
Auto Reset	16 May 1998 1998136T08:01:00Z	Self-initiated Reset (#16).
Manual Reset	21 May 1998 1998141T16:45:00Z	Manual Reset (#17).
Manual Reset	22 May 1998 1998142T04:03:00Z	Manual Reset (#18).
Auto Reset	28 May 1998 1998148T20:58:00Z	Self-initiated Reset (#19).
S/W Change	29 May 1998 1998149T00:00:00Z	Algorithm change - Changed delta_h_init from 000.0000 km to -0.019893 km.

Table 2-2 GFO Key Events (Continued)

Event	Date & Time of Event	Comments
S/W Change	09 Jun 1998 1998160T00:00:00Z	Algorithm change - Changed swh_lower_bound from 0.00 m to 0.01 m.
S/W Change	09 Jun 1998 1998160T00:00:00Z	Algorithm change - Changed swh_upper_bound from 0.00 m to 20.0 m.
S/W Change	10 Jun 1998 1998161T00:00:00Z	Algorithm change - Changed agc_lower_bound from 0.0 dB to 0.1 dB.
S/W Change	10 Jun 1998 1998161T00:00:00Z	Algorithm change - Changed delta_agc_init from 32.0 dB to 33.0 dB.
S/W Change	16 Jun 1998 1998167T00:00:00Z	Algorithm change - Changed delta_h_init from -0.01989 km to 0.020904 km.
S/W Change	16 Jun 1998 1998167T00:00:00Z	Algorithm change - Changed scc.dat file.
Auto Reset	17 Jun 1998 1998168T17:22:00Z	Self-initiated Reset (#20). No data until 08:45Z on 19 Jun (170).
S/W Change	24 Jun 1998 1998175T00:00:00Z	Started flight software upload.
S/W Change	25 Jun 1998 1998176T00:00:00Z	Algorithm change.
Auto Reset	28 Jun 1998 1998179T11:30:00Z	Self-initiated Reset (#21.) No data until 9 July 1998 (190).
S/W Change	30 Jun 1998 1998181T00:00:00Z	Algorithm change - Changed delta_swh_init to time_bias and set to -0.049001 sec.
S/W Change	01 Jul 1998 1998182T00:00:00Z	Algorithm change - Changed ra_time delay to 0.0783488.
S/W Change	01 Jul 1998 1998182T00:00:00Z	To solve sqrt error.
Manual Reset	02 Jul 1998 1998183T20:01:00Z	Manual Reset (#22).
Auto Reset	06 Jul 1998 1998187T21:56:00Z	Self-initiated Reset (#23).
Manual Reset	09 Jul 1998 1998190T21:24:00Z	Manual Reset (#24).
Manual Reset	12 Jul 1998 1998193T21:32:00Z	Manual Reset (#25).
Manual Reset	15 Jul 1998 1998196T21:39:00Z	Manual Reset (#26).
Manual Reset	18 Jul 1998 1998199T21:45:00Z	Manual Reset (#27).
Manual Reset	21 Jul 1998 1998202T21:53:00Z	Manual Reset (#28).
Manual Reset	22 Jul 1998 1998203T21:22:00Z	Manual Reset (#29).
Manual Reset	24 Jul 1998 1998205T21:59:00Z	Manual Reset (#30).
Manual Reset	26 Jul 1998 1998207T20:59:00Z	Manual Reset (#31) Payload off; no data received.
Manual Reset	31 Jul 1998 1998212T21:44:00Z	Manual Reset (#32).
Manual Reset	03 Aug 1998 1998215T21:50:00Z	Manual Reset (#33). Switch to IAP#1.

Table 2-2 GFO Key Events (Continued)

Event	Date & Time of Event	Comments
Manual Reset	04 Aug 1998 1998216T21:20:00Z	Manual Reset (#34). Switch to IAP #2 with Rev. B Code.
S/W Change	04 Aug 1998 1998216T00:00:00Z	Algorithm correction - Changed delta_h_cg from 1.00000 mm to 292.00000 mm.
S/W Change	04 Aug 1998 1998216T00:00:00Z	Algorithm correction - Changed delta_h_init from 0.020904 km to 0.020815 km.
S/W Change	05 Aug 1998 1998217T00:00:00Z	Algorithm correction - Changed RA constant tables.
Payload On	08 Aug 1998 1998220T00:00:00Z	Payloads on.
Auto Reset	16 Aug 1998 1998228T18:13:00Z	Self-initiated Reset (#35). Payloads off.
Manual Reset	19 Aug 1998 1998231T00:04:00Z	Manual CPU Reset (#36). Payloads off.
Payload On	04 Sep 1998 1998247T00:00:00Z	Payloads on.
Auto Reset	10 Sep 1998 1998253T12:20:00Z	Self-initiated Reset (#37).
Auto Reset	15 Sep 1998 1998258T13:46:00Z	Self-initiated Reset (#38).
Maneuver	16 Sep 1998 1998259T00:00:00Z	ERO Maneuver.
Manual Reset	22 Sep 1998 1998265T00:53:00Z	Manual Reset (#39). Switch to IAP#1.
Auto Reset	22 Sep 1998 1998265T02:35:00Z	Self-initiated Reset (#40).
Auto Reset	23 Sep 1998 1998266T01:36:00Z	Self-initiated Reset (#41). AC-2 Fault.
Maneuver	08 Oct 1998 1998281T00:00:00Z	ERO Maneuver.
Auto Reset	09 Oct 1998 1998282T12:20:00Z	Self-initiated Reset (#42).
Auto Reset	19 Oct 1998 1998292T01:36:00Z	Self-initiated Reset (#43).
Manual Reset	19 Oct 1998 1998292T16:33:00Z	Manual Reset (#44). IAP #2 Swap.
S/W Change	20 Oct 1998 1998293T00:00:00Z	Battery charging level changed from VT 4.5 to VT 5.0.
Maneuver	21 Oct 1998 1998294T00:00:00Z	ERO Maneuver.
Manual Reset	28 Oct 1998 1998301T18:35:00Z	Manual Reset (#45).
Manual Reset	04 Nov 1998 1998308T14:56:00Z	Manual Reset (#46) Rev D-1 Flight SW Upload.
Manual Reset	05 Nov 1998 1998309T14:26:00Z	Manual Reset (#47) Rev D-1 Flight SW Upload.
Manual Reset	06 Nov 1998 1998310T13:56:00Z	Manual Reset (#48) Rev D-1 Flight SW Upload.
Manual Reset	07 Nov 1998 1998311T15:03:00Z	Manual Reset (#49) Rev D-1 Flight SW Upload.
Manual Reset	08 Nov 1998 1998312T14:33:00Z	Manual Reset (#50) Rev D-1 Flight SW Upload.
Manual Reset	09 Nov 1998 1998313T15:41:00Z	Manual Reset (#51) Rev D-1 Flight SW Upload.
Manual Reset	10 Nov 1998 1998314T15:10:00Z	Manual Reset (#52) Rev D-1 Flight SW Upload.

Table 2-2 GFO Key Events (Continued)

Event	Date & Time of Event	Comments
Manual Reset	11 Nov 1998 1998315T14:40:00Z	Manual Reset (#53) Rev D-1 Flight SW Upload.
Manual Reset	12 Nov 1998 1998316T15:48:00Z	Manual Reset (#54).
Maneuver	13 Nov 1998 1998317T00:00:00Z	ERO Maneuver.
Powered Down	16 Nov 1998 1998320T18:43:00Z	Manual Reset (#55). Powered down due to onset of Leonid Meteor Swarm.
In Track	20 Nov 1998 1998320T00:00:00Z	RA in Track1. No damage due to Meteors.
Manual Reset	23 Nov 1998 1998327T15:08:00Z	Manual Reset (#56).
Manual Reset	30 Nov 1998 1998334T19:49:00Z	Manual Reset (#57).
Manual Reset	01 Dec 1998 1998335T16:00:00Z	Manual Reset (#58).
Maneuver	02 Dec 1998 1998336T00:00:00Z	ERO Maneuver.
Payload Off	03 Dec 1998 1998337T00:00:00Z	Payload off.
Payload On	05 Dec 1998 1998339T00:00:00Z	Payload on. RA in standby.
Manual Reset	10 Dec 1998 1998344T16:21:00Z	Manual Reset (#59).
Maneuver	12 Dec 1998 1998346T00:00:00Z	ERO Maneuver.
Manual Reset	16 Dec 1998 1998350T18:14:00Z	Manual Reset (#60).
Auto Reset	22 Dec 1998 1998356T10:03:00Z	Self-initiated Reset (#61).
Manual Reset	30 Dec 1998 1998364T19:20:00Z	Manual Reset (#62).
Manual Reset	06 Jan 1999 1999006T19:03:00Z	Manual Reset (#63).
Maneuver	07 Jan 1999 1999007T00:00:00Z	ERO Maneuver.
Manual Reset	13 Jan 1999 1999013T23:43:00Z	Manual Reset (#64).
Payload Off	18 Jan 1999 1999018T00:00:00Z	Payloads off. Transferred operation to Rev. D software.
Manual Reset	19 Jan 1999 1999019T18:57:00Z	Manual Reset (#65). Flight Software Initialization.
Maneuver	21 Jan 1999 1999021T00:00:00Z	ERO Maneuver.
Payload On	21 Jan 1999 1999021T00:00:00Z	Payloads on. RA in standby.
In Track	29 Jan 1999 1999029T00:00:00Z	RA in Track 1.
Battery Test	01 Feb 1999 1999032T00:00:00Z	Battery testing. Data outage 1359Z to 1424Z.
Battery Test	04 Feb 1999 1999035T00:00:00Z	Battery testing. Data outage 1728Z to 1803Z.
Battery Test	11 Feb 1999 1999042T00:00:00Z	Battery testing. Data outage 1850Z to 1925Z.
Maneuver	19 Feb 1999 1999050T00:00:00Z	ERO Maneuver.

Table 2-2 GFO Key Events (Continued)

Event	Date & Time of Event	Comments
Auto Reset	08 Mar 1999 1999067T11:00:00Z	Self-initiated Reset (#66A). Anomaly - Bit stuck on Zero in IAP#2.
Auto Reset	08 Mar 1999 1999067T00:00:00Z	Self-initiated Reset (#66B). Failed to Re-load Rev.D
Auto Reset	08 Mar 1999 1999067T00:00:00Z	Self-initiated Reset (#66C). Successful load Rev.B: EEPROM #1/IAP#1.
Payload On	10 Mar 1999 1999069T00:00:00Z	Payloads on. RA in standby.
In Track	12 Mar 1999 1999071T00:00:00Z	RA in Track 1.
Manual Reset	12 Mar 1999 1999071T23:47:00Z	Manual Reset (#67).
Manual Reset	19 Mar 1999 1999078T17:14:00Z	Manual Reset (#68).
Payload Off	25 Mar 1999 1999084T00:00:00Z	Payloads off.
Manual Reset	25 Mar 1999 1999084T17:26:00Z	Manual Reset (#69). Rev.D-1 Initialization Attempt.
Manual Reset	29 Mar 1999 1999088T16:55:00Z	Manual Reset(#70). Rev.D-1 Initialization Attempt.
Manual Reset	02 Apr 1999 1999092T18:20:00Z	Manual Reset (#71).
Manual Reset	05 Apr 1999 1999095T16:42:00Z	Manual Reset (#72). Rev. D-I Initialization Attempt.
Auto Reset	07 Apr 1999 1999097T04:37:00Z	Self-initiated Reset (#73).
Manual Reset	12 Apr 1999 1999102T19:49:00Z	Manual Reset (#74).
Manual Reset	13 Apr 1999 1999103T19:19:00Z	Manual Reset (#75).
Manual Reset	19 Apr 1999 1999109T16:10:00Z	Manual Reset (#76).
Manual Reset	22 Apr 1999 1999112T17:51:00Z	Manual Reset (#77).
Manual Reset	23 Apr 1999 1999113T01:57:00Z	Manual Reset (#78).
Manual Reset	30 Apr 1999 1999120T17:06:00Z	Manual Reset (#79).
Manual Reset	03 May 1999 1999123T18:50:00Z	Manual Reset (#80A). RAM & EDAC Chip Test.
Manual Reset	03 May 1999 1999123T20:35:00Z	Manual Reset (#80B). RAM & EDAC Chip Test.
Manual Reset	03 May 1999 1999123T20:38:00Z	Manual Reset (#80C). RAM & EDAC Chip Test.
Manual Reset	04 May 1999 1999124T16:41:00Z	Manual Reset (#81A). RAM & EDAC Chip Validation.
Manual Reset	04 May 1999 1999124T18:19:00Z	Manual Reset (#81B). RAM & EDAC Chip Validation.
Manual Reset	04 May 1999 1999124T20:10:00Z	Manual Reset (#81C). RAM & EDAC Chip Validation.

Table 2-2 GFO Key Events (Continued)

Event	Date & Time of Event	Comments
Manual Reset	06 May 1999 1999126T17:21:00Z	Manual Reset (#82). Swap IAP #2 to IAP #1. Note Daily resets with the upload of software to the IAP. Rev D (1) software.
Manual Reset	11 May 1999 1999131T18:07:00Z	Manual Reset (#83).
Manual Reset	12 May 1999 1999132T17:37:00Z	Manual Reset (#84).
Manual Reset	13 May 1999 1999133T18:44:00Z	Manual Reset (#85).
Manual Reset	14 May 1999 1999134T18:14:00Z	Manual Reset (#86).
Manual Reset	15 May 1999 1999135T17:44:00Z	Manual Reset (#87).
Manual Reset	16 May 1999 1999137T18:52:00Z	Manual Reset (#88).
Manual Reset	17 May 1999 1999137T18:22:00Z	Manual Reset (#89).
Manual Reset	19 May 1999 1999139T03:31:00Z	Manual Reset (#90).
Manual Reset	20 May 1999 1999140T18:29:00Z	Manual Reset (#91).
Maneuver	20 May 1999 1999140T00:00:00Z	ERO Maneuver.
RA On	20 May 1999 1999140T00:00:00Z	RA on.
WVR On	22 May 1999 1999142T00:00:00Z	WVR on.
Manual Reset	24 May 1999 1999144T21:25:00Z	Manual Reset (#92A). Rev D (1) on IAP1 & EEPROM #2.
Manual Reset	24 May 1999 1999144T21:25:00Z	Manual Reset (#92B). Rev D (1) on IAP1 & EEPROM #2.
Manual Reset	26 May 1999 1999146T18:41:00Z	Manual Reset (#93). IAP1 to IAP2 SWP.
Manual Reset	08 Jun 1999 1999159T20:16:00Z	Manual Reset (#94). Swap to IAP2, transmitter #2, and Rev. B.
In Track	09 Jun 1999 1999160T00:00:00Z	RA in Track 1. Swap to EEPROM #2 of IAP #1 (Rev D-1).
Manual Reset	10 Jun 1999 1999161T20:00:00Z	Manual Reset (#95).
Maneuver	12 Jun 1999 1999163T00:00:00Z	ERO Maneuver.
In Track	15 Jun 1999 1999166T20:00:00Z	RA in Track 1.
Cal/Val	15 Jun 1999 1999166T00:00:00Z	Began Cal/Val.
Maneuver	24 Jun 1999 1999175T00:00:00Z	ERO Maneuver.
Auto Reset	25 Jun 1999 1999176T04:48:00Z	Self-initiated Reset (#96).
RA On	28 Jun 1999 1999179T00:00:00Z	RA On.
WVR On	28 Jun 1999 1999179T00:00:00Z	WVR On.

Table 2-2 GFO Key Events (Continued)

Event	Date & Time of Event	Comments
Cal/Val	30 Jun 1999 1999181T00:00:00Z	Start of first attempt at Cal/Val.
Data Lost	08 Jul 1999 1999179T00:00:00Z	Lost data from 0124Z to 0139Z.
Auto Reset	10 Jul 1999 1999191T04:48:00Z	Self-initiated Reset (#97).
Manual Reset	14 Jul 1999 1999195T00:00:00Z	Manual Reset (#98). IAP #1 & EEPROM #2 with new BootLoader/VTCW patch.
Manual Reset	21 Jul 1999 1999202T23:05:00Z	Manual Reset (#99).
Manual Reset	28 Jul 1999 1999209T02:42:00Z	Manual Reset (#100).
Manual Reset	04 Aug 1999 1999216T13:38:00Z	Manual Reset (#101).
Maneuver	10 Aug 1999 1999222T01:20:00Z	ERO Maneuver.
Payload	18 Aug 1999 1999230T03:30:00Z	Payload in standby.
H/W Failure	26 Aug 1999 1999238T00:00:00Z	GPSR #4 software upload completed. Receiver locks onto 8 GPS satellites after auto-reboot.
Loses Lock	02 Sep 1999 1999245T02:23:00Z	GPSR #4 loses lock. NOTE: Since 2 Sep. the GPSR locks after being power cycled, but then fails to retain lock for more than 48 hours.
Manual Reset	02 Sep 1999 1999245T15:18:00Z	Manual Reset (#102). IAP#1 - IAP#2, Patched for Failed Bit (Stuck on Zero).
Manual Reset	03 Sep 1999 1999246T01:53:00Z	Manual Reset (#103) EEPROM #2 w/patch, could not go to point per schedule.
Auto Reset	24 Sep 1999 1999267T13:30:00Z	Spontaneous Reset (#104). PCU Fault.
Maneuver	30 Sep 1999 1999273T15:15:00Z	Orbit Adjustment Maneuver.
Auto Reset	05 Oct 1999 1999278T17:44:00Z	Self-initiated Reset (#105).
Commanded	06 Oct 1999 1999279T14:27:00Z	Satellite Commanded to Point.
Manual Reset	14 Oct 1999 1999287T18:38:00Z	Manual Reset (#106). VTCW patch uploaded prior to reset.
Maneuver	16 Oct 1999 1999289T00:30:00Z	Propulsion Maneuver. ERO maintenance.
Auto Reset	16 Oct 1999 1999289T23:25:00Z	Self-initiated Reset (#107). Went to acquire sun mode.
Commanded	17 Oct 1999 1999290T15:33:00Z	Satellite Commanded to Point.
Manual Reset	21 Oct 1999 1999294T18:23:00Z	Manual Reset (#108). Prior to Patch Upload.
In Point	21 Oct 1999 1999294T18:29:00Z	Satellite back in Point.
Manual Reset	22 Oct 1999 1999295T19:28:00Z	Manual Reset (#109).
In Point	22 Oct 1999 1999295T19:35:00Z	Satellite back in Point.

Table 2-2 GFO Key Events (Continued)

Event	Date & Time of Event	Comments
Maneuver	02 Nov 1999 1999306T00:54:00Z	ERO Maintenance Maneuver. 29.76 mm/s with a 0 deg yaw.
Maneuver	16 Nov 1999 1999320T02:01:00Z	ERO Maintenance Maneuver. 35.43 mm/sec.
Manual Reset	17 Nov 1999 1999321T16:06:00Z	Manual Reset (#110). Switch to IAP #1, EEPROM #2.
Manual Reset	18 Nov 1999 1999322T18:52:00Z	Manual Reset (#111A). Part of IAP Update (left in sun orientation for next reset).
Manual Reset	18 Nov 1999 1999322T20:34:00Z	Manual Reset (#111B). Second Reset in series, back to point at 2039Z.
Manual Reset	19 Nov 1999 1999323T18:23:00Z	Manual Reset (#112). Reset to establish IAP #1, Image 2, with Rev Dvl. To point at 18:28Z.
Maneuver	30 Nov 1999 1999334T03:10:00Z	ERO Maintenance Maneuver. 36.03 mm/s with a 0 deg yaw.
Maneuver	10 Dec 1999 1999344T05:20:00Z	ERO Trim Maneuver. 6 mm/s at 180 deg yaw.
Intrusion	17 Dec 1999 1999351T13:46:00Z	Moon Intrusion. Caused nadir attitude error of 0.4 degrees for 1 minute.
Maneuver	20 Dec 1999 1999354T22:10:00Z	ERO Maintenance Maneuver. 33 mm/s at 0 deg yaw.
Auto Reset	25 Dec 1999 1999359T18:58:35Z	Self-initiated reset - “Smile patch” lost. In standby till activated by a Cal, returned to track. Returned to track 25 Dec 1999, 1999359T23:27:40Z.
Maneuver	29 Dec 1999 1999363T07:15:00Z	ERO Trim Maneuver. 3 mm/s at 180 deg yaw.
Manual Reset	06 Jan 2000 2000006T14:29:49Z	In standby till activated by a Cal, returned to track. No data available between 006t04:21 and 006t14:29, patch uploaded during this time. Returned to track 06 Jan 2000, 2000006T23:55:23Z.
Maneuver	17 Jan 2000 2000017T14:45:00Z	ERO Trim Maneuver. 22 mm/s at 0 deg yaw.
Intrusion	17 Jan 2000 2000017T21:40:00Z	Moon Intrusion. Caused nadir attitude error of 0.475 degrees for 10 sec.
Intrusion	18 Jan 2000 2000018T14:58:00Z	Moon Intrusion. Caused nadir attitude error of 0.520 degrees for 10 sec. Note: The three events on 17, 18 Jan that did not cause the satellite to exceed 0.27 deg.
Maneuver	13 Feb 2000 2000044T13:35:00Z	ERO Maintenance Maneuver.
Configure	23 Feb 2000 2000054T17:29:00Z	Reconfiguration. Both Horizon Scanners Selected.
Maneuver	07 Mar 2000 2000067T01:35:00Z	ERO Maintenance Maneuver. 27 mm/sec at 0 deg yaw.

Table 2-2 GFO Key Events (Continued)

Event	Date & Time of Event	Comments
Maneuver	21 Mar 2000 2000081T12:45:00Z	ERO Maintenance Maneuver. 36 mm/sec at 0 deg yaw.
Maneuver	01 Apr 2000 2000092T00:18:00Z	ERO Maintenance Maneuver. 36 mm/sec at 0 deg yaw.
Maneuver	08 Apr 2000 2000099T00:01:00Z	ERO Maintenance Maneuver. 4 mm/sec at 0 deg yaw.
Maneuver	08 Apr 2000 2000099T01:41:00Z	ERO Maintenance Maneuver. 20 mm/sec at 0 deg yaw.
Maneuver	19 Apr 2000 2000110T01:01:00Z	ERO Maintenance Maneuver.
Maneuver	19 Apr 2000 2000110T02:41:00Z	ERO Maintenance Maneuver. Net result of two maneuvers on 19 Apr, is 42 mm/sec at 0 deg yaw.
Reconfigure	01 May 2000 2000122T20:40:00Z	Reconfiguration. Switch IAPs, Satellite out of point.
Reconfigure	01 May 2000 2000122T22:30:00Z	Reconfiguration. Satellite back in point.
ERO	04 May 2000 2000125T04:00:00Z	Satellite back in ERO.
Maneuver	11 May 2000 2000132T16:25:00Z	ERO Maintenance Maneuver. 35 mm/sec at 0 deg yaw.
Maneuver	24 May 2000 2000145T04:48:00Z	ERO Maintenance Maneuver. 25 mm/sec at 0 deg yaw.
Maneuver	16 Jun 2000 2000168T06:15:00Z	ERO Maintenance Maneuver. 18 mm/sec at 0 deg yaw.
Auto Reset	17 Jun 2000 2000169T03:10:53Z	Self-initiated reset - patch lost. In standby till activated by a Cal, returned to track. Returned to track 17 Jun 2000, 2000169T11:12:13Z.
Auto Reset	17 Jun 2000 2000169T18:59:31Z	Self-initiated reset - patch lost. Returned to track 20 Jun 2000, 2000172T00:00:00Z.
Trim Burn	23 Jun 2000 2000175T06:23:00Z	Reduce Eccentricity and Argument of Perigee. 135mm/sec at 180 deg yaw.
Trim Burn	23 Jun 2000 2000175T07:28:00Z	Reduce Eccentricity and Argument of Perigee. 135mm/sec at 0 deg yaw.
Trim Burn	24 Jun 2000 2000176T00:00:00Z	Replay of above. Second burn in the series completed.
Trim Burn	28 Jun 2000 2000180T02:29:00Z	ERO Trim Burn. 24 mm/sec at 180 deg yaw.
Trim Burn	20 Jul 2000 2000202T12:54:00Z	ERO Trim Burn. 24 mm/sec at 0 deg yaw.
Trim Burn	04 Aug 2000 2000217T05:00:00Z	ERO Trim Burn and Raise SMA. 15 mm/sec at 0 deg yaw.

Table 2-2 GFO Key Events (Continued)

Event	Date & Time of Event	Comments
Auto Reset	10 Aug 2000 2000223T11:35:42Z	Self-initiated reset - patch lost. Time of reset is approximate due to no data available between 223t06:45 and 223t11:35. In standby till activated by a Cal to return to track. Returned to track 10 Aug 2000, 2000223T14:57:46Z.
Auto Reset	10 Aug 2000 2000223T22:52:57Z	Second reset - still no patch. In standby till activated by a Cal, returned to track. Returned to track 10 Aug 2000 2000224T02:21:30Z.
Manual Reset	11 Aug 2000 2000224T15:47:00Z	Commanded power cycle of the RA and upload of patch. Patch still not installed. Time of reset is approximate due to no data available between 224t11:51 and 224t15:47.
Auto Reset	12 Aug 2000 2000225T09:00:36Z	Self-initiated reset - no patch. In standby till activated by a Cal. Returned to track 12 Aug 2000, 2000225T15:36:07Z.
Manual Reset	14 Aug 2000 2000227T15:44:29Z	In standby. Power cycled and patch uploaded. Returned to track 14 Aug 2000, 2000227T17:30:16Z.
Auto Reset	16 Aug 2000 2000229T01:04:10Z	In Standby till activated by a Cal. Returned to track 16 Aug 2000, 2000229T03:06:15Z.
Auto Reset	20 Aug 2000 2000233T04:45:51Z	Spontaneous reset. In standby. Returned to track without a CAL 20 Aug 2000, 2000233T06:37:23Z .
Manual Reset	20 Aug 2000 2000233T08:52:00Z	RA power cycle to get RA back in track and s/w patch reloaded. Data variables have constant values up to day 2000235t18:20.
RA Turned Off	22 Aug 2000 2000235T18:20:00Z	Current indications from telemetry are that the receiver power monitor flag is indicating failed and the temperatures are higher than expected.
RA Turned On	23 Aug 2000 2000236T03:22:36Z	RA and WVR turned on, patch loaded and RA put in track.
Trim Burn	24 Aug 2000 2000237T04:33:00Z	ERO Trim Burn. 22.8 mm/sec at 0 deg yaw.
Trim Burn	14 Sep 2000 2000258T18:45:00Z	ERO Trim Burn. 28.7 mm/sec at 0 deg yaw.
Trim Burn	29 Sep 2000 2000273T00:53:00Z	ERO Trim Burn to Raise SMA. 31.8 mm/sec at 0 deg yaw.
Trim Burn	09 Oct 2000 2000283T12:28:00Z	ERO Trim Burn. 36 mm/sec at 0 deg yaw.
Auto Reset	20 Oct 2000 2000294T23:30:09Z	Self-initiated reset - Loss of patch. In standby till activated by a Cal. Returned to track 21 Oct 2000, 2000295T09:00:11Z. Patch was not restored.
Manual Reset	21 Oct 2000 2000295T11:11:29Z	Power cycled and patch uploaded. Returned to track 21 Oct 2000, 2000295T11:17:18Z.

Table 2-2 GFO Key Events (Continued)

Event	Date & Time of Event	Comments
Trim Burn	26 Oct 2000 2000300T03:40:00Z	ERO Trim Burn. 39.2 mm/sec at 0 deg yaw.
Trim Burn	08 Nov 2000 2000313T03:43:00Z	ERO Trim Burn. 36 mm/sec at 0 deg yaw.
Trim Burn	22 Nov 2000 2000327T04:47:00Z	ERO Trim Burn. 17.4 mm/sec at 0 deg yaw. Purpose is to raise the SMA and maintain the ERO.
Acceptance	29 Nov 2000 2000334T00:00:00Z	GFO Acceptance. SPAWAR authorizes DD250s.

Section 3

Assessment of Instrument Performance

In addition to assessing the altimeter's internal measurement consistency, Wallops has also been comparing the GFO results with other spaceborne ocean sensors, and has been examining the altimeter's waveforms.

The following sections report several assessments performed by the WFF GFO team. In some cases, the same parameter was analyzed with different methods and there are some variations in the exact performance estimates that have not been fully explained; however, the results seem to be consistent with each other. All analysis indicates the altimeter instrument is performing within specification.

Section 3.1 addresses the range noise performance. Sections 3.2, 3.4, and 3.5 address the sigma naught parameter and its related wind speed estimates using two different methods. Sections 3.3 and 3.5 address SWH. Section 3.6 describes the SWH and range results of GFO waveform fitting. Sections 3.7 and 3.8 discuss GFO range and SWH estimation consequences of a "smile patch" and of thermal changes. Section 3.9 describes the effects of "sigma0 blooms" in the GFO altimeter data. Early in our GFO altimeter assessment, we studied the acquisition time to provide good data from non-normal tracking and found that the 5 second specification was being met and that GFO over land was tracking and acquiring surfaces better then GEOSAT or TOPEX. We plan to report more details on this in a later report.

3.1 Range Measurement Noise

On behalf of Wallops, Mavis Driscoll and Richard Sailor (both of TASC) have determined the range measurement noise for the GFO altimeter. Driscoll and Sailor (personal communication) employed the same noise determination techniques as they had for all other satellite altimeter mission data.

Their technique is based on observing the noisy time series obtained by differencing repeat tracks to cancel out the geoid. Spectral estimation is then applied to the difference time series, showing 'colored' noise due to oceanography plus a 'white noise floor' due to the sought-after altimeter instrument noise. The rms white noise level is obtained by integrating, from -0.5 to +0.5 Hz, the noise under the noise floor.

Data from 17 pairs of open-ocean repeat GFO groundtracks over a variety of sea states and a variety of geoid signatures were used in the study. The duration of each pair of repeating groundtracks was about eight minutes. Data were edited to remove a few spikes per arc. The resultant estimates of spectra compare very favorably with other satellite altimeter results, as depicted in Figure 3-1 "Noise in Altimetry - Spectra Derived by Differencing Repeat Tracks".

The GFO noise estimates, plotted versus SWH, are shown in Figure 3-2 "GFO Noise Level". For a typical SWH of 2.0 m, the altimeter noise level is observed to be about 2.6 cm.

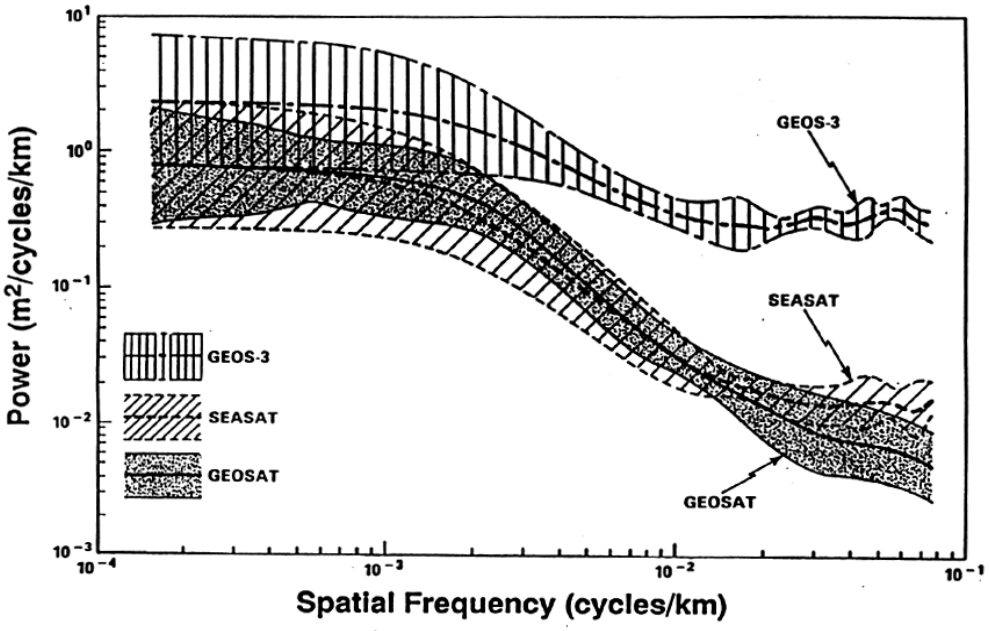

Figure 3-1 Noise in Altimetry - Spectra Derived by Differencing Repeat Tracks

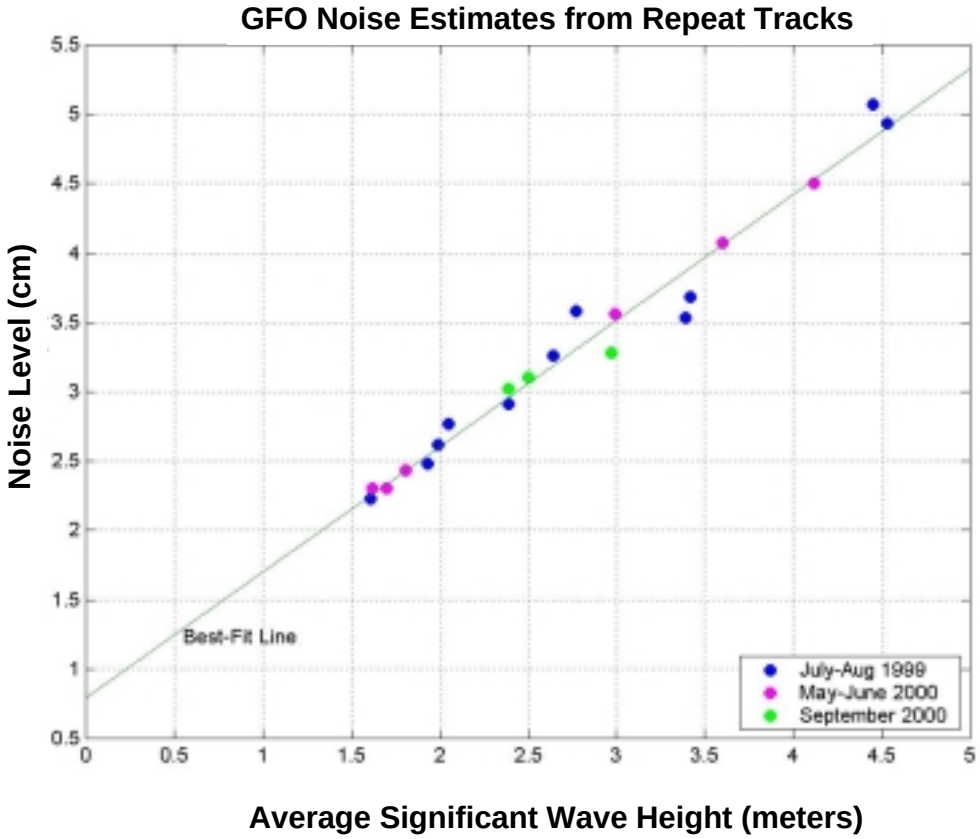

Figure 3-2 GFO Noise Level

3.2 GFO Sigma Naught Comparison with TOPEX

One of the quantities estimated by a spaceborne radar altimeter is the ocean surface's radar backscattering cross-section. For typographical convenience, this quantity is often referred to as sigma0, sigma naught, or sigma-naught. We will try to use sigma0 throughout this report.

Wallops has compared GFO Sigma0 with TOPEX Ku-Band Sigma0 over concurrent time periods. This was accomplished by averaging global GFO sigma0 over 10-day periods, corresponding to TOPEX 10-day cycles. Since GFO is in a 17 day repeat cycle and TOPEX a 10 day repeat cycle, an approximate 10 day set of GFO data was made using the same start and end time boundaries as the TOPEX cycle.

The TOPEX data, prior to the cycle averaging, were edited, using 60 second averages, to remove any data with Sigma0 > 16.0 dB and Off-nadir > 0.12 deg.

The GFO data, prior to the cycle averaging, were edited, using 60 second averages, to remove any data with Sigma0 > 16.0dB and SWH > 12.0m, and were truncated to delete measurements beyond +/- 66 degrees latitude so as to match TOPEX's latitude coverage.

The results of the Sigma0 comparisons, for 15 TOPEX cycles, are listed in Table 3-1 "Comparison of GFO and TOPEX (Ku) Sigma0 Means for 10-Day TOPEX Cycles".

Table 3-1 Comparison of GFO and TOPEX (Ku) Sigma0 Means for 10-Day TOPEX Cycles

TOPEX Cycle Number	Start Day-of-Year	End Day-of-Year	GFO Number of Data Points Processed	TOPEX Number of Data Points Processed	GFO Mean Sigma0 (dB)	TOPEX Ku Mean Sigma0 (dB)	Delta Sigma0 (dB) GFO-TOPEX
252	1999-198t23:28	1999-208t21:25	413683	331139	10.77	11.11	-0.34
253	1999-208t21:26	1999-218t19:24	358801	333620	10.96	11.20	-0.24
254	1999-218t19:25	1999-228t17:22	392855	331624	10.24	11.14	-0.90
281	2000-121t12:45	2000-131t10:42	347018	369181	10.87	11.02	-0.15
282	2000-131t10:43	2000-141t08:40	367795	360068	10.85	10.98	-0.13
283	2000-141t08:42	2000-151t06:43	344198	349607	11.07	11.14	-0.07
284	2000-151t06:44	2000-161t04:40	300143	349022	11.06	11.09	-0.03
285	2000-161t04:41	2000-171t02:45	284381	349171	10.96	11.03	-0.07
286	2000-171t02:46	2000-181t00:35	142788	342918	10.99	11.09	-0.10
287	2000-181t00:36	2000-190t22:40	384752	342273	10.98	11.10	-0.12
293	2000-240t12:27	2000-250t10:25	369654	328836	11.03	11.11	-0.08
294	2000-250t10:26	2000-260t08:23	384319	328926	10.94	11.07	-0.13

Table 3-1 Comparison of GFO and TOPEX (Ku) Sigma0 Means for 10-Day TOPEX Cycles (Continued)

TOPEX Cycle Number	Start Day-of-Year	End Day-of-Year	GFO Number of Data Points Processed	TOPEX Number of Data Points Processed	GFO Mean Sigma0 (dB)	TOPEX Ku Mean Sigma0 (dB)	Delta Sigma0 (dB) GFO-TOPEX
295	2000-260t08:24	2000-270t06:22	415464	315313	10.99	11.13	-0.14
296	2000-270t06:23	2000-280t04:20	431374	326753	10.94	11.08	-0.14
297	2000-280t04:21	2000-290t02:20	412300	334559	10.90	11.06	-0.16

The Table headings are, left-to-right: the TOPEX cycle number, the start date/time and the end date/time for the cycle, the number of GFO data points averaged, the number of TOPEX data points averaged, the GFO mean sigma0 in dB, the TOPEX mean sigma0 in dB, and the sigma0 difference (GFO minus TOPEX) in dB.

While the sigma0 differences are generally small, that was not the case for the first three listed TOPEX cycles (cycles 252-254) in Table 3-1. At the time, in late-1999, when these rather large differences were initially noted, Wallops sought the reason. We determined that the sign of the temperature correction to AGC during GFO routine processing needed to be reversed, and that the temperature correction coefficient needed to be modified. We notified the GFO project of our findings, and they instituted the changes (see Section 4.1).

The 12 subsequent sigma0 differences in Table 3-1 are indicative of the GFO sigma0 improvement resulting from the change in the temperature correction algorithm. The combined cycle 281-287 grouping and the cycle 293-297 grouping have a mean difference with respect to TOPEX of -0.11dB. Figure 3-3 "Comparison of GFO and TOPEX Sigma0" provides a plot, for the ten-day periods, of GFO sigma0 versus TOPEX sigma0.

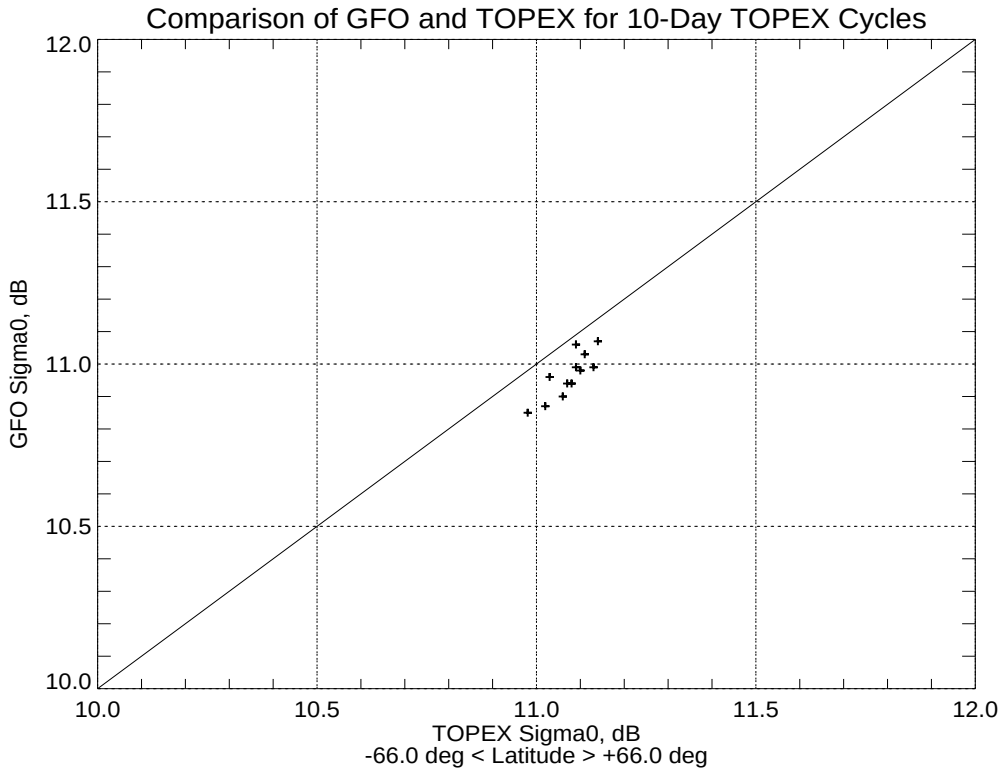

Figure 3-3 Comparison of GFO and TOPEX Sigma0

3.3 GFO SWH Comparison of GFO and TOPEX

Using the same 15 10-day cycles as for the sigma0 comparison, Wallops has compared the GFO significant waveheight (SWH) with TOPEX Ku-Band SWH. The SWH comparison results are tabulated in Table 3-2 "Comparison of GFO and TOPEX (Ku) SWH Means for 10-Day TOPEX Cycles". The Delta SWH (GFO minus TOPEX) in meters is listed in the rightmost column in the table.

Table 3-2 Comparison of GFO and TOPEX (Ku) SWH Means for 10-Day TOPEX Cycles

TOPEX Cycle Number	Start Day-of-Year	End Day-of-Year	GFO Number of Data Points Processed	TOPEX Number of Data Points Processed	GFO Mean SWH (m)	TOPEX Ku Mean SWH (m)	Delta SWH(m) GFO-TOPEX
252	1999-198t23:28	1999-208t21:25	413683	331139	2.59	2.91	-0.32
253	1999-208t21:26	1999-218t19:24	358801	333620	2.53	2.81	-0.28
254	1999-218t19:25	1999-228t17:22	392855	331624	2.54	2.86	-0.32
281	2000-121t12:45	2000-131t10:42	347018	369181	2.62	3.00	-0.38
282	2000-131t10:43	2000-141t08:40	367795	360068	2.80	3.17	-0.37
283	2000-141t08:42	2000-151t06:43	344198	349607	2.49	2.78	-0.29
284	2000-151t06:44	2000-161t04:40	300143	349022	2.52	2.88	-0.36
285	2000-161t04:41	2000-171t02:45	284381	349171	2.52	2.87	-0.35
286	2000-171t02:46	2000-181t00:35	142788	342918	2.61	2.88	-0.27
287	2000-181t00:36	2000-190t22:40	384752	342273	2.51	2.79	-0.28
293	2000-240t12:27	2000-250t10:25	369654	328836	2.45	2.76	-0.31
294	2000-250t10:26	2000-260t08:23	384319	328926	2.52	2.81	-0.29
295	2000-260t08:24	2000-270t06:22	415464	315313	2.55	2.85	-0.30
296	2000-270t06:23	2000-280t04:20	431374	326753	2.63	2.94	-0.31
297	2000-280t04:21	2000-290t02:20	412300	334559	2.56	2.82	-0.26

With respect to TOPEX, the mean GFO SWH delta is -0.31m. The consistency of the delta for a variety of seastates is depicted in Figure 3-4 "Comparison of GFO and TOPEX SWH".

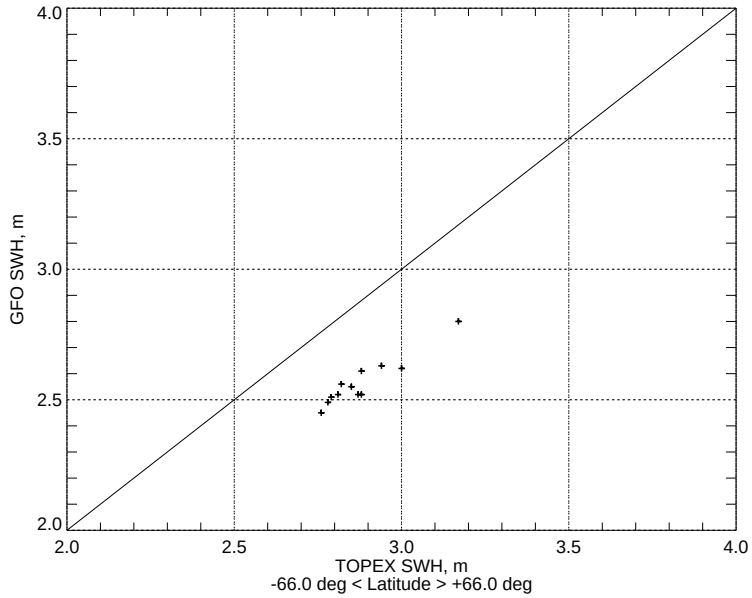

Figure 3-4 Comparison of GFO and TOPEX SWH

3.4 Wind Speeds

A wind speed comparison study has been carried out between the GFO altimeter and the SeaWinds scatterometer on board the NASA QuikSCAT satellite (QSCAT). For each GFO measurement, the closest scatterometer footprint is selected whenever it is within 25 km and within 60 min of the GFO location. Due to various orbit characteristics, geographical distributions of data are very different from one sensor to the other. The phasing is such that all the collocated data are at high latitudes, above 50 degrees, during the period of 17 days from 3 May 2000 to 19 May 2000 (Figure 3-5). Figure 3-6 presents the comparison between the GFO and QSCAT wind speeds. The GFO wind speeds are generally larger than the QSCAT ones. The bin-averaged data in Figure 3-7, computed by filtering the outliers, show a difference between the two sources of about 2 m/s in the wind speed range from 5 to 12 m/s.

Due to the limitations of the number of crossovers between GFO and QSCAT, and their locations at latitudes above 50 degrees which cannot give a good representation of the wind speed distribution over the entire globe, we additionally chose to collocate GFO data with interpolated surface model winds from the National Centers for Environmental Prediction (NCEP). By then reproducing the same procedure with the TOPEX altimeter data, we are able to compare the two altimeters using the same meteorological wind speed reference. Our comparison study leading to GFO altimeter sigma0 and significant wave height calibration correction with respect to TOPEX

measurements is enclosed in this document as Appendix A, and is further addressed in Section 3.5.

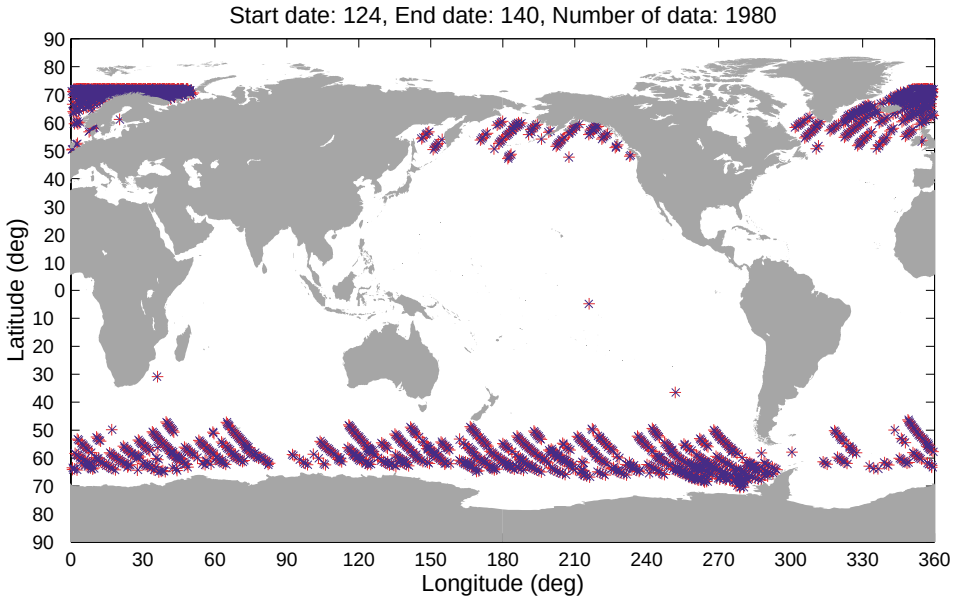

Figure 3-5 Distribution of Open Ocean Collected Data

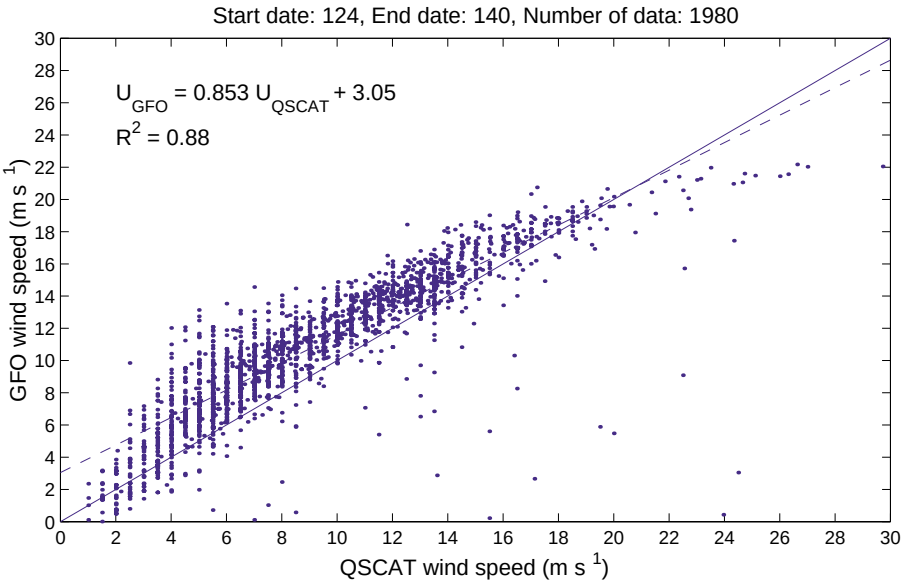

Figure 3-6 Comparison Between GFO and QSCAT Wind Speeds

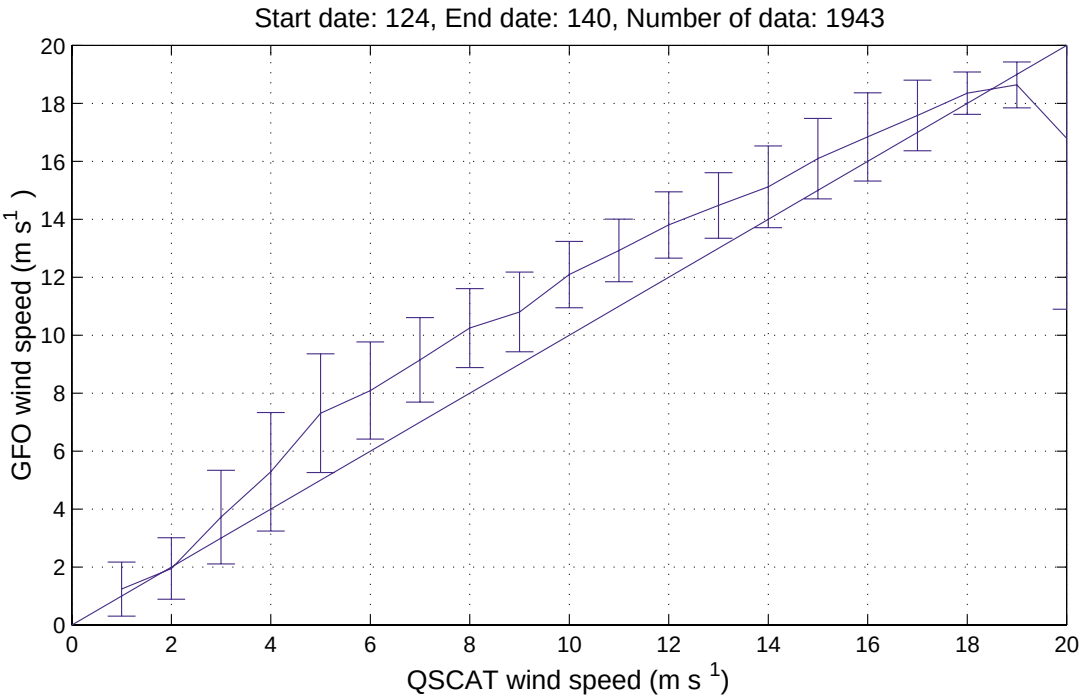

Figure 3-7 Standard Deviation Comparison Between GFO and QSCAT Wind Speeds

3.5 GFO Sigma0 and SWH Calibration Correction

The study in this report's Appendix A used NCEP as an intermediate reference for comparison of the GFO and TOPEX sigma0 and SWH. This study showed that the GFO cross-section values are biased about 0.37 dB lower than the TOPEX cross-section, and the GFO significant wave height values are biased about 0.24 m lower than the TOPEX significant waveheight. Attachment A ("GFO altimeter sigma0 and SWH calibration correction," by Tran, et al) describes how these GFO calibration corrections were generated, and recommends these additive contributions to both the GFO cross-section and significant waveheight to improve the wind speed retrieval.

The correction to GFO sigma0 leads to statistically significant global error reductions for the GFO windspeed. The overall bias between GFO and NCEP windspeeds decreases from 1.75 m/s to 0.53 m/s, and the root-mean-square (rms) error decreases from 2.44 m/s to 1.59 m/s with the operational algorithm.

3.5.1 Implementation

The recommendation for the Sigma0 correction was implemented in the Payload Operations Center (POC) Systems effective 7 December 2000. The first ngdr dataset with the "AGC_CALIBRATION_BIAS = -0.370000" was 2000342_00835_86399.

3.6 Waveform Fitting in GFO Data

This section will describe results from waveform fitting to 1-second averages of GFO waveform data but first will examine typical GFO Calibration Mode 1 and Calibration Mode 2 waveform data. The first thing to do is to verify that the GFO point-target response, in effect the transmitted pulse shape as observed by the altimeter's receiver, has the expected sinc^2 shape, where sinc x = (sin x) / x. The GFO Calibration Mode 1 samples the point-target response at the fundamental altimeter sample spacing of 3.125 nanoseconds, and Figure 3-8 shows the 2000 day 147 Cal Mode 1 waveform samples and a least-squares fit of a sinc^2 function to those waveform samples. The vertical axis of the upper plot in Figure 3-8 is in waveform amplitude counts which is proportional to power. Only the first several sidelobes of the actual Cal Mode 1 waveform data are plotted in these figures, because the rest of the values have no meaning as a result of the finite resolution of the 8-bit resolution of the individual GFO waveform samples. The lower plot of Figure 3-8 shows the same data as the upper plot except that the vertical axis is in dB relative to the peak value of the sinc^2 fit. These results indicate that the actual point-target response is a very good approximation to the theoretical sinc^2 shape.

In the GFO Calibration Mode 2 the waveform samplers look at receiver thermal noise only, with no signal from the transmitter. Ideally the noise spectrum should be flat and the Cal Mode 2 observed amplitude would be the same in each of the GFO altimeter's 128 on-board waveform samples. The upper plot of Figure 3-9 shows the waveform samples from a typical GFO Cal Mode 2 waveform on 2000 day 147, together with the individual sample standard deviation. The lower plot of Figure 3-9 shows the individual sample waveform gain adjustments derived from the data of the upper plot and from the assumption that upper plot should have been completely flat. Notice that the gain adjustments from Cal Mode 2 are only of the order of a couple of tenths of a percent, extremely small corrections in a practical sense.

As the Cal Mode 1 and Cal Mode 2 results indicated adequacy of a sinc^2 model for the point-target response and flatness of the waveform sampler relative response, we assembled a set of GFO over-ocean waveform sample 1-second averages for portions of 2000 days 124, 134, 137, and 150. These data were edited to be over deep water only, in latitudes where no ice could be present, and the average waveforms were then least-squares fitted by a zero-skewness waveform model having five variable fit parameters: amplitude, delta range, SWH, noise baseline, and attitude angle. The fit results were edited to remove obvious bad fits, and we were left with about 170 minutes of 1-second fit results. Figure 3-10 shows typical fit results for the 1-second waveform averages: one example is at relatively low SWH and the other example is at relatively high SWH.

The second of the five fit parameters, the delta range, indicates how far the fitted model waveform is away from the altimeter's track point (the track point is sample 32.5 of the waveform sample set numbered 1 - 128). This waveform fit delta range will be a function of attitude angle and SWH; in fact it should agree with the attitude / SWH range correction in the GFO data processing if the GFO attitude / SWH range correction is correctly implemented. The attitude / SWH range correction is dif-

ferent for the five different gate index values in the GFO tracker. Gate index 1 occurs for the lowest SWH values and gate index 5 for the highest, but most of the GFO over-ocean operation will use gate index values 2 or 3. Figure 3-11 and Figure 3-12 show the differences between the waveform fit delta range and the GFO attitude / SWH range correction as a function of the GFO SWH, in separate plots for the four separate gate index values in our trial waveform data set. There were no gate index 5 values in the data. As indicated in the legends on the plots in Figure 3-11 and Figure 3-12, the waveform fit delta range and the GFO attitude / SWH range correction agreed on average to a couple of centimeters or so. The errors in the comparison could presumably be driven down by comparing a lot more data, but we think that Figure 3-11 and Figure 3-12 indicate that the GFO attitude / SWH range correction is performing well within the needs of the GFO mission.

Figure 3-13 compares the waveform fit attitude angle estimates with those from the GFO SDR (or NGDR). The 1-second waveform fit attitude estimates are noisier than the GFO SDR attitudes, because the GFO attitude is computed from the fitted Vatt which is a highly smoothed quantity. However Figure 3-13 indicates that the agreement of waveform fit attitude and GFO SDR attitude is very good, within 0.04 degrees on average. The attitude angle is of no particular interest in itself except in its use in correcting sigma0 estimates, and the agreement shown in Figure 3-13 is also within the needs of the GFO mission.

Finally, Figure 3-14 and Figure 3-15 compare the 1-second waveform fit SWH estimates with those on the GFO SDR (or NGDR); as in Figure 3-11 and Figure 3-12 there are separate subplots for the four gate index values in the waveform data set. There appears to be a consistent small bias between two SWH estimates, with the waveform fit SWH estimates being 0.1 to 0.2 m higher than the GFO SDR SWH estimates. This small SWH difference is very well within the limits set by the GFO requirements and mission needs.

There is one small question about GFO waveform data. The noise baseline values are too good, i.e., too low for the nominal 13 dB GFO signal to noise ratio (SNR). As an example, Figure 3-15 shows a magnified portion of the typical GFO waveforms already shown in Figure 3-10. Notice for the low SWH example that equivalent waveform sample 28 (telemetry sample 20) and below have zero amplitude. For the higher SWH example all equivalent waveform samples 18 (telemetry sample 10) and below have zero amplitude. For a 13 dB SNR and the typical waveform maximum value of 1100 in Figure 3-10, the average waveform value in the early noise-only region should have been around 55, not zero.

This GFO situation is different than our experience with data from the TOPEX radar altimeter. The original TOPEX SNR specification was 13 dB but the Ku-band system actually had about 6 dB of additional margin, for a system SNR of almost 20 dB. The typical TOPEX Ku-band waveform has a maximum amplitude of about 8000, and the noise baseline in the early samples is typically between 80 and 100. For the GFO maximum waveform amplitude of 1100 we would expect to see noise baseline values of around 11 if the GFO SNR were as high as 20 dB. It is true that because the waveform samples are telemetered in 8-bit words there are limits on how small a non-zero

waveform sample will be, but for GFO we would still expect to see non-zero sample values as low as 6 or so, solely based on the telemetry limits. A GFO early noise region signal of 6 would imply a SNR of about 23 dB. That all the early samples are zero therefore implies a highly unlikely SNR of greater than 23 dB for GFO.

These numbers are approximate, for illustration only, to indicate why we are surprised to see zeros for all the early waveform samples in GFO. We had noticed that the baseline looked too clean in the preflight GFO data, and this same behavior persists in GFO on-orbit data. Although only the two examples in Figure 3-17 are presented in this report, we see the zero values in early waveform samples in all GFO data. This too-clean baseline should have no effect on GFO's performing to its specifications in range and SWH estimation, and we point it out here only as a curiosity.

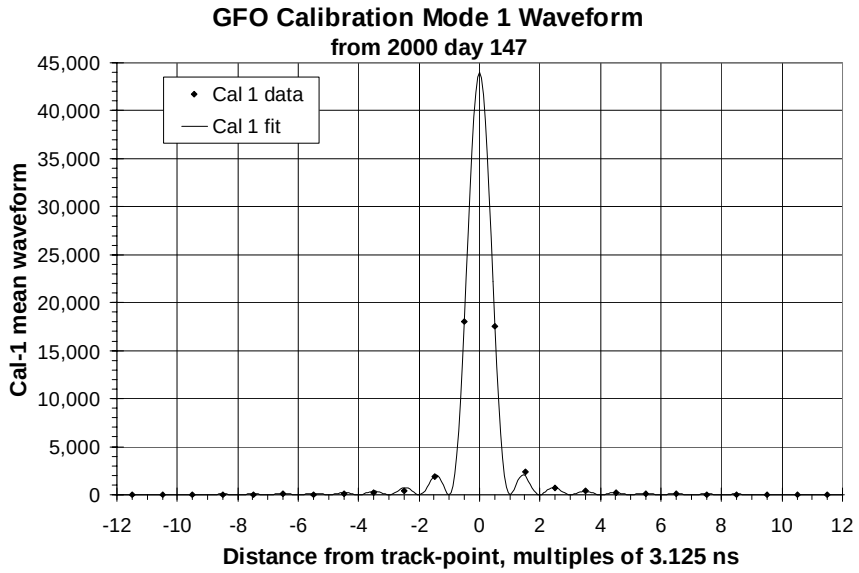

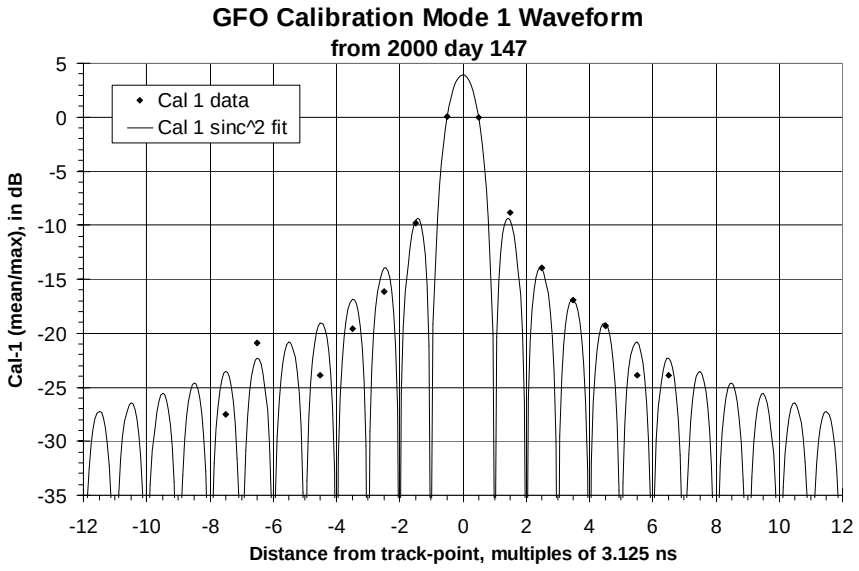

Figure 3-8 GFO Waveform Data from Calibration Mode 1 Fitted to Ideal Sinc^2 with 3.125 ns Width

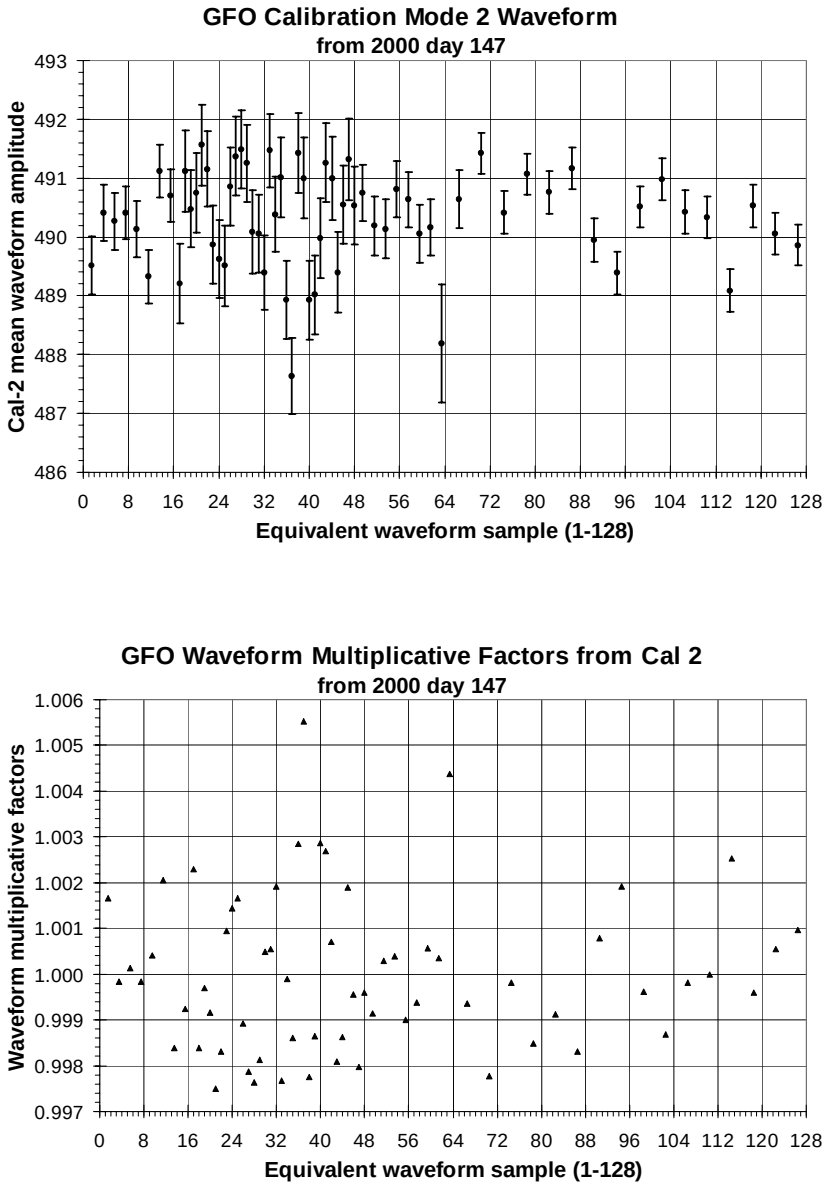

Figure 3-9 GFO Waveform Data from Calibration Mode 2

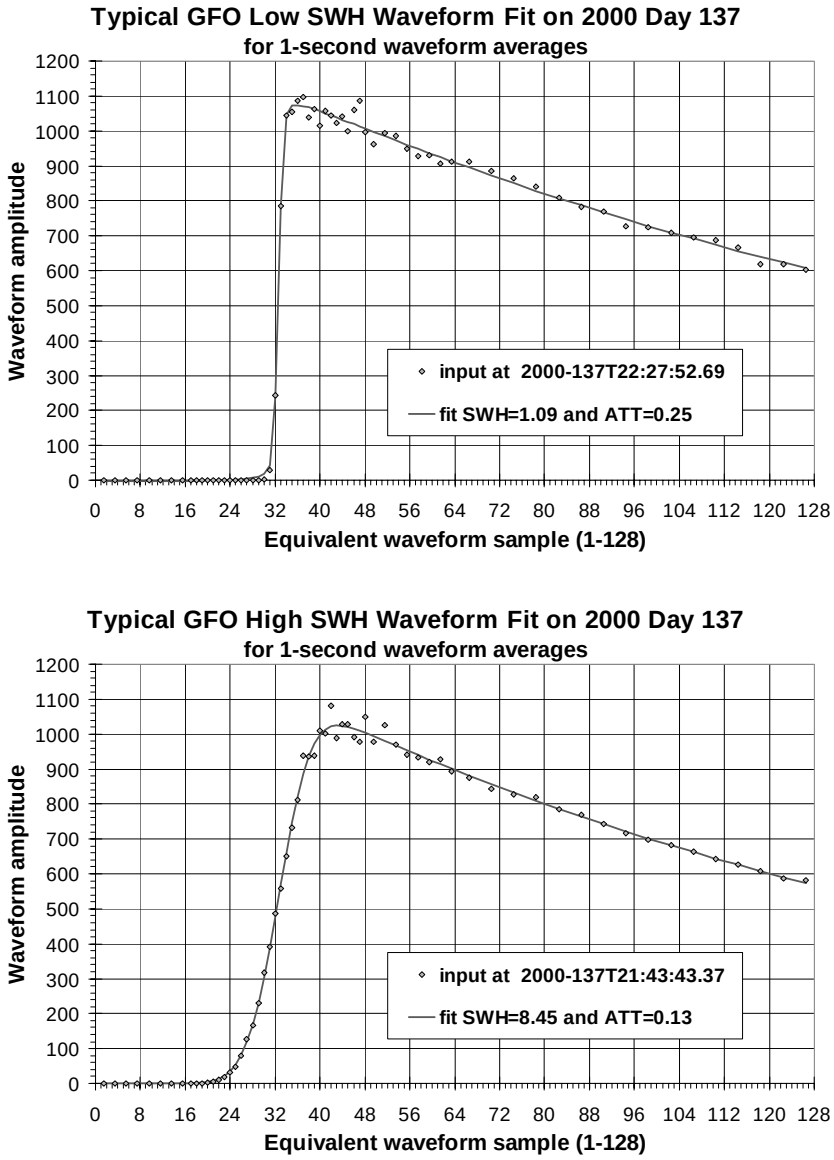

Figure 3-10 GFO Waveform Sample Data and Model Waveform Fits

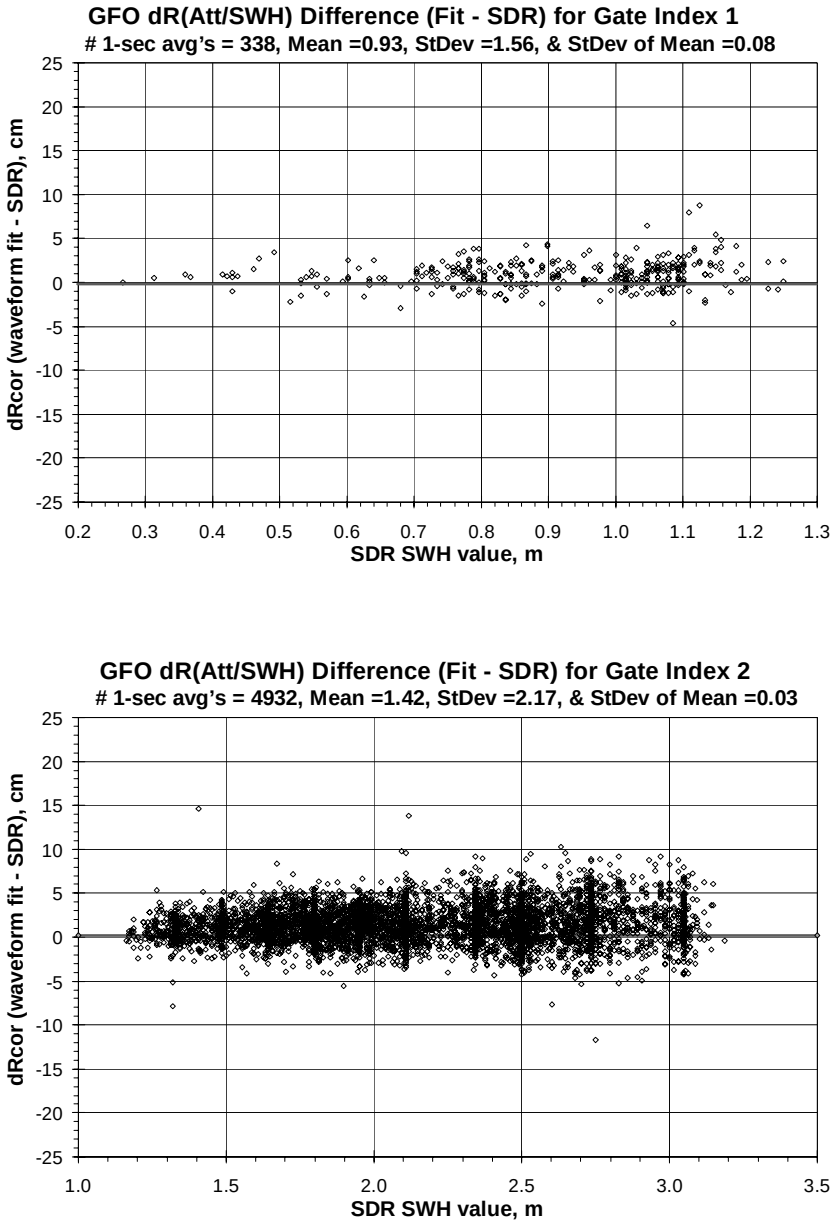

Figure 3-11 GFO Waveform Fit Comparisons of Attitude/SWH Correction to Range for Gate Index 1 and 2

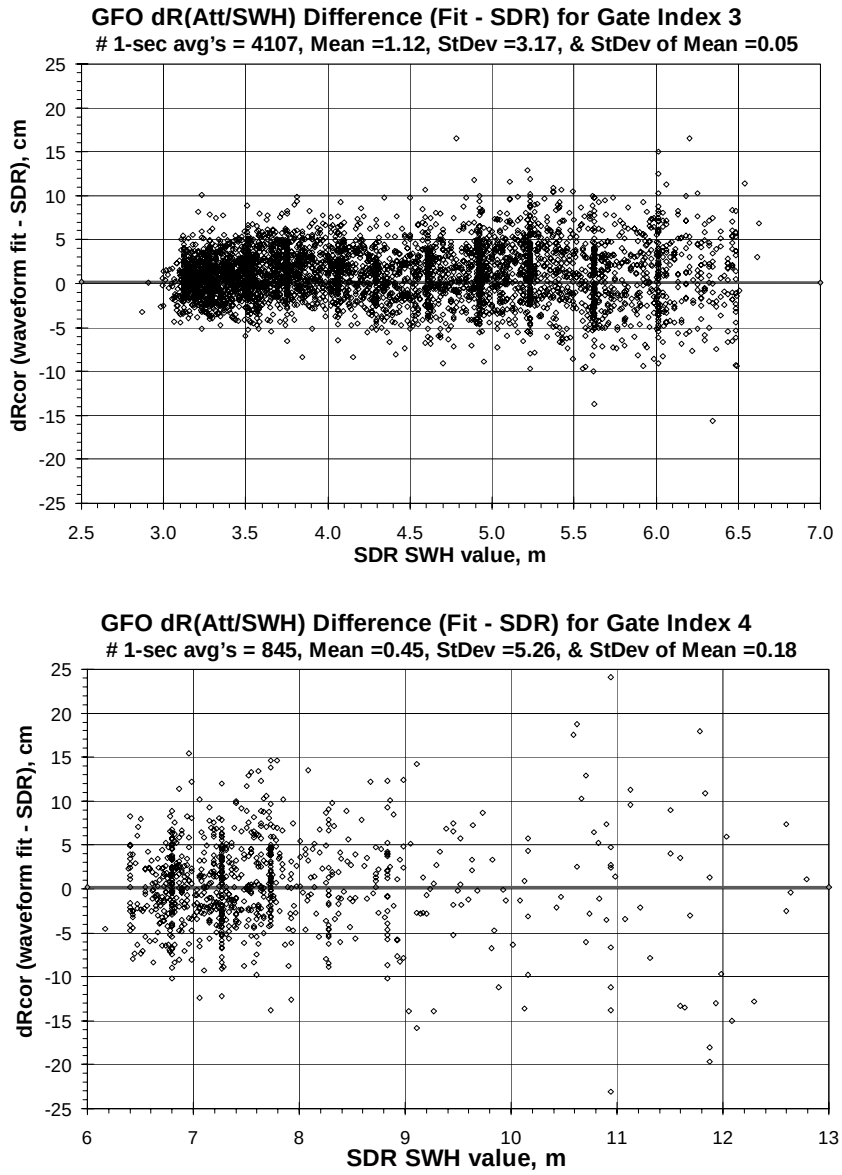

Figure 3-12 GFO Waveform Fit Comparisons of Attitude/SWH Correction to Range for Gate Index 3 and 4

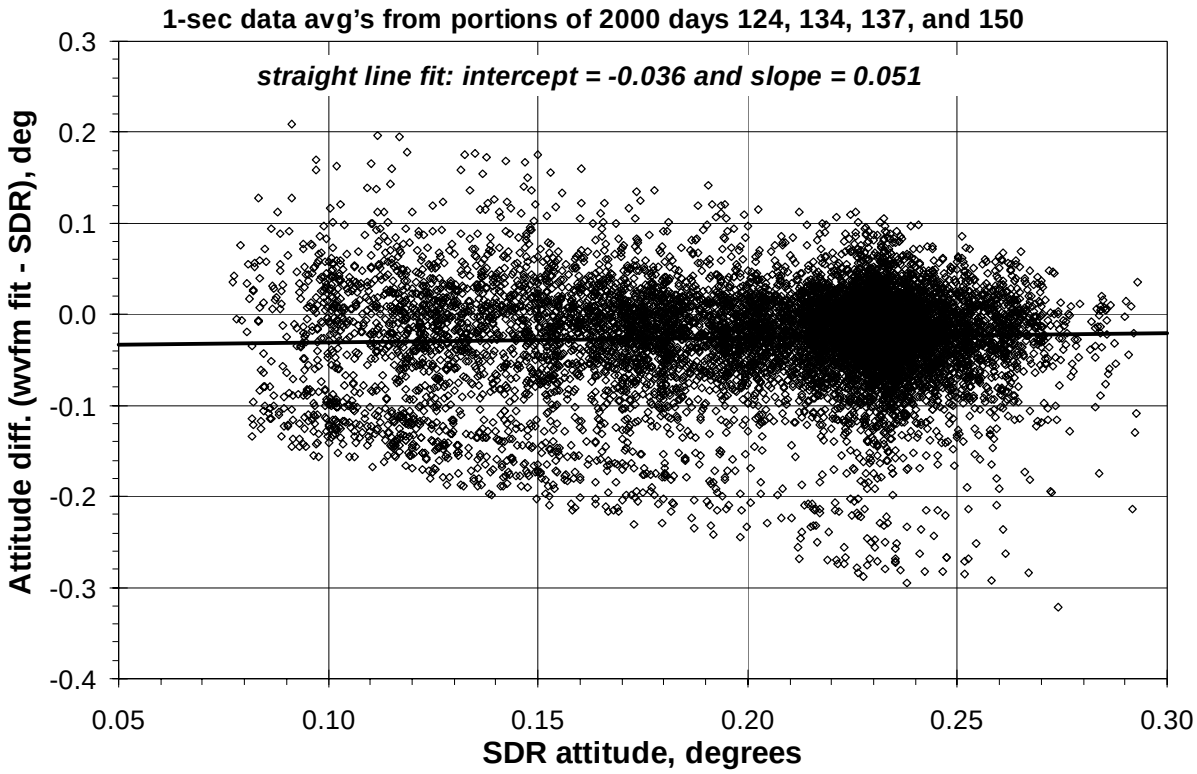

Figure 3-13 GFO Attitude Diff. (Fit - SDR) for All Gate Index (1-4)

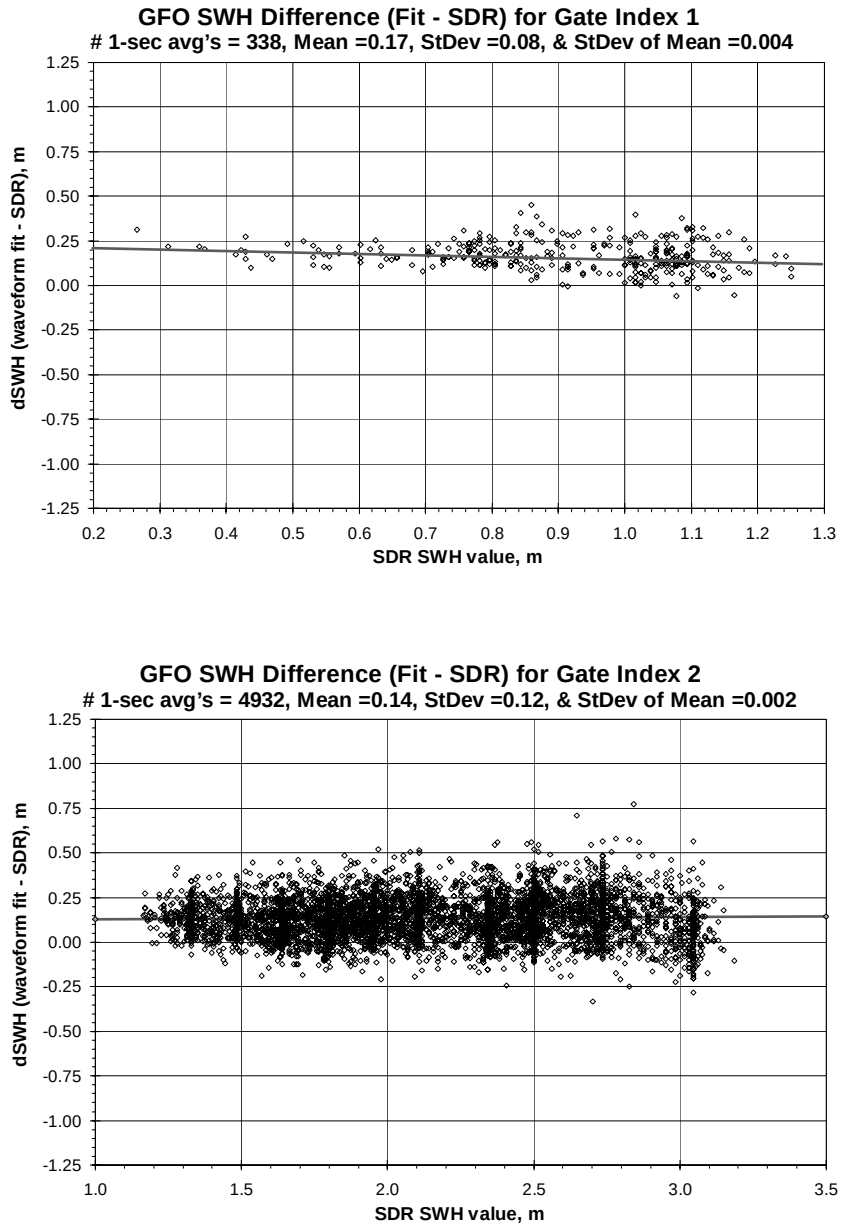

Figure 3-14 GFO Waveform Fit Comparisons of SWH Estimates for Gate Index 1 and 2

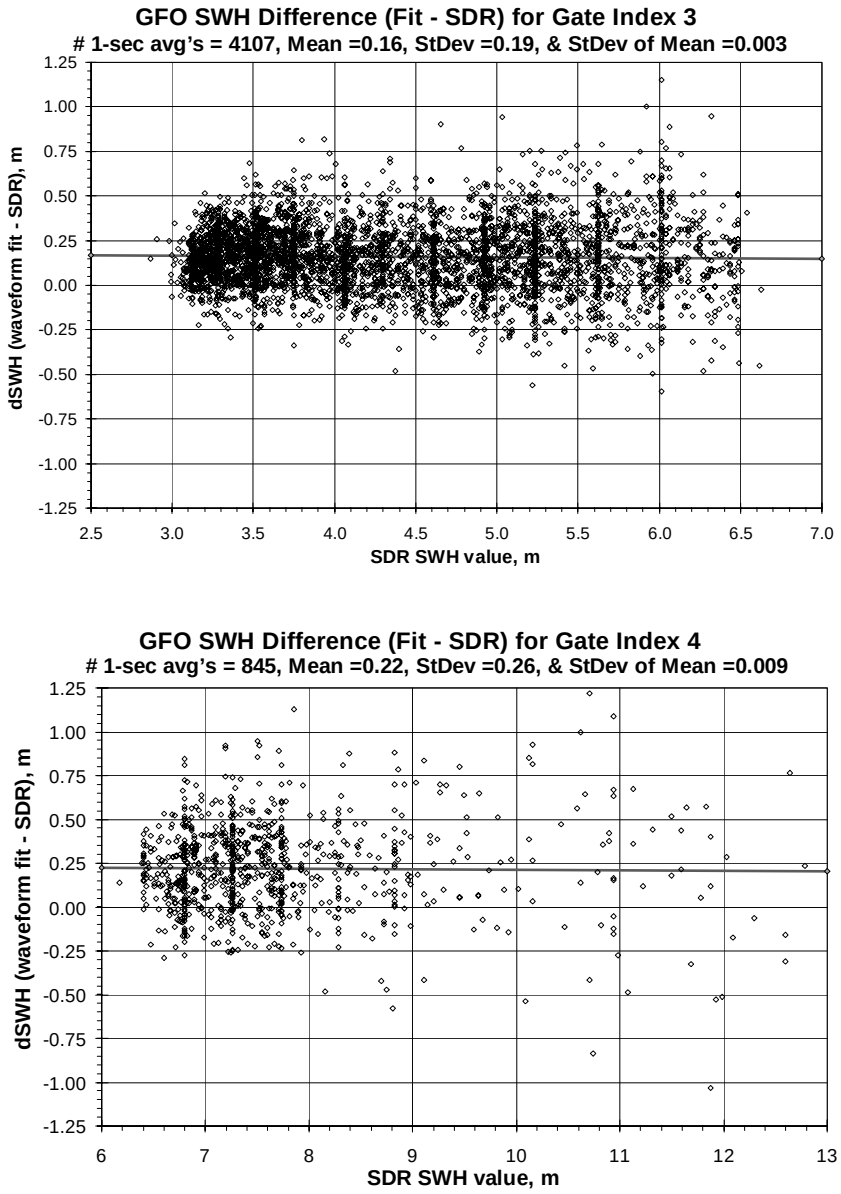

Figure 3-15 GFO Waveform Fit Comparisons of SWH Estimates for Gate Index 3 and 4

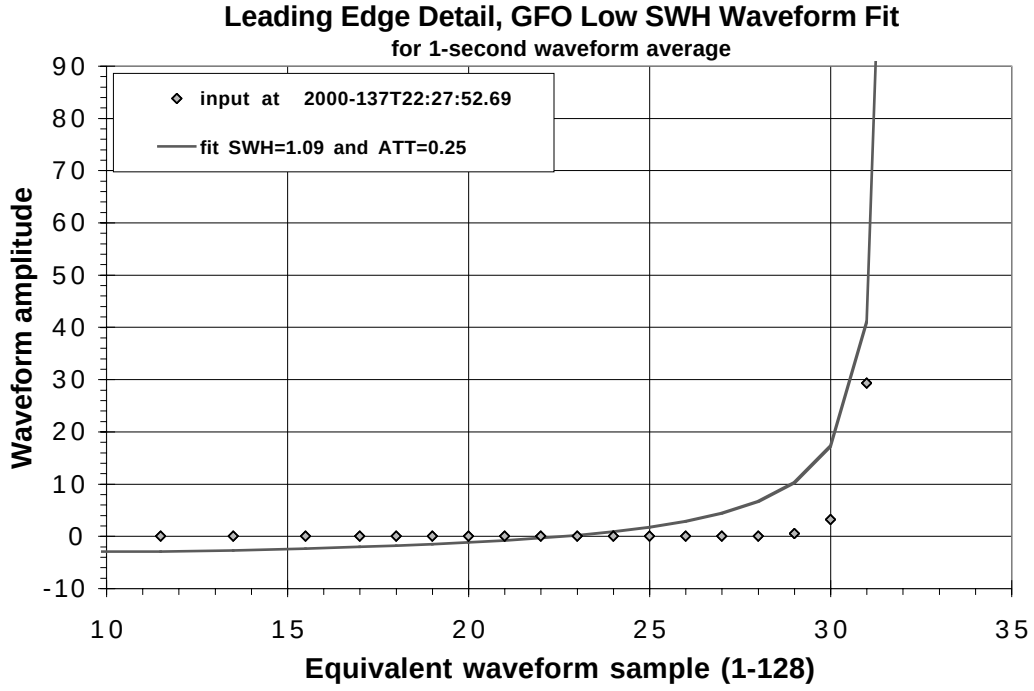

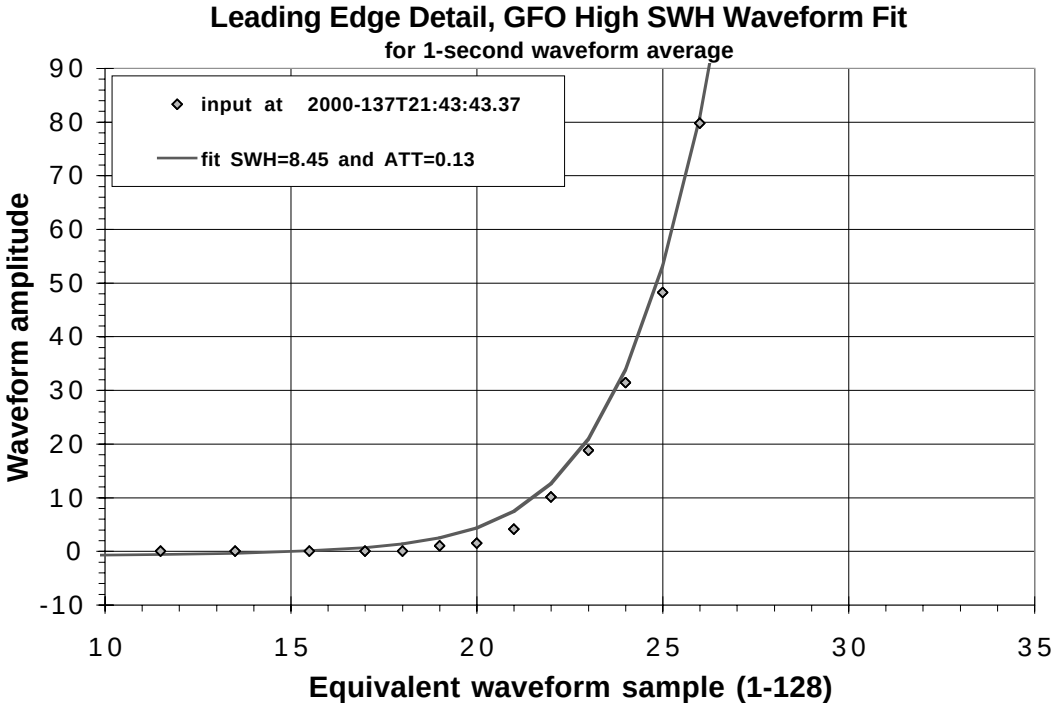

Figure 3-16 GFO Noise Baseline Examples

3.7 GFO "Smile Patch" and its Consequences

Ideally the Calibration Mode 2 should be flat, meaning it should have uniform output across the set of waveform samples. Relatively late in the GFO preflight testing it was noted that the Calibration Mode 2 data exhibited a "smile" pattern, with the samples at either end of the set having higher effective gain than the samples in the middle of the set. The flight software had already been developed and installed. Since the on-board algorithms were designed assuming a flat waveform sample response, a software patch was developed by the altimeter developers at E-Systems to be uploaded to the GFO altimeter. This "smile patch" is basically a set of 128 multiplicative waveform sample adjustments, gains in effect, with a "frown" shape to compensate for the smile pattern. The patch values are not well documented so we will list them here. Table 3-3 lists the GFO smile patch values for a waveform set numbered 1 through 128.

Table 3-3 GFO "Smile Patch" Values for Waveform Samples 1 - 128

Waveform Sample #	Patch Value	Waveform Sample #	Patch Value	Waveform Sample #	Patch Value	Waveform Sample #	Patch Value
1	0.953013	33	1.011715	65	0.959713	97	0.945683
2	0.953013	34	1.010947	66	0.959713	98	0.945683
3	0.956746	35	1.011187	67	0.959713	99	0.945683
4	0.956746	36	1.012150	68	0.959713	100	0.945683
5	0.959180	37	1.012316	69	0.983433	101	0.934026
6	0.959180	38	1.016388	70	0.983433	102	0.934026
7	0.963749	39	1.016750	71	0.983433	103	0.934026
8	0.963749	40	1.015712	72	0.983433	104	0.934026
9	0.966890	41	1.015808	73	0.978832	105	0.921097
10	0.966890	42	1.016903	74	0.978832	106	0.921097
11	0.970482	43	1.017324	75	0.978832	107	0.921097
12	0.970482	44	1.018602	76	0.978832	108	0.921097
13	0.976526	45	1.016327	77	0.981061	109	0.909145
14	0.976526	46	1.017834	78	0.981061	110	0.909145
15	0.980738	47	1.016709	79	0.981061	111	0.909145
16	0.980738	48	1.014588	80	0.981061	112	0.909145
17	0.979146	49	1.011463	81	0.982289	113	0.896047
18	0.986360	50	1.011463	82	0.982289	114	0.896047
19	0.987668	51	1.004834	83	0.982289	115	0.896047

Table 3-3 GFO "Smile Patch" Values for Waveform Samples 1 - 128 (Continued)

Waveform Sample #	Patch Value	Waveform Sample #	Patch Value	Waveform Sample #	Patch Value	Waveform Sample #	Patch Value
20	0.989496	52	1.004834	84	0.982289	116	0.896047
21	0.992460	53	1.000536	85	0.976700	117	0.884578
22	0.995203	54	1.000536	86	0.976700	118	0.884578
23	0.995020	55	0.996737	87	0.976700	119	0.884578
24	0.996716	56	0.996737	88	0.976700	120	0.884578
25	0.997351	57	0.994990	89	0.967161	121	0.873742
26	0.999910	58	0.994990	90	0.967161	122	0.873742
27	1.004239	59	0.996192	91	0.967161	123	0.873742
28	1.004929	60	0.996192	92	0.967161	124	0.873742
29	1.004551	61	0.997144	93	0.955166	125	0.864794
30	1.006474	62	0.997144	94	0.955166	126	0.864794
31	1.005611	63	0.957526	95	0.955166	127	0.864794
32	1.008372	64	0.957526	96	0.955166	128	0.864794

The data of Table 3-3 are plotted in Figure 3-17.

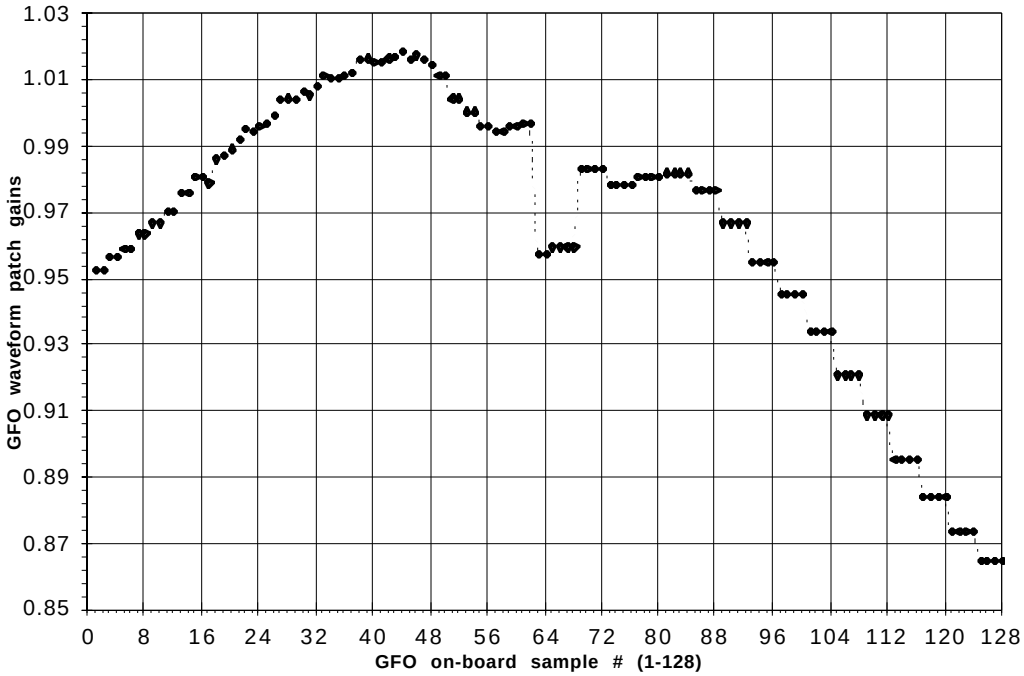

Figure 3-17 GFO Waveform "Smile Patch" Values

Among the GFO events listed in Table 2-2 is a system self-initiated reset on 25 December 1999 in which the smile patch was lost. The GFO altimeter operated without the smile patch until 06 January 2000 when the smile patch was reinstalled. The altimeter algorithms and ground processing corrections for SWH and attitude effects all assume the patch to have been present, and there will be range and SWH errors in the system output (i.e., in the distributed GFO results) for data taken during the smile patch's absence. We'll refer to these as the "no-patch" errors.

Now we will describe a simulation exercise which we carried out to assess the magnitude of the no-patch errors. The simulation assumed 800 kilometers satellite height and 1.6 degrees antenna beamwidth. We have a digital computer program which simulates the response of the GFO altimeter to a model altimeter waveform, and we executed that program for a large set of SWH values between 0 and 20 meters and attitude values between 0.0 and 0.4 degrees under the assumption of perfectly uniform waveform sample response. From this set of "perfect GFO" simulation data we built a large table of GFO range and SWH corrections as a function of SWH and attitude. Then we ran the altimeter simulator for waveforms which the altimeter's tracker would have seen if the smile patch had been omitted (i.e., with the "frown" pattern present in the waveform sample gains); we produced simulated GFO no-patch output for a range of SWH and attitude inputs. We used the no patch outputs to enter the correction look-up tables which had been produced for the "perfect GFO". In this way we could estimate the range and SWH errors for GFO no patch data at the output of the GFO ground processing (and correction) system.

Figure 3-18 shows the simulation's estimate of the no-patch error in GFO range for

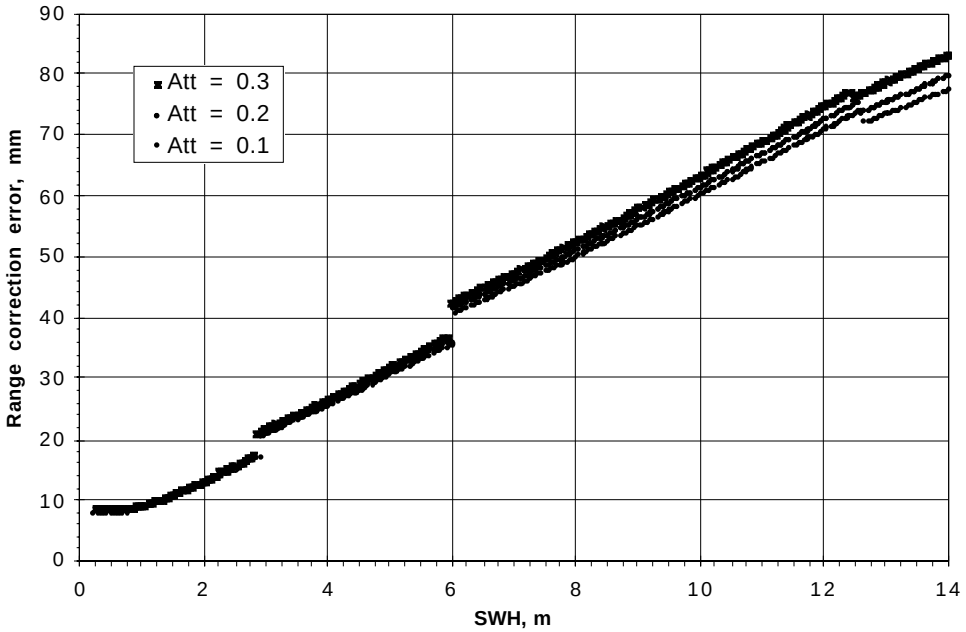

Figure 3-18 GFO Range Correction Error vs. SWH, With NO Patch

SWH from 0 to 14 m for the three attitude values 0.1, 0.2, and 0.3 degrees. This range

error has relatively little attitude dependence, and varies almost linearly from a 1 centimeter error at very low SWH to a 8 centimeter error at 14 m SWH. Figure 3-19 shows the corresponding simulation estimate of the GFO no-patch error in SWH, for the same SWH and attitude ranges as Figure 3-18. The no-patch SWH error is not as easily characterized as the range error, but the SWH error is in all cases less than 0.15 m for SWH up to 14 m. The obvious breaks or discontinuities in Figure 3-19 are

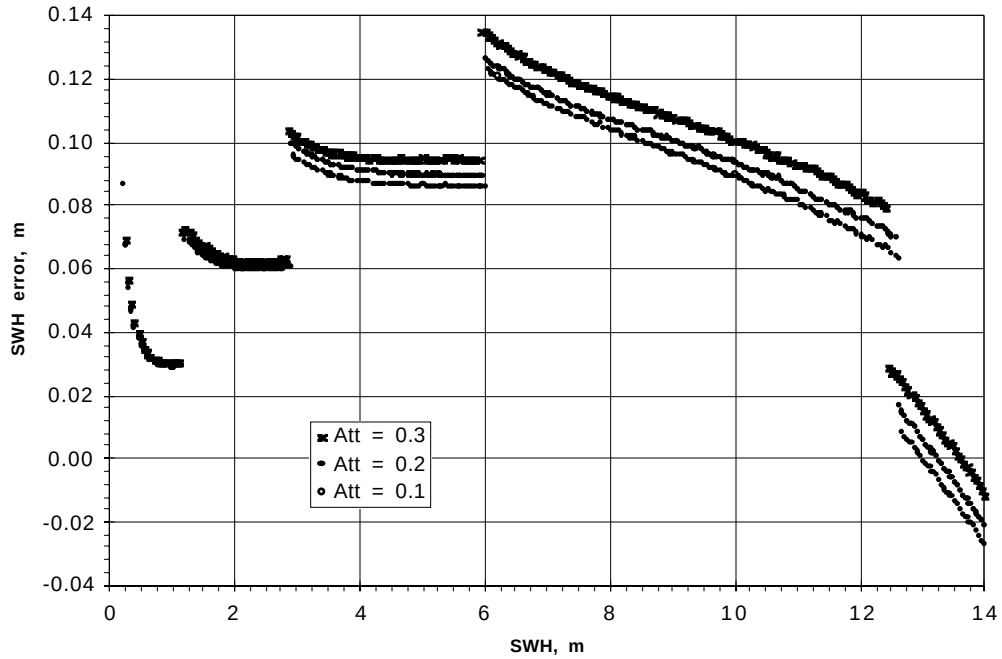

Figure 3-19 GFO SWH Error vs. SWH, With NO Patch

where the GFO altimeter switches between its five gate index values. The same gate index discontinuities are visible in Figure 3-18 except at the switch from gate index 1 to gate index 2.

Details of the actual GFO ground correction algorithms could change the range error by a centimeter or two. There are no doubt a number of other small effects not included in our simulation. It was not the intent of this section to produce a correction to be applied directly to the GFO no-patch estimates, but we have showed the importance of the patch, as well as providing some estimate of the errors in GFO data should the smile patch ever again fail to be uploaded after a system reset.

3.8 GFO Range and SWH Consequences of Thermal Change

The GFO on-orbit temperature generally is within 5 degree C of a mean temperature somewhere around 35 C. See for example Figure 2-4 which plots a GFO receiver temperature for parts of year 2000. Later in this report in Section 4.1 there is an analysis of temperature effects on AGC and sigma0. One consequence of a GFO temperature change is a change in the relative gains of the waveform samples. The Calibration Mode 2 looks at the waveform sample response to a noise-only signal which should be uniform across the sample set, so that all waveform samples would ideally have the same average value in this calibration mode. When the Calibration Mode 2 result is not completely uniform, the renormalized inverse of the Calibration Mode 2 output can be taken as a set of corrective gains. See Section 3.7 for a discussion of the "smile patch" gains derived from Calibration Mode 2 data.

The smile patch removes most of the nonuniform response of the waveform samples, but there are expected to be small residual temperature effects. That is, the Calibration Mode 2 shape will be a function of temperature, and we now want to estimate the magnitudes of the range and SWH estimation errors resulting from the on-orbit temperature changes. Figure 3-20 shows the GFO residual gain adjustments obtained

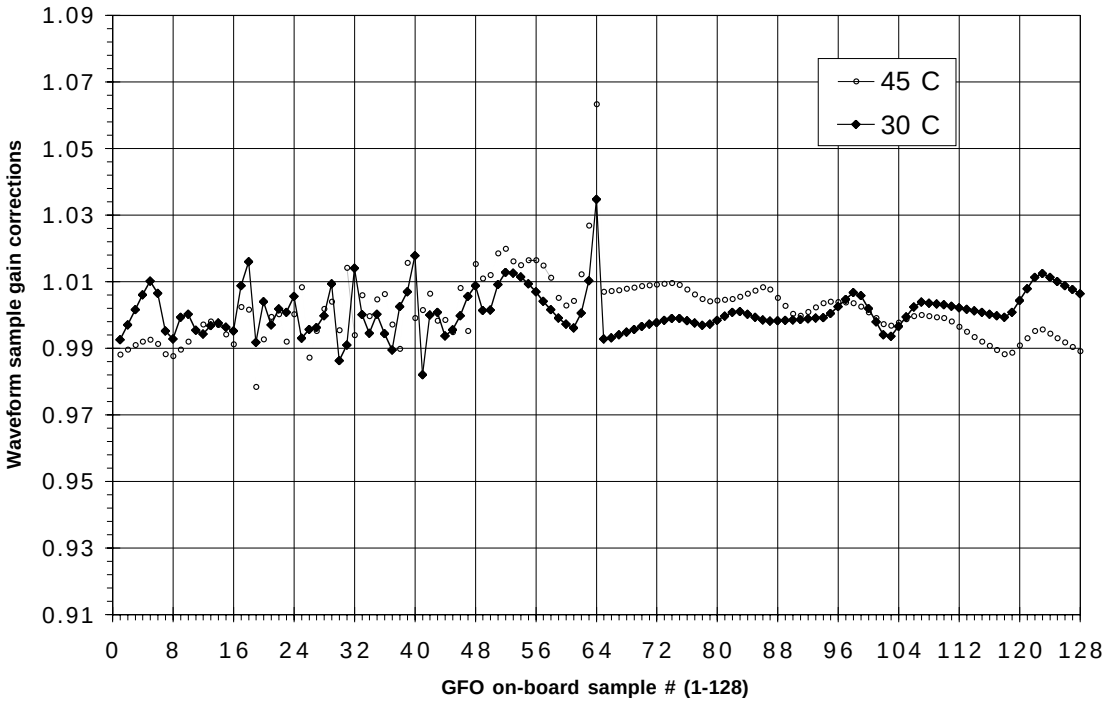

Figure 3-20 GFO Individual Waveform Sample Gains from Cal-2 with Patch, at Temperatures 30 and 45C

as the inverse of Calibration Mode 2 data from GFO thermal testing in September 1996 for two different temperatures, 30 C and 45 C. The GFO smile patch was already loaded into the GFO altimeter for these tests.

We can use the same type of simulation study as in the no-patch investigation in Section 3.7. This time we produced a large simulated set of GFO responses to waveforms generated for SWH from 0 to 20 m and attitude 0.0 to 0.4 degrees assuming that the waveform sample response would have been perfectly corrected by the 30C gains of Figure 3-20. This set of simulated data was used to build a table look-up correction procedure. Then we ran the simulation for a set of SWH and attitudes using the 45 C gains of Figure 3-20. We then entered these 45 C results into the 30C table look-up procedure, and were thus able to estimate the range and SWH estimation consequences of a change from 30 to 45 C.

The range correction error is plotted in Figure 3-21 for SWH 0 to 14 m and for attitude 0.2, 0.3, and 0.4 degrees. There is little attitude sensitivity in this result. The gate index transitions are readily seen in this Figure. The range estimation change is less than 3 millimeters for all SWH less than 13 m. At the gate index change from 4 to 5 at about 13 m, SWH the range estimation error suddenly increases to 7 millimeters, and increases with increasing SWH. Figure 3-21 is for a 15 degree C temperature change, from 30 C to 45 C. We expect the waveform sample shape effects (as shown by Calibration Mode 2) to be relatively linear with temperature, so we expect that the GFO range variations for a 5 C temperature change to be only 1/3 of the size of the Figure 3-21 range error estimate. Thus we're predicting sub-centimeter range estimation consequences of the 5 degree C variations of the GFO on-orbit temperature.

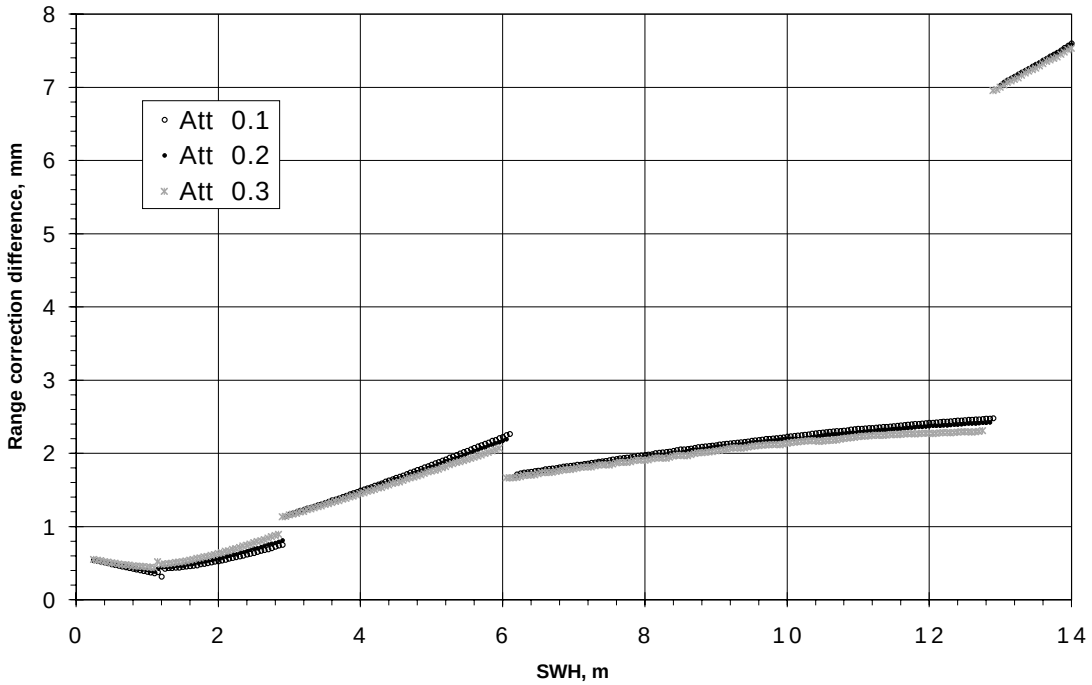

Figure 3-21 GFO Range Correction Difference vs. SWH Comparing 45C to 30C Cal-2 Data

Figure 3-22 shows the SWH estimation error resulting from the 30 C to 45 C temperature change and the largest SWH error shown, at 14 m SWH, is only about 0.15 m.

Therefore the GFO estimation error for SWH is expected to be within 0.05 m for a 5 degree change in GFO temperature.

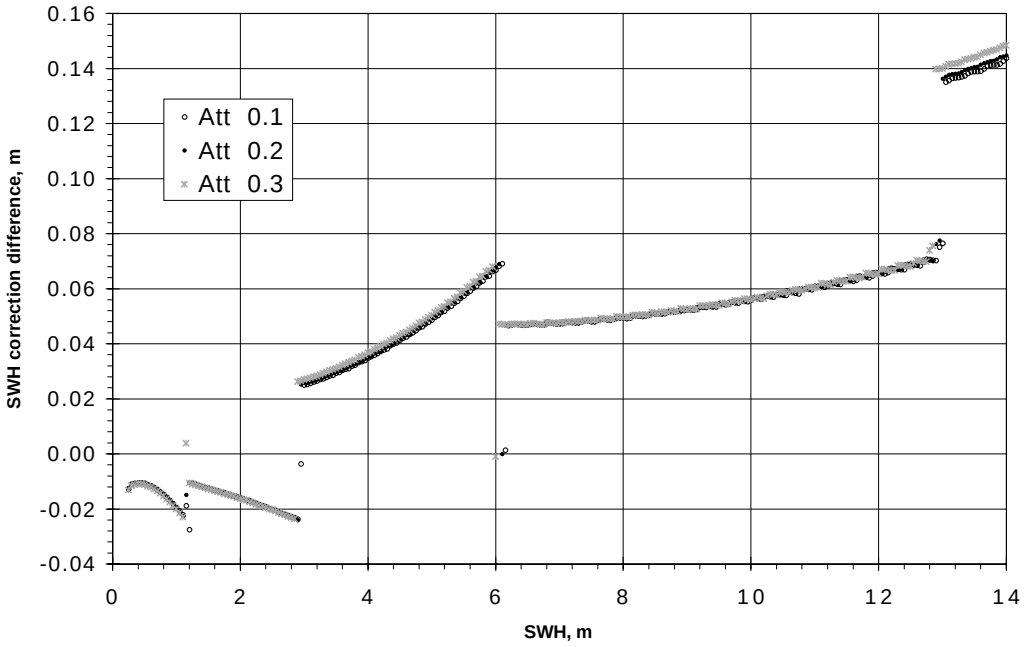

Figure 3-22 GFO SWH Correction Difference vs. SWH Comparing 45C to 30C Cal-2 Data

This simulation study has shown that GFO range and SWH estimation errors for a 15 C temperature change are much less than the errors for no-patch operation (Section 3.6), as we expect. More importantly, this study shows that normal GFO thermal variations will have no practical consequences to range and SWH estimates. No thermal corrections were planned for GFO range and SWH, and we are pleased to have shown that no such corrections are needed.

3.9 Sigma0 Blooms and Examples in GFO Data

Over several years of our continuing assessment of TOPEX Altimeter performance, we have been investigating a phenomenon we designated as the sigma0 bloom. A sigma0 bloom is characterized by abnormally high sigma0 values, typically persisting for some tens of seconds. The occurrence of sigma0 blooms is generally correlated with regions of lower significant waveheights. The strong radar returns from the sigma0 blooms are apparently the result of very smooth ocean surfaces within the radar altimeter footprint, either as a result of very calm winds or as a consequence of surface slicks. The slick regions may be irregularly distributed within the altimeter footprint. In a sigma0 bloom region the classical radar altimeter waveform model is not valid, and the range results can be affected by the departure of the return shape from the ocean surface scattering model for which the over-ocean radar altimeter was designed. We have estimated that almost 5% of the TOPEX over-ocean data are contaminated by sigma0 blooms, and we have found examples of blooms in data from other radar altimeters including Geosat, ERS-1, and Poseidon-1. As expected, the GFO data also have regions of sigma0 blooms.

In this section we will present a pair of typical sigma0 blooms from GFO data, and will discuss a possible scheme for identifying data regions in which blooms are present. Figure 3-23 shows the 1-second sigma0 for an approximately 13 minute portion of 2000 day 252 data. The horizontal axis of this, and all subsequent figures in the GFO bloom examples, is time in seconds relative to an arbitrary J2000 time of 21664440.497 seconds. Notice the obvious sigma0 bloom examples at about 200 and 700 seconds on the horizontal axis of Figure 3-23.

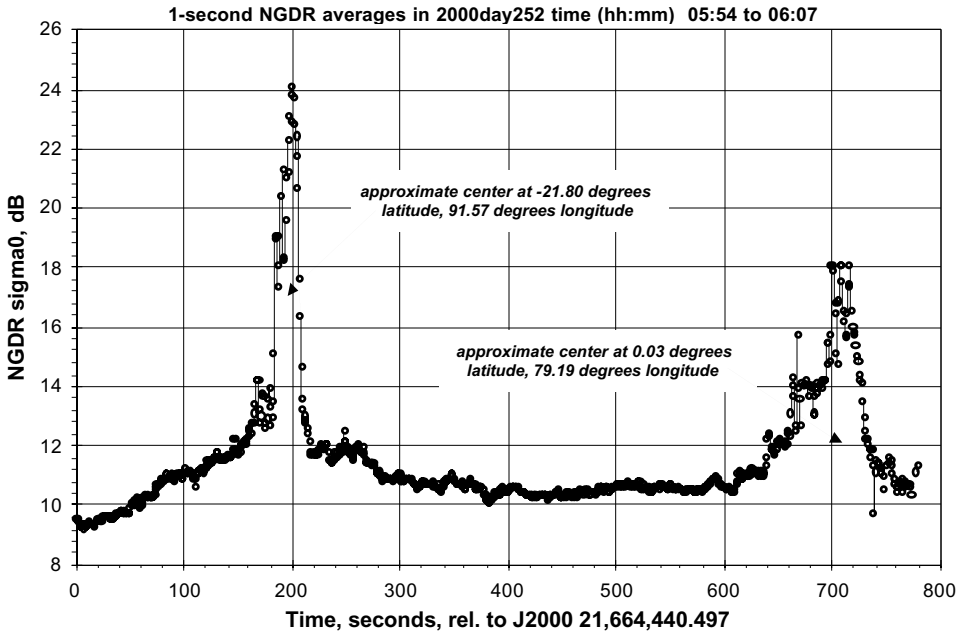

Figure 3-23 NGDR Sigma0 vs. Time

Figure 3-24 shows the GFO wind speed estimates for the same time as Figure 3-23,

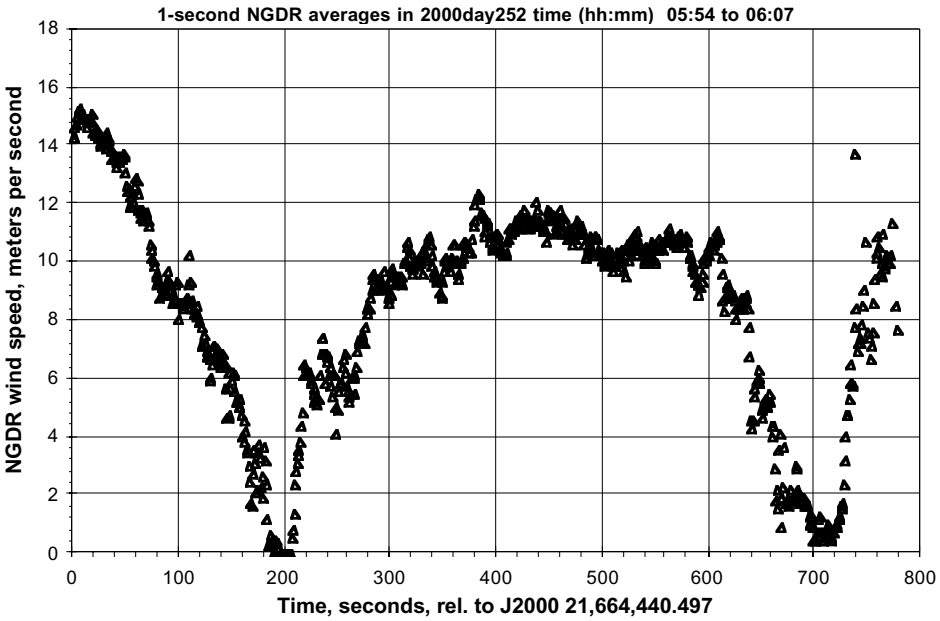

Figure 3-24 NGDR Wind Speed vs. time

and Figure 3-25 shows the corresponding 1-second significant waveheight estimates.

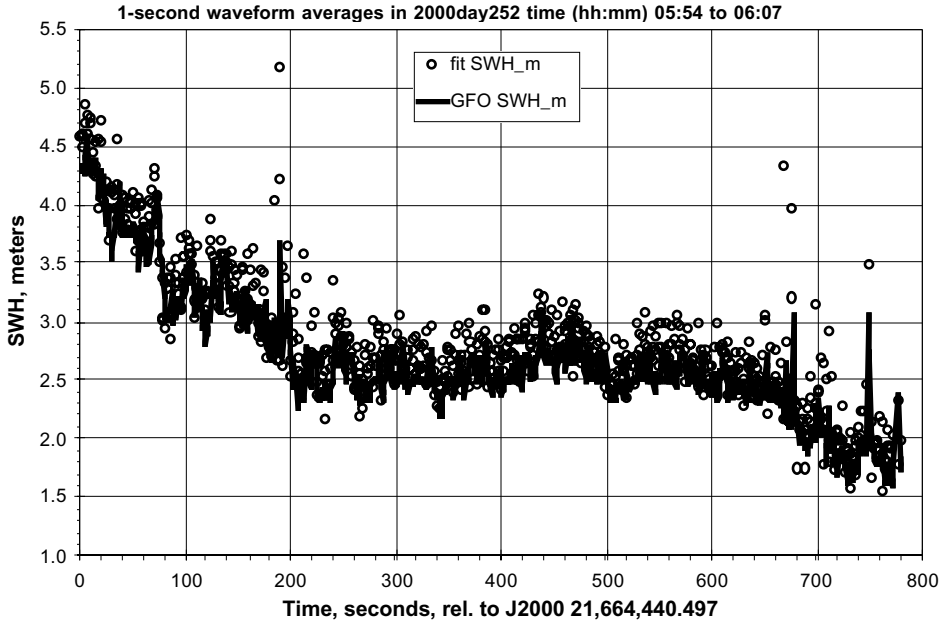

Figure 3-25 GFO 1-Sec Waveform Fit SWH vs. Time

Figure 3-25 shows both the GFO SWH estimates (available from the NGDR or the SDR) and the SWH estimates from waveform fits to 1-second averages of the GFO waveform samples.

Figure 3-26 shows the GFO attitude-related quantity Vatt for this 2000day 252 bloom

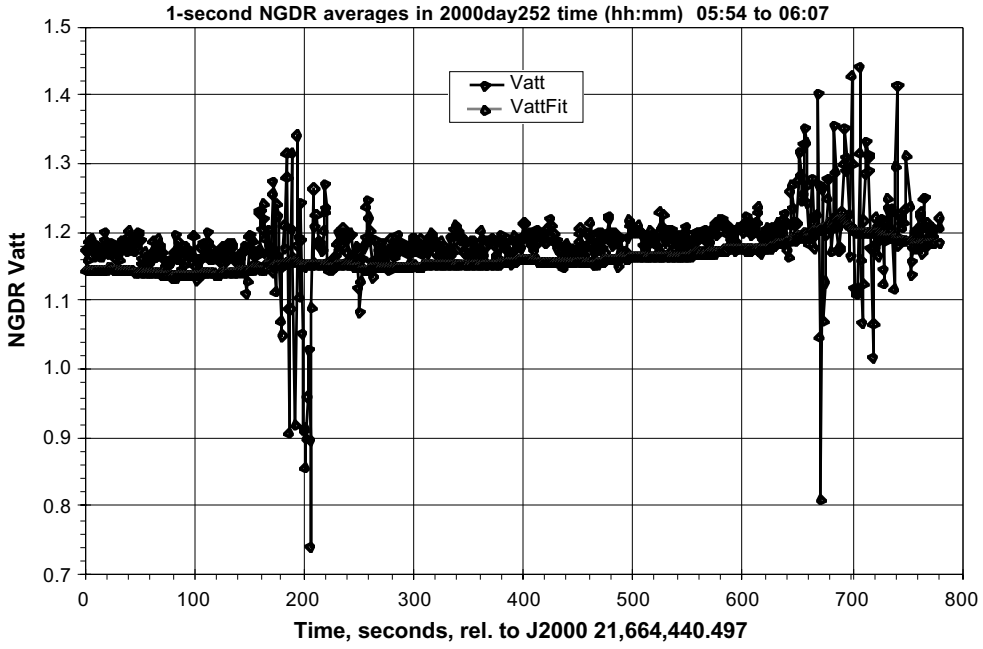

Figure 3-26 NGDR Vatt vs. Time

region. The NGDR contains both the 1-second Vatt and the fitted Vatt which is in effect a smoothed and shifted version of the 1-second Vatt. The fitted Vatt is not particularly sensitive to the sigma0 blooms but the 1-second Vatt values do show marked increase in noise and amplitude in the regions of the two sigma0 blooms. Figure 3-27 shows two different GFO attitude angle estimates: the first estimate, the NGDR Attitude, is a function of the fitted Vatt; and the second, the fit ATT, is obtained from the waveform fits to 1-second averages of the GFO waveform samples. The attitude estimates from the waveform fits show behavior similar to the 1-second Vatt. Notice that the attitude estimates from waveform fits have some negative attitude estimates. There is of course no physical meaning to a negative attitude angle, which is instead a fitting procedure artifact which signals that the plateau region of the waveform is decaying more rapidly than allowed by even a zero attitude angle for the waveform return model being used in the fitting. This just another way of saying that the model waveform return on which radar altimeter design is based is partially invalid in regions of the sigma0 blooms.

Figure 3-28 plots the NGDR quantity SSHU STD in the bloom example region. The SSHU STD is the standard deviation of the ten individual SSHU estimates within the nominal 1-second data frame of the GFO altimeter, and SSHU is the sea-surface height without any environmental corrections. Figure 3-28 shows noisier behavior in the regions of the two blooms, at 200 and 700 seconds on the time axis, but except for a few higher spikes it,s not particularly easy to see the change in noise relative to the rest of the data. To show the noise change more clearly, a 15-second time window was chosen and a standard deviation was estimated for the 15 SSHU STD values in this

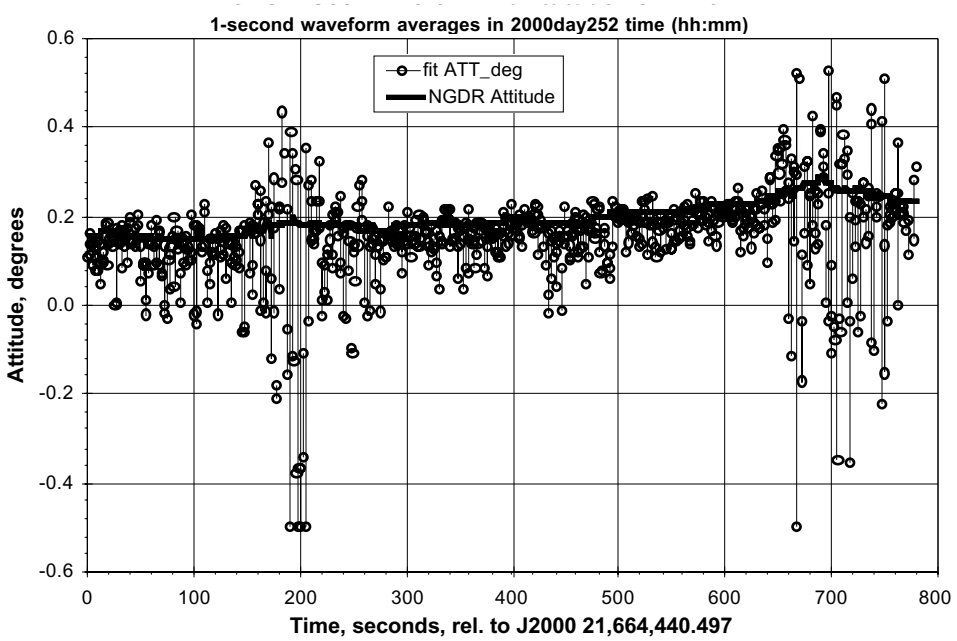

Figure 3-27 GFO 1-Sec Waveform Fit Attitude vs. Time

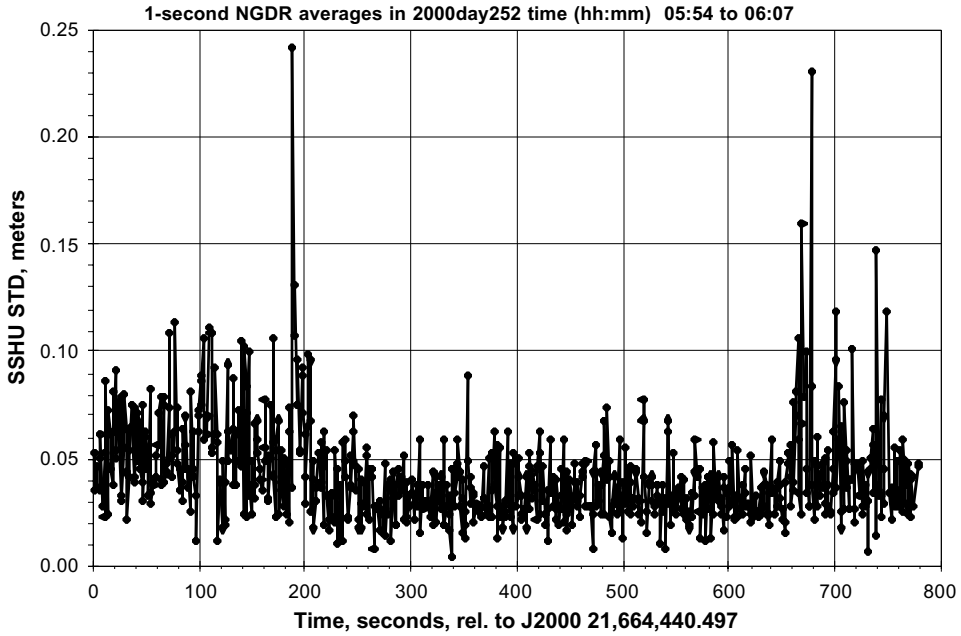

Figure 3-28 SSHU STD vs. Time for GFO Data Segment B, in 2000 Day 252

window. This 15-second window was slid through the entire set of data and the results were plotted every (nominal) second in Figure 3-29. There is nothing special about the choice of a 15-second window, and the results are not highly sensitive to the particular time width chosen. The point of this exercise was to show that there were range estimation noise consequences of the presence of sigma0 blooms.

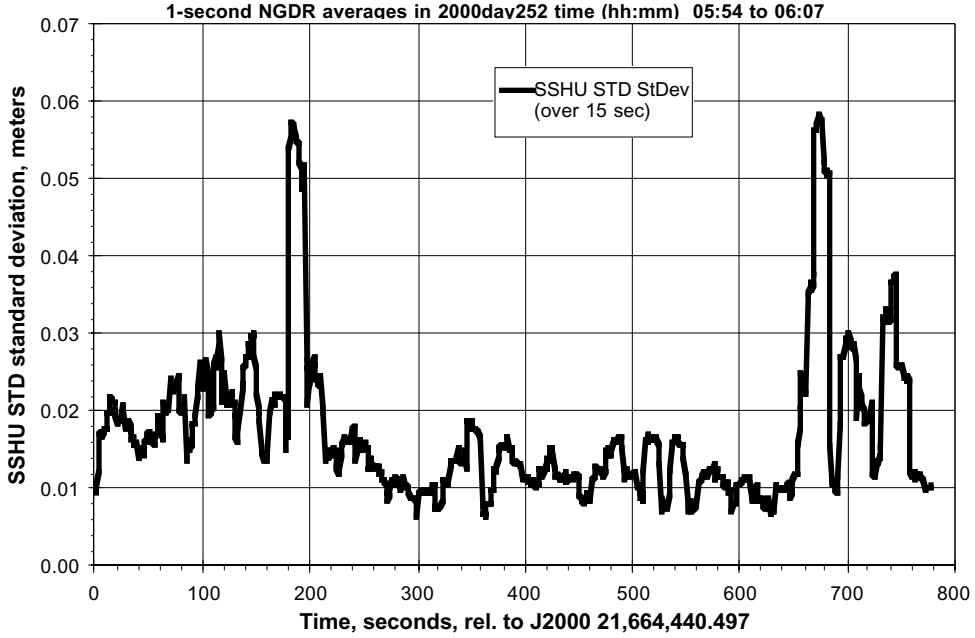

Figure 3-29 NGDR SSHU STD Standard Deviation vs. Time

There is no reason not to expect that there would be range biases as well in presence of sigma0 blooms. In absence of a clearly characterizable waveform shape evolution through a bloom event, it is not possible to estimate how large a bloom-caused range bias would be. A very rough guess would be several centimeters. Therefore anyone trying to use radar altimeter data in problems requiring better than 10 centimeter resolution would be well advised to develop editing criteria to remove bloom-contaminated data from those problems.

Our studies of sigma0 blooms in the TOPEX data, as well as our more limited bloom studies to date in the GFO data, indicate that the anomalously increased sigma0 estimates are always accompanied by waveform shape changes which would manifest themselves in an increase in the noise of the 1-second Vatt. There would be no particular concern about high sigma0 values if there were no accompanying waveform shape changes; it is the shape changes which lead to the possible range estimate changes. Figure 3-30 shows the standard deviation of 1-second Vatt estimates within a 15-second sliding time window; it is the same technique used for the standard deviations of SSHU STD shown in Figure 3-29.

A first guess at a bloom-editing recipe for GFO might be:

1) Edit out any data for which the 1-second sigma0 value is greater than 14 dB. (Actually in our TOPEX experience, we,re suspicious of any sigma0 greater than 13 or 13.5 dB.)

2) Form the set of 15-second sliding time window standard deviation estimates of the 1-second Vatt values (as plotted in Figure 3-30), and remove any data for which the 15-second Vatt standard deviation exceeds some threshold. Figure 3-30 suggests that 0.04 might be a reasonable threshold.

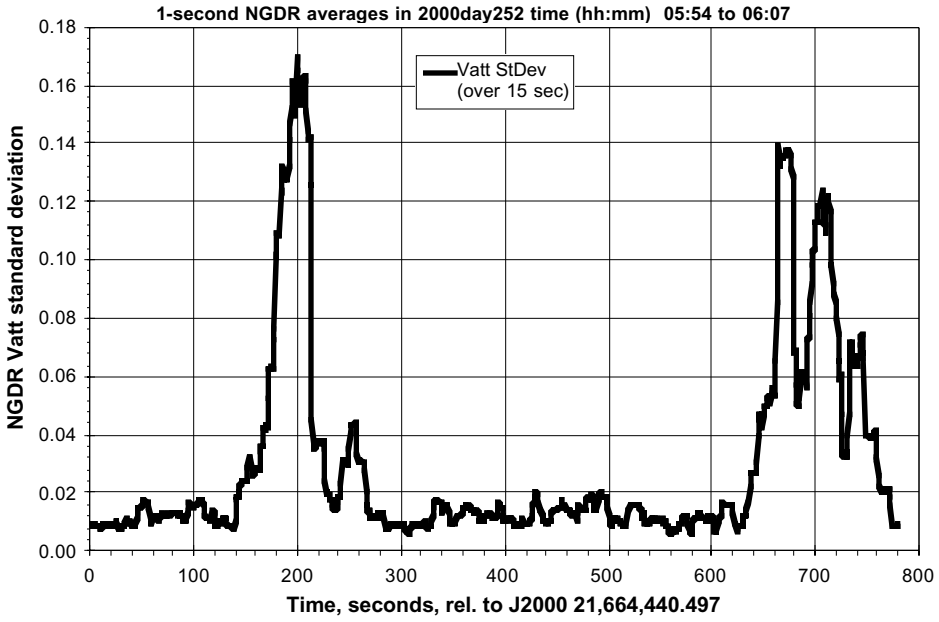

Figure 3-30 NGDR Vatt Standard Deviation vs. Time

Section 4

WFF's Processing Recommendations to GFO Project

Wallops has made specific processing recommendations to the GFO Project, with respect to:

- temperature correction for AGC
- bias corrections to sigma0 and SWH

The basis for these recommendations is discussed in the following.

4.1 Temperature Correction for AGC

4.1.1 Findings

Examination of early NGDR data showed that GFO's AGC and Sigma0 were both strongly correlated with Receiver Temperature. Their slopes were both negative with respect to increasing temperature.

The WFF-calculated additive temperature-effect correction (normalized at 41.8 degrees), applicable to both NGDR AGC and NGDR Sigma0, is:

WFF Corr (NGDR) = -9.1492 dB + 0.2188 dB / degree * temperature.

4.1.2 Background

Prior to any temperature correction, AGC was observed to have a negative slope with respect to increasing temperature.

Pre-Launch TV testing showed CAL-1 AGC temperature correction (normalized at 41.8 degrees) of:

WFF Corr (TV_Cal) = -3.6191 dB + 0.0865 dB / degree * temperature

In-Flight CAL-1 AGC shows temperature effect (normalized at 41.8 degrees) of:

WFF Corr (FLT_Cal) = -5.5301 dB + 0.1323 dB / degree * temperature

The GFO-processing correction for temperature (normalized at 41.8 degrees) was:

Corr(GFO) = +3.6191 dB - 0.0865 dB / degree * temperature

4.1.3 Analysis

For our analysis, one-minute averages of AGC, Sigma0 and SWH from NGDRs between 1999030 and 1999213 were accumulated and temperature-binned (0.1 degree bins); and then the mean of each bin was computed. The mean AGC and Sigma0 were then normalized to 2.85 m SWH, based on a WFF empirical model (derived from TOPEX data) relating SWH to backscatter. Figure 4.1 shows the analysis of the temperature correction applied to the AGC and Sigma0.

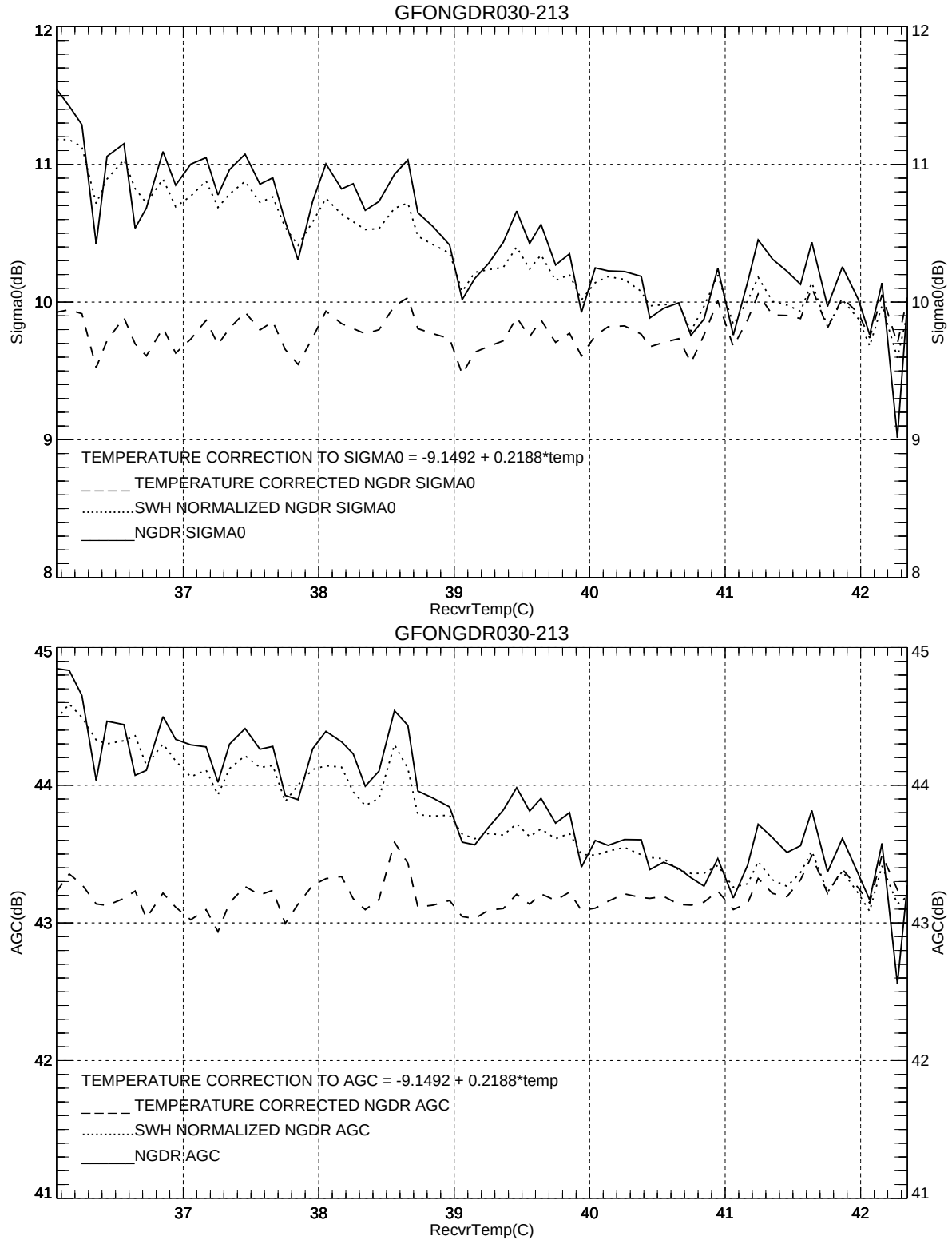

Figure 4-1 Temperature Correction Analysis Plots

Our conclusion is that the AGC temperature correction coefficients used during GFO processing had the wrong sign. [The GFO coefficients made the AGC slope, with respect to increasing temperature, more negative.]

4.1.4 Recommendation

The WFF recommendation, for AGC temperature correction, was to change the temperature correction coefficients:

- Change recv_1k_t0 from +3.6191 to -5.5301
- Change recv_1k_t1 from -0.0865 to +0.1323
- recv_1k_t2 would remain 0.0

4.1.5 Implementation

This recommendation was implemented in the Payload Operations Center (POC) Systems on 11 February 2000. The first POC dataset following the change was 00042 / 173349Z. The first sdr dataset following the change was 00042 / 134745Z.

4.2 WFF Recommended Sigma0 and SWH Corrections

Based on the various studies in section 3, WFF recommends using the sigma0 and SWH corrections that resulted from the windspeed study using NCEP winds as the reference as summarized in section 3.5 and attached as this report's Appendix A. We believe this method is our best sigma0 calibration method and have chosen to keep the matching SWH calibration as our recommendation. This analysis determined that the GFO sigma0 needs to be increased by 0.37 dB and the SWH needs to be increased about 0.24 meters.

Section 5

Engineering Assessment Synopsis

5.1 Performance Overview

Our analyses of the GFO altimeter demonstrate that it is performing well. Its range measurement precision is comparable with contemporaneous satellite radar altimeters, including TOPEX. Its internal calibrations and its cycle-to-cycle global averages have been very consistent. Comparisons with other sensors indicate that measurement biases are within GFO's pre-flight specifications of: SWH +/- 0.5m, sigma0 +/-01 dB, and windspeed +/- 2 m/s.

During the assessment of the GFO altimeter performance, WFF encountered a number of data problems that were the results of the errors in the ground data processing. Considerable time was spent in the analysis of each problem and the communication of these back to the GFO project. These problems made our performance analysis difficult and often were wrongly associated with the altimeter performance. The major ground software problems have been fixed, but several ground processing software changes that will improve the data integrity remain to be implemented. Some fine-tuning of GFO altimeter data correction algorithms and data processing algorithms have been shown to be necessary, and most have been implemented. However, fine-tuning has also occurred for every satellite radar mission flown to date.

We are continuing our GFO altimeter performance assessment on a daily basis, and are continuing to develop improved analysis techniques. Supplemental performance reports will be issued on a regular basis, and special reports will be prepared as warranted.

5.2 Open Issues

There are some remaining open issues regarding our assessment of the performance of the GFO altimeter. Those issues are:

- Definitive study of land-to-water acquisition times
- SWH Bias

Some of the remaining issues regarding data integrity are:

- Time-tag assignment to bad data caused by bad down link
  - SDR/NGDR occasional data misalignment - Example: Day 2000150
  - Erroneous datasets are occasionally received for future dates - Example: Day 2003246
- Occasional tropospheric correction problem at 0 degree longitude
- NGDR quality assurance - Example: Day 2000147

- Data sets are received that are processed with a constant composite receiver temperature. This causes data correction errors.

Section 6

References

6.1 Supporting Documentation

D.W. Hancock III, 1995, GFO Altimeter Height Noise Comparison with TOPEX, NASA / WFF report. http: / / gfo.wff.nasa.gov / docs.html

D.W. Hancock III, et al, 1998, On the Evaluation of the GEOSAT Follow-on (GFO) Altimeter. NASA / WFF presentation at the AGU meeting in San Francisco, CA, on December 10, 1998. http: / / gfo.wff.nasa.gov / docs.html

G.S. Hayne, 1996, Geosat Follow-On Altimeter Height Loop and AGC Loop Step Responses from Ground Testing. NASA / WFF report. http: / / gfo.wff.nasa.gov / docs.html

G.S. Hayne and D.W. Hancock III, 2000, GFO Radar Altimeter Performance. NASA / WFF GFO presentation at GFO meeting in Washington, D.C., on July 20, 2000. http: / / gfo.wff.nasa.gov / docs.html

G.S. Hayne and D.W. Hancock III, 1998, GFO Preliminary Results for Waveform Fitting to On-Orbit Waveform Sample Data. NASA / WFF report. http: / / gfo.wff.nasa.gov / docs.html

J.E. Lee, Documentation for the GFO File Transfer System. NASA / WFF report. http: / / gfo.wff.nasa.gov / docs.html

Naval Oceanographic Office, 2000, Navy-IGDR Users Handbook. http: / / gfo.bmpcoe.org / Gfo / Data_val / Cal_formats / formats.htm

Naval Oceanographic Office, 1998, SDR Format, Contents and Algorithms. http: / / gfo.bmpcoe.org / Gfo / Data_val / Cal_formats / formats.htm

Naval Oceanographic Office, 1998, NGDR Format, Contents and Corrections. http: / / gfo.bmpcoe.org / Gfo / Data_val / Cal_formats / formats.htm

N. Tran, D.W. Hancock III, G.S. Hayne, D.W. Lockwood and D. Vandemark, 2000, GFO Altimeter Sigma0 and SWH Calibration Correction. NASA / WFF report.

Appendix A

GFO altimeter sigma-naught and swh calibration correction

N. Tran, D. W. Hancock III, G. S. Hayne, D. W. Lockwood and D. Vandemark

NASA Goddard Space Flight Center, Wallops Flight Facility, Wallops Island, Virginia

DRAFT - 8 December 2000

Abstract

A comparison study has been carried out between GEOSAT Follow-on (GFO) and TOPEX altimeters for the radar cross section (sigma-naught) and the significant wave height (swh) by using National Centers for Environmental Prediction (NCEP) wind. This study shows that the GFO cross section values are biased about 0.37 dB lower than the TOPEX cross section, and the GFO significant wave height values are biased about 0.24 m lower than the TOPEX significant wave height. This paper describes how these GFO calibration corrections were generated and recommends these additive contributions to both GFO cross section and significant wave height to improve the wind speed retrieval. The correction on GFO sigma-naught leads to statistically significant global error reductions for the GFO wind speed. The overall bias between GFO and NCEP wind speeds decreases from 1.75 m to 0.53 m s^{-1} and the root-mean-square (rms) error from 2.44 to 1.59 m s^{-1} with the operational algorithm.

1 Introduction

The GEOSAT Follow-on (GFO) program is a United States Navy project. It was launched on 10 February 1998. This paper presents some results as part of the calibration and validation projet for GFO. Data products examined include radar cross section, significant wave height and surface wind speed. Comparison of GFO and TOPEX altimeter measurements is intended to check the proper functioning of GFO instrument.

2 Methods

Because the number of crossovers between GFO and TOPEX altimeters would be too limited to draw significant features during the period of 17 days from 3 May 2000 to 19 May 2000, we chose to compare these two sensors through the use of collocations with the National Centers for Environmental Prediction (NCEP) wind. In order to avoid problems linked to low and high wind speed, we select data between $\pm$ 1 standard deviation from the mean of the NCEP wind speed. These subsets contain 69.55% and 69.30% of data from the global sets GFO/NCEP and TOPEX/NCEP respectively. The minimum value of wind speed is about 4.8-4.9 m s^{-1} and the maximum value is about 11.0-11.2 m s^{-1}.

These subsets are used to determine biases between the two altimeters and we evaluated the relevancy of these corrections on GFO measurements by comparing respectively GFO and TOPEX wind speeds with NCEP winds over the whole wind speed range. We used in both cases their operational modified Chelton and Wentz (MCW) algorithms [1986] on the 10 second average radar cross sections to compute the altimeter wind speed.

3 Data

GFO data are from NGDR files and TOPEX data are from GDR during the same period of time of 17 days from 3 May 2000 to 19 May 2000. We applied TOPEX Side B sigma-naught calibration Table adjustements [Hayne and Hancock III, 2000] to the TOPEX GDR cross section. The different measurements used are a 10 second average. These altimeter data are limited in space between 60^oN and 60^oS.

The NCEP model provides near-surface wind vector estimates for an altitude of 10 meters above the ground and for neutral stability. Their output is on a 1.0 x 1.0 degree grid every 6 hours. For our purpose we interpolated the model outputs in space and time to derive a wind estimate colocated with GFO (or TOPEX) observations.

After completing comparisons between altimeter wind speeds and NCEP winds over the entire wind speed range, we repeated the TOPEX/GFO radar cross section and significant wave height comparisons for two later 17-day periods to demonstrate consistency of the biases found in the 3-19 May 2000 dataset.

4 Results

For the subsets described previously the comparisons show that the GFO cross section values are biased about 0.37 dB lower than the TOPEX cross section, and the GFO significant wave height values are biased about 0.24 m lower than the TOPEX significant wave height.

	Days	GFO	TOPEX	TOPEX-GFO
$< \sigma_0 >$ (dB)	124-140	10.86	11.23	0.37
$< swh >$ (m)	124-140	2.33	2.57	0.24

Table 1: Mean values for GFO and TOPEX radar cross section and significant wave height on the respective subset for year 2000, days 124-140.

We define the wind speed difference at 10 meters, U_{err}:

$$U_{err} = U_{altimeter} - U_{NCEP} \tag{1}$$

Winds are in m s^{-1},and the wind error standard deviation is simply:

$$std = (< U_{err}^2 > - < U_{err} >^2)^{\frac{1}{2}} \tag{2}$$

This factor will be of some value in providing a relative algorithm assessments but is obviously equivalent to the rms when the bias nears zero. Denoting the wind error e, α_{swh} is defined as the slope in the linear regression $e = \alpha_{swh}\ swh + \beta$. This slope is checked because numerous past studies have suggested that long scale gravity waves, which do not adjust to wind as quickly as the short gravity-capillary waves, have a measurable influence on interpretation of altimeter returns in term of wind speed. Most studies appear to agree that the effect is clearly of second order and that swh serves as a limited proxy for removing sea-state impacts from the altimeter wind speed estimate. In our case, we used such a parameter to valid our proposed corrections both on radar cross section and significant wave height.

Tables 2 to 5 present some statistical comparisons between altimeter wind speeds and NCEP winds over the whole wind speed range: Table 2 for GFO wind speed retrieved by using GFO MCW algorithm as on NGDR without correction on cross section and Table 5 with correction of 0.3725 dB on cross section before

computing the new GFO wind speed. For comparison purposes, Table 3 presents the same statistical parameters about the comparison between TOPEX and NCEP wind speeds. In Table 4 we used a new TOPEX algorithm, described in [Gourrion et al., 2000], on the GFO measurements in order to take into account both corrections on cross section and on significant wave height. This new model relates TOPEX altimeter measurements of radar cross section and significant wave height to near-surface wind speed.

Nb total	Nb after filter	$< U_{GFO} >$ (m/s)	$< U_{NCEP} >$ (m/s)	bias $< U_{err} >$	std (m/s)	rms (m/s)	% error $> 2m/s$	α_{swh}
91215	66389	9.58	7.84	1.75	1.71	2.44	51.79	0.31

Table 2: Statistical parameters of the comparison between GFO and NCEP wind speeds by using GFO MCW algorithm without correction on (σ^0) on the whole wind speed range for year 2000, days 124-140.

Nb total	Nb after filter	$< U_{TPX} >$ (m/s)	$< U_{NCEP} >$ (m/s)	bias $< U_{err} >$	std (m/s)	rms (m/s)	% error $> 2m/s$	α_{swh}
101371	70475	8.43	8.02	0.41	1.47	1.53	18.89	0.39

Table 3: Statistical parameters of the comparison between TOPEX and NCEP wind speeds by using TOPEX MCW algorithm on the whole wind speed range for year 2000, days 124-140.

Nb total	Nb after filter	$< U_{GFO} >$ (m/s)	$< U_{NCEP} >$ (m/s)	bias $< U_{err} >$	std (m/s)	rms (m/s)	% error $> 2m/s$	α_{swh}
91215	66466	7.80	7.83	-0.04	1.47	1.47	16.85	0.06

Table 4: Statistical parameters of the comparison between GFO and NCEP wind speeds by using a new TOPEX algorithm [Gourrion et al.,2000], $U_{10} = f(\sigma_0, swh)$, with correction on $(swh_{cor} = swh + 0.2381)$ and on $(\sigma^0_{cor} = \sigma^0 + 0.3725)$ on the whole wind speed range for year 2000, days 124-140.

We note that the correction on GFO sigma-naught leads to statistically-significant global error reductions for the GFO wind speed. The overall bias between GFO and NCEP wind speed decreases from 1.75 m to 0.53 m s^{-1} and the root-mean-square (rms) error from 2.44 to 1.59 s^{-1} with the operational algorithm. The percentage of data for which the difference between GFO and NCEP wind speeds are greater than 2 m s^{-1} decreases more than half. As an additional note, when we computed new GFO winds by using the new TOPEX algorithm [Gourrion et al.,2000] with correction both on sigma-naught and swh the values of the overall bias and of the slope α_{swh} are close to zero.

Figure 1 presents the comparison between GFO wind speeds without correction and NCEP winds with respect to the wind speed. Between 7 and 15 m s^{-1} the difference between the two sources is in average greater than 2 m s^{-1}. Figure 2 presents the same results when we used the correction on cross section to compute a new GFO wind. We can note that when we take into account the correction on cross section, the new GFO wind speeds appear to be more coherent with NCEP over the whole wind speed range. This second scatter diagram shows that the data are closer to the perfect line and the difference between these new GFO wind speed values and those of NCEP are in average almost between $\pm$ 1 m s^{-1}. Figure 2 is similar to Figure 3 which presents the comparison between TOPEX wind speeds and NCEP winds with respect to the wind speed.

Nb total	Nb after filter	$< U_{GFO} >$ (m/s)	$< U_{NCEP} >$ (m/s)	bias $< U_{err} >$	std (m/s)	rms (m/s)	% error $> 2m/s$	α_{swh}
91215	66362	8.37	7.84	0.53	1.50	1.59	20.50	0.28

Table 5: Statistical parameters of the comparison between GFO and NCEP wind speeds by using GFO MCW algorithm with correction on $(\sigma^0_{cor} = \sigma^0 + 0.3725)$ on the whole wind speed range for year 2000, days 124-140.

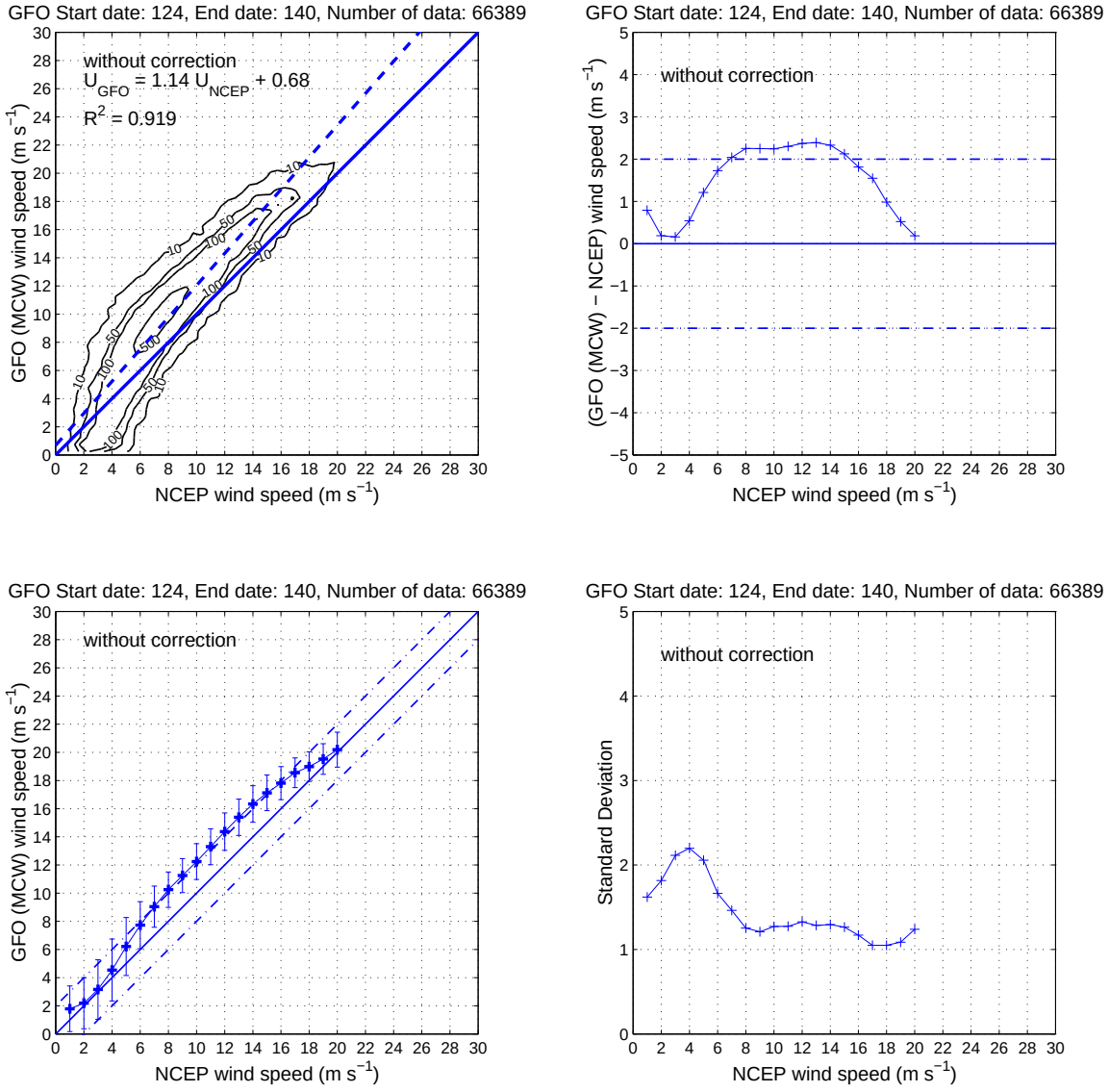

Figure 1: Comparison between GFO winds by the GFO MCW algorithm without correction and NCEP winds with respect to NCEP wind speed.

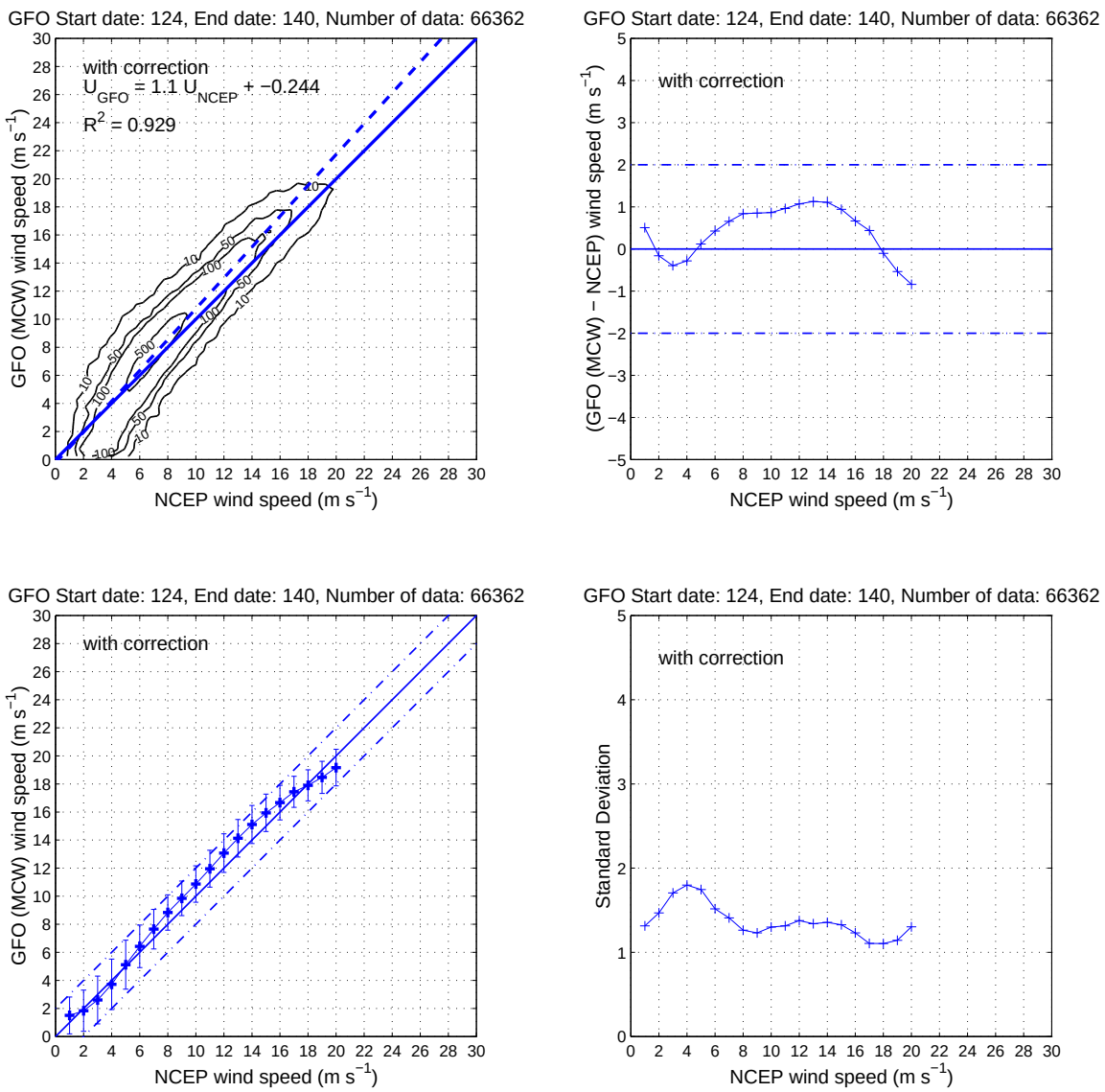

Figure 2: Comparison between GFO winds by the GFO MCW algorithm with correction on radar cross section and NCEP winds with respect to NCEP wind speed.

	Days	GFO	TOPEX	TOPEX-GFO
$< \sigma_0 >$ (dB)	245-260	10.95	11.32	0.37
	(244 missing)			
	261-277	10.97	11.33	0.36
$< swh >$ (m)	245-260	2.16	2.38	0.22
	(244 missing)			
	261-277	2.24	2.49	0.25

Table 6: Mean values for GFO and TOPEX radar cross section and significant wave height on the respective subset for year 2000, days 245-277.

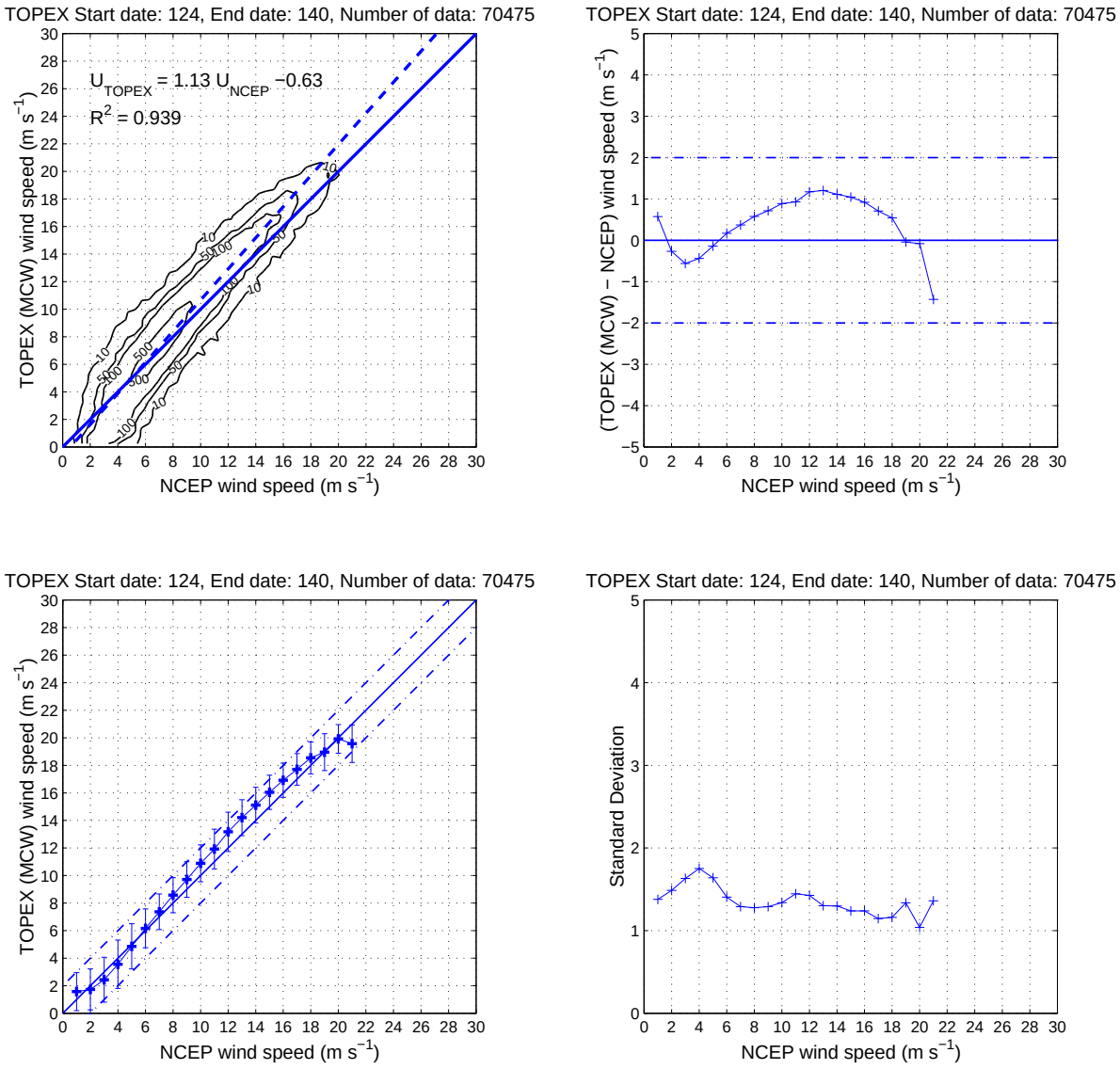

Figure 3: Comparison between TOPEX winds by the TOPEX MCW algorithm and NCEP winds with respect to NCEP wind speed.

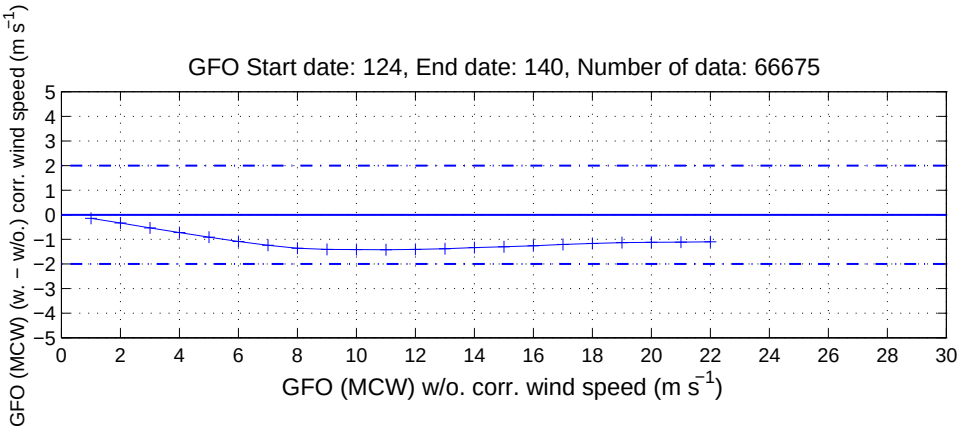

Figure 4: Comparison between GFO wind speed retrieval by using GFO MCW algorithm with and without correction on radar cross section

Figure 4 presents a comparison between GFO wind speed retrieval by using GFO MCW algorithm with and without correction on radar cross section with respect to GFO wind without correction. The improvement appears to be for all wind speeds. Above 5 m s^{-1}, the difference between these two GFO wind speeds is close to 1 m s^{-1}.

To evaluate the consistency of the biases on sigma-naught and on SWH pointed out in Table 1, we used two other periods of 17 days from 31 August 2000 to 3 October 2000. The results are presented in Table 6 and the agreement of the TOPEX/GFO differences in Table 1 and Table 6 confirms the values of the biases found.

5 Conclusion

We have determined that the GFO altimeter calibration bias to be added to SWH is 0.24 m. This will be a constant shift from the current SWH values that we feel needs to be applied based using TOPEX as the standard. The calibration bias to be added to sigma-naught is 0.37 dB; this implies a variable wind speed correction. Using GFO MCW wind speed algorithm the effects on the estimated wind speed on the GFO products is shown in the previous Figure 4. The maximum error is less than 2 m s^{-1}. Both of these calibrations are less than the specification (swh $\pm$ 0.5 m, sigma-naught $\pm$ 1 dB, wind speed $\pm$ 2 m s^{-1}) but we recommend that they be implemented in the standard GFO data processing.

6 References

- Chelton D. B. and Wentz F. J., Further development of an improved altimeter wind-speed algorithm, J. of Geophys. Res., 91, C12, 14250-14260, 1986.
- Gourrion J., Vandemark D., Bailey S., Chapron B., Satellite altimeter models for surface wind speed developed using ocean satellite crossovers, IFREMER Tech. Report, DRO/OS-00/01, 2000.
- Hayne G. S. and Hancock III D. W., TOPEX Side B sigma0 calibration table adjustements, WFF TOPEX documents, November 2000.

Abbreviations & Acronyms

CAL	Calibration Mode or Calibration Mode data
Cal/Val	Calibration and Validation
CPU	Central Processing Unit
EDAC	Error Detection and Correction Circuits
EEPROM	Electrically Erasable Programmable Read Only Memory
ENG	Engineering Data
ERO	Exact Repeat Orbit
FTP	File Transfer Protocol
GEOSAT	Geodetic Satellite
GFO	GEOSAT Follow-On
GPSR	Global Positioning Satellite Receiver
GSFC	Goddard Space Flight Center
HW	Hardware
IAP	Integrated Avionics Processor
IDL	Interactive Data Language
NCEP	National Centers for Environmental Prediction
NGDR	NOAA Geophysical Data Record
NSI	NASA Science Internet
OODD	Operational Orbit Determination Data
POC	Payload Operations Center
QSCAT	NASA QuikSCAT satellite
RA	Radar Altimeter
RAM	Read Access Memory
RASE	Radar Altimeter System Evaluator
SCI	Science Data
SDR	Science Data Record
SDT	Science Definition Team
SMA	Semi-Major Axis of the orbit
SW	Software

UTC	Universal Time Code
VTCW	Vehicle Time Code Word
WF	Waveform Data
WFF	Wallops Flight Facility
WVR	Water Vapor Radiometer